



# HABILITATION A DIRIGER DES RECHERCHES

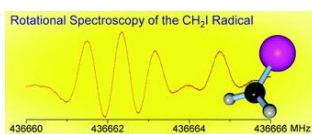
N° d'ordre : 40640

Stéphane Baillex

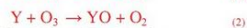
Maitre de Conférences – section 30 du CNU (milieux dilués & optique)

Laboratoire de Physique des Lasers, Atomes et Molécules

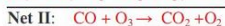
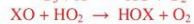
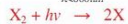
## High Resolution Spectroscopic Studies of Radicals of Atmospheric and Astrophysical Importance



$X = Cl, Br, \text{ or } I$



$\lambda < 600\text{nm}$



Tropospheric halogen chemistry







# HABILITATION A DIRIGER DES RECHERCHES

N° d'ordre : 40640

Stéphane Bailleux

Maitre de Conférences – section 30 du CNU (milieux dilués & optique)

Laboratoire de Physique des Lasers, Atomes et Molécules

## High Resolution Spectroscopic Studies of Radicals of Atmospheric and Astrophysical Importance

---

soutenue le 2 décembre 2011

devant le jury composé de

### Rapporteurs

**Luca Dore** Professeur, Université de Bologne (Italie)

**Agnès Perrin** Directeur de Recherches (CNRS), Universités Paris Est Créteil/Paris Diderot

**Maryvonne Gerin** Directeur de Recherches (CNRS), Université Paris 6

### Examineurs

**Svatopluk Civiš** Professeur, J. Heyrovský Institute of Physical Chemistry (Rép. Tchèque)

**Bernard Pinchemel** Professeur, Université Lille 1 Sciences et Technologies

### Garant de l'habilitation

**Georges Wlodarczak** Professeur, Université Lille 1 Sciences et Technologies



## Abstract

Chemically reactive (but thermodynamically stable) species are often key intermediates involved in the chemistry of a wide variety of complex systems. These include Earth and non-terrestrial planetary atmospheres, combustion engines, microcircuits manufacturing and both the interstellar medium and circumstellar shells. Among the transient species, many are radicals (ions or neutrals), *i.e.* open-shell molecules characterized by the presence of at least one unpaired electron.

The very short lifetime of these unstable molecules, ranging typically from tens of microseconds to hundreds of milliseconds, makes it complicated to produce them with a sufficient number density, which is a prerequisite to conduct laboratory experiments devoted to their studies. Thus for a large number of reactive molecules, the amount of data available is either scarce or even non-existent, on both experimental and theoretical point of view. Basic research on these molecules is highly desirable in order to better understand the chemistry occurring in the above-mentioned environments.

In the past eight years I have carried out several research projects related to this matter. In collaboration with teams from Germany, Czech Republic and Japan, a number of radicals have been characterized for the first time by millimetre-wave spectroscopy. The high-resolution inherent to this technique makes it possible to resolve the fine- and hyperfine- structures which are often observed in the rotational spectra of open-shell molecules. Their analyses provide remarkable insights on the electronic and molecular structure.

The research has potential applications in two fields. On the one hand, the rotational spectra of halogen-bearing species which are minor atmospheric constituents have been investigated. They include the  $\text{CH}_2\text{X}$  radicals, with  $\text{X} = \{\text{Br}, \text{I}\}$  and the stable mixed halogen species  $\text{ICl}$  and  $\text{CH}_2\text{ICl}$ . Likewise, the  $\text{FCO}_2$  radical is a key intermediate involved in the stratospheric degradation of hydrofluorocarbons (HFCs). The  $\nu_4$  rotation-vibration band (asymmetric  $\text{CO}_2$  stretching) measured by Fourier-transform infrared spectroscopy in Germany has been analysed.

On the other hand, a number of open-shell species involved in interstellar and circumstellar chemistry have been detected for the first time by millimetre-wave spectroscopy up to the terahertz range:  $\text{CS}^+$ , the bi-radical  $\text{CHD}$ , and the 15-nitrogen isotopologues of the  $\text{NH}$  and  $\text{NH}_2$  radicals as well as the  $\text{HNC}$  unstable, close-shell molecules.

## Résumé

Les molécules chimiquement instables (mais stables sur le plan thermodynamique) sont souvent des intermédiaires très réactifs jouant un rôle prépondérant dans un grand nombre de réactions dont les mécanismes sont encore relativement méconnus. Celles-ci se déroulent en général dans des environnements complexes, tels que ceux rencontrés dans les processus de combustion, dans l'atmosphère terrestre, ou encore dans le milieu interstellaire et les enveloppes circumstellaires. Parmi les espèces labiles, nombreuses sont des radicaux (ions ou molécules neutres), des molécules dites à couche ouverte caractérisées par la présence d'au moins un électron non apparié à l'origine de nombreuses interactions intramoléculaires. La très courte durée de vie qui caractérise ce type de molécules (ordre de grandeur compris entre quelques microsecondes et quelques centaines de millisecondes) posent de sérieux problèmes de production en concentration suffisante afin de permettre leur étude en laboratoire. Nombreuses sont ainsi les espèces qui restent à identifier et à caractériser par des techniques adéquates. Les travaux fondamentaux qui s'y rapportent sont fortement souhaitables si l'on veut mieux comprendre et modéliser la chimie de ces milieux.

C'est dans ce contexte que se sont inscrits mes projets de recherche menés au cours des huit dernières années, en collaboration avec des équipes tchèque, allemande et japonaise. J'ai ainsi identifié et caractérisé pour la première fois par spectroscopie millimétrique essentiellement des molécules à couche ouverte. La haute résolution inhérente à cette technique permet de résoudre les structures fines et hyperfines des spectres rotationnels, dont l'analyse conduit à des informations importantes sur leur configuration électronique et leur structure moléculaire.

J'ai orienté mes travaux autour de deux axes majeurs. D'une part je me suis intéressé à des molécules halogénées susceptibles de jouer un rôle dans les réactions catalytiques en chaîne perturbant la concentration de l'ozone atmosphérique. Il s'agit des radicaux  $\text{CH}_2\text{X}$ , avec  $\text{X} = \{\text{Br}, \text{I}\}$  et de deux composés stables doublement halogénés,  $\text{ICl}$  et  $\text{CH}_2\text{ICl}$ . Le radical  $\text{FCO}_2$  est un intermédiaire clé impliqué dans la dégradation stratosphérique des hydrofluorocarbones. La bande de vibration  $\nu_4$  (mode d'élongation asymétrique de  $\text{CO}_2$ ) mesurée par spectroscopie infrarouge à transformée de Fourier en Allemagne a été analysée.

D'autre part, l'ion radicalaire  $\text{CS}^+$ , la variété mono-deutérée du bi-radical méthylène ( $\text{CHD}$ ), et la variété  $^{15}\text{N}$  des radicaux  $\text{NH}$ ,  $\text{NH}_2$  et des isotopologues de  $\text{HNC}$ , ont aussi été identifiés et caractérisés pour la première fois par spectroscopie millimétrique jusqu'au térahertz. Ces travaux permettront d'aboutir à une meilleure connaissance de leur rôle clé dans la chimie du milieu interstellaire.

## Acknowledgements

I started the millimetre-wave spectroscopic studies of chemically unstable species in the mid 1990's in the laboratory of Marcel Bogey, Claire Demunck and Jean-Luc Destombes. I particularly owe much to M. Bogey who gave me the impetus to study transient molecules. Although the complexity in characterising transient species by the use of spectroscopic methods is continuously increasing, my wish is to be able to pursue this activity for many more years.

I am also grateful to G. Wlodarczak who supported my investigations of labile molecules by millimetre-wave spectroscopy after M. Bogey and J.L. Destombes have retired.

Since the early stage of my scientific career, I have been very fortunate to collaborate with a number of visiting scientists, in particular with S. Civiš, Z. Zelinger and H. Ozeki. It always was a pleasure to discuss and work with them and I express here my deep gratitude to them.

Finally I would be remiss if I did not recognize the importance of my wife's support and encouragement. She accepted to leave her sweet home which was recently hit by one of the biggest earthquake ever measured. She still grudges the fact that she had to give up her lifestyle in Japan, her own carrier as well and needless to mention that I feel responsible for that. A very special thanks also to our beloved daughter Ayumi for her constant cheerfulness and for gifts too numerous to detail.



# Table of Contents

<b>Part 1- Academic Survey</b> .....	1
<b>Curriculum Vitae</b> .....	2
<b>Scientific Supervision</b> .....	4
<b>Peer Reviewed Papers</b> .....	5
<b>List of Communications</b> .....	9
<b>Part 2- Scientific Records</b> .....	15
<b>Chapter 1- Introduction</b> .....	16
1.1 Motivations and scientific background .....	16
1.2 Characterizing reactive species by millimetre-wave spectroscopy .25	
1.2.a Specificities, difficulties and ... ..	25
1.2.b ... naturally, some of my research projects failed .....	33
1.2.b.i The case of $\text{H}_2\text{O}^+$ .....	33
1.2.b.ii The case of deuterated isotopologues of $\text{CH}_3^+$ .....	41
1.3 The Lille submillimetre-wave spectrometer .....	45
<b>Chapter 2- Environmental-Related Spectroscopy of Halogen-Containing Species</b> .....	52
2.1 Introduction .....	52
2.2 The $\nu_4$ band of the $\text{FCO}_2$ radical analyzed: evidence for the strong <i>pseudo</i> Jahn-Teller effect .....	57
2.3 The rotational spectrum of the $\text{CH}_2\text{X}$ radicals, with $\text{X}=\text{Br}, \text{I}$ .....	60
2.4 Stable iodine-bearing species: $\text{ICl}$ and $\text{CH}_2\text{ICl}$ .....	64
2.4.a $\text{ICl}$ .....	64
2.4.b $\text{CH}_2\text{ICl}$ .....	66
2.5 Future prospects .....	72
<b>Chapter 3- Small Transients of Astrophysical Significance</b> .....	74
3.1 Introduction .....	74
3.2 The $\text{CS}^+$ radical cation .....	79
3.3 The $\text{CHD}$ bi-radical .....	81
3.4 Future prospects .....	84



# Part 1

## Academic Survey

# Curriculum Vitae

Stéphane Bailleux

Born 18 October, 1969

## Contact

Laboratoire de **Physique des Lasers, Atomes et Molécules** (PhLAM)

UMR CNRS 8523

Université Lille 1

UFR de Physique – Bat. P5

FR-59655 Villeneuve d'Ascq Cedex

[stephane.bailleux@univ-lille1.fr](mailto:stephane.bailleux@univ-lille1.fr)

## Academic employment & Education

2003 -today: Associate Professor – Université Lille 1

Laboratoire PhLAM – Millimetre-wave Spectroscopy Group

Research topic: characterization by millimetre-wave spectroscopy of chemically reactive species of atmospheric and astrophysical importance.

1999 -2003: Associate Professor – Université Lille 1

Laboratoire PhLAM – Photonics Group

Subject: Permanent  $\chi^{(2)}$  susceptibility induced by 193-nm insulation under high electric field gradient in Ge-doped bulk silica glasses (known as UV poling): characterization by VUV spectroscopy and the Maker fringe technique. Potential applications in nonlinear optical active devices.

This activity was stopped when it was worldwide realized that the magnitude of the induced  $\chi^2$  was insufficient ( $\sim 0.05$  pm/V, with an objective of  $\sim 5$  pm/V) to develop efficient optical active devices. This situation prompted me to return to high-resolution spectroscopic studies of reactive species.

1998 -1999: Post-doctoral fellowship (**J**apan **S**ociety for the **P**romotion of **S**cience, JSPS)

Institute for Molecular Science, Okazaki, Japan  
supervisor: Prof. K. Tanaka

Subject: Pulsed supersonic jet millimetre-wave spectroscopy for the detection of the van der Waals bending band of Ar-HCN, Ar-DCN and Ar-HBr clusters.

1994 -1997: PhD in Physics (defended the 10 December 1997)

Laboratoire PhLAM – Université Lille 1

co-supervisors: M. Bogey and C. Demuyneck

Subject: High-resolution spectroscopy studies of reactive species: production and molecular structure of  $\text{H}_2\text{CSiH}_2$  and  $\text{P}_2\text{O}$

Short-term research scholarship awarded by the DAAD (German Academic Exchange Service) in 1996 to carry out the high-resolution spectroscopic analysis of ro-vibration bands of  $\text{H}_3\text{Si}^{37}\text{Cl}$  with Prof. H. Bürger (Wuppertal, Germany, 4 months).

1992 -1993: Postgraduate Diploma

PhLAM – Université Lille 1

co-supervisors: M. Bogey and C. Demuyneck

Laboratory project: Millimetre-wave spectroscopy of silicon-bearing reactive species: detection of silanone,  $\text{H}_2\text{SiO}$ , produced in a pulsed-discharge.

## **Miscellaneous**

2008 –today: elected member at the **C**onseil **N**ational des **U**niversités

(University National Board) section 30: diffuse materials and optics. The advisory and decision-making Board is in charge of the career of both Full and Associate Professors.

## Scientific supervision

I have co-supervised with Z. Zelinger (J. Heyrovský Institute of Physical Chemistry, Academy of Science of the Czech Republic, Prague, Czech Republic) two PhD students to completion (in December 2010):

Eva Grigorová and Jan Skřinský (Faculty of Safety Engineering, VŠB - Technical University of Ostrava, Czech Republic).

E. Grigorová participated in the analysis of the  $\nu_4$  band of the FCO<sub>2</sub> radical (see Part 2, chap. 2) measured by Fourier transform infrared spectroscopy at the University of Wuppertal (Germany) and in the detection by millimetre-wave spectroscopy of the CS<sup>+</sup> radical ion (Part 2, chap. 3). J. Skřinský was involved in the detection of the iodiomethyl radical, CH<sub>2</sub>I (Part 2, chap. 2).

In 2008, Patrik Kania (Institute of Chemical Technology, Department of Analytical Chemistry, Prague, Czech Republic) was a post-doctorate researcher in the PhLAM Laboratory under my scientific supervision. He contributed to the detection for the first time in the gas-phase of the rotational spectra of the CH<sub>2</sub>I radical and of the stable interhalogen molecules ICl and CH<sub>2</sub>ICl. He also assisted in detecting the <sup>15</sup>N isotopologues of the hydrogen isocyanide molecule.

In 2000-2001, I have co-supervised (~50 %) the postgraduate student M. Lancry, now lecturer at University Paris-Sud XI.

## Peer reviewed papers:

I published twenty-six papers in peer-reviewed journal that are of significance in various fields of high-resolution molecular spectroscopy and in particular in astrophysics, atmospheric chemistry and quantum chemistry. Additional papers have been submitted (FCO<sub>2</sub>) or are in preparation (CH<sub>2</sub>ICl, ICl, <sup>15</sup>NH, <sup>15</sup>NH<sub>2</sub>, <sup>15</sup>HNC...). To a large extent, the studies deal with the *first* detection by microwave and millimetre-wave spectroscopy of transient species.

## Post-PhD thesis

---

### 26. Terahertz Spectroscopy of the CHD Radical ( $X^3A''$ )

H. Ozeki, S. Bailleux and G. Wlodarczak

*Astron. & Astrophys.* **527**, A64 (2011)

### 25. Hyperfine Resolved Fourier Transform Microwave and Millimeter-Wave Spectroscopy of the Iodomethyl Radical, CH<sub>2</sub>I ( $X^2B_1$ )

S. Bailleux, P. Kania, J. Skřínský, T. Okabayashi, M. Tanimoto, S. Matsumoto and H. Ozeki

*J. Phys. Chem. A* **114**, 4776 – 4784 (2010)

### 24. Dispersion of Light and Heavy Pollutants in Urban Scale Models: CO<sub>2</sub> Laser Photoacoustic Studies

Z. Zelinger, M. Strížík, P. Kubát, S. Civiš, E. Grigorová, R. Janečková, O. Zavila, V. Nevrlý, L. Herecová, S. Bailleux, V. Horká, M. Ferus, J. Skřínský, M. Kozubková, S. Drábková and Z. Janour

*Appl. Spectrosc.* **63**, 430 – 436 (2009)

### 23. Rotational transitions within the $\nu_2$ , $\nu_3$ , $\nu_4$ and $\nu_6$ bands of formaldehyde H<sub>2</sub><sup>12</sup>C<sup>16</sup>O

L. Margulès, A. Perrin, R. Janečková, S. Bailleux, C. P. Endres, T. F. Giessen and S. Schlemmer

*Can. J. Phys.* **87**, 425 – 435 (2009)

### 22. The Submillimeter-Wave Spectrum of the CS<sup>+</sup> Radical Ion

S. Bailleux, A. Walters, E. Grigorová and L. Margulès

*AstroPhys. J.* **678**, 73163 (2008)

- 21. High resolution rotational spectrum of FCO<sub>2</sub> radical (extension to lower frequencies)**  
 Z. Zelinger, S. Bailleux, D. Babánková, M. Šimečková, L. Strítěská, L. Kolesníková, P. Musil, P. Kania, Š. Urban, H. Beckers and H. Willner  
*J. Mol. Spectrosc.* **243**, 292 (2007)
- 20. Hyperfine Resolved Spectrum of the Bromomethyl Radical, CH<sub>2</sub>Br, by Fourier Transform Microwave Spectroscopy**  
 H. Ozeki, T. Okabayashi, M. Tanimoto, S. Saito and S. Bailleux  
*J. Chem. Phys.* **127**, 224301 (2007)
- 19. Millimeterwave Spectrum of Bromomethyl Radical, CH<sub>2</sub>Br**  
 S. Bailleux, P. Dréan, Z. Zelinger, S. Civiš, H. Ozeki and S. Saito  
*J. Chem. Phys.* **122**, 134302 (2005)
- 18. The Submillimeter-wave Spectrum of the Chloromethyl Radical, CH<sub>2</sub>Cl, in the ground vibronic state**  
 S. Bailleux, P. Dréan, Z. Zelinger and M. Godon  
*J. Mol. Spectrosc.*, **229**, 140 – 144 (2005)
- 17. First Observation of the Rotational Spectrum of the Bromomethyl Radical, CH<sub>2</sub>Br**  
 S. Bailleux, P. Dréan, M. Godon, Z. Zelinger and C. Duan  
*Phys. Chem. Chem. Phys.* **6**, 3049 – 3051 (2004)
- 16. Thermal Poling with Alternating Voltage: a Way to Increase the Second Order Nonlinearity**  
 G. Martinelli, Y. Quiquempoix, A. Kudlinski, S. Bailleux and H. Zeglache  
*Proc. SPIE - Int. Soc. Opt. Eng.* **4943**, 176 – 183 (2003)
- 15. Thermal Stability of the 248 nm Induced Presensitization Process in Standard H<sub>2</sub>-loaded Germanosilicate Fibers**  
 M. Lancry, P. Niay, S. Bailleux, M. Douay, C. Depecker, P. Cordier and I. Riant  
*App. Optics – OT* **41**, 7197 – 7204 (2002)
- 14. Third and Second Order Nonlinear Optical Properties of Ge-Se-S-As Chalcogenide Glasses**  
 F. Smektala, J. Troles, V. Couderc, A. Berthelemy, G. Boudebs, F. Sanchez, H. Zeglache, G. Martinelli, Y. Quiquempoix and S. Bailleux  
*Proc. SPIE - Int. Soc. Opt. Eng.* **4628**, 30 – 38 (2002)

**13. Millimeter-wave Spectroscopy of PO in Excited Vibrational States up to  $v = 7$**

S. Bailleux, M. Bogey, C. Demuynck, Y. Liu and A. Walters

*J. Mol. Spectrosc.* **216**, 465 – 471 (2002)

**12. Van der Waals Bending Bands of the ArDCN Cluster Observed by Millimeter-Wave Spectroscopy Combined with a Pulsed Supersonic Jet Technique**

K. Tanaka, S. Bailleux, A. Mizoguchi, K. Harada, T. Baba, I. Ogawa and M. Shirasaka

*J. Chem. Phys.* **113**, 1524 (2000)

**During my PhD thesis**

---

**11.  $\text{H}_3\text{Si}^{37}\text{Cl}$  Revisited with High Resolution: The Ground State and the  $\nu_2 = 1$ ,  $\nu_3 = 1, 2$  and  $3$ ,  $\nu_5 = 1$  and  $2$ , and  $\nu_3 = \nu_6 = 1$  States**

H. Bürger, S. Bailleux, G. Graner, S. Bosc, and Y. Hennequin

*J. Mol. Spectrosc.* **196**, 296 (1999)

**10. Gas-phase Generation of Silicon Oxysulfide by Flash Vacuum Thermolysis**

V. Lefèvre, J. Levillain, J. L. Ripoll, S. Bailleux, M. Bogey and W. Wojnowski

*Phosphorus, Sulfur and Silicon & Relat. Elem.* **140**, 73 (1998)

**9. Sub-Millimeter Wave Spectroscopy of the  $\text{Ar}\cdot\text{H}_3^+$  and  $\text{Ar}\cdot\text{D}_3^+$  Ionic Complexes**

S. Bailleux, M. Bogey, H. Bolvin, S. Civiš, M. Cordonnier, A. F. Krupnov, M. Yu Tretyakov, A. Walters and L. H. Coudert

*J. Mol. Spectrosc.* **190**, 130 (1998)

**8. Submillimeter-Wave Spectral Lines of Negative Ions ( $\text{SH}^-$  and  $\text{SD}^-$ ) Identified by their Doppler Shift**

S. Civiš, A. Walters, M. Yu. Tretyakov, S. Bailleux, M. Bogey

*J. Chem. Phys.* **108**, 8369 (1998)

**7. The Rotational Spectrum of Isobutane up to 640 GHz**

D. Priem, J.M. Colmont, D. Petitprez and S. Bailleux

*J. Mol. Spectrosc.* **184**, 84 (1997)

6. **Ab-Initio Study and Millimeter-Wave Spectroscopy of P<sub>2</sub>O**  
 S. Bailleux, M. Bogey, C. Demuyneck, J.L. Destombes, Y. Liu and A.G. Császár  
*J. Chem. Phys.*, **107** (20), 8317 (1997)
5. **Millimeter-Wave Spectroscopy of Silene CH<sub>2</sub>=SiH<sub>2</sub>**  
 S. Bailleux, M. Bogey, H. Bolvin, R. Fajgar, Y. Liu, J. Pola and M. Senzlober  
*Proc. SPIE - Int. Soc. Opt. Eng.* **3090**, 158 (1997)
4. **The Equilibrium Structure of Silene H<sub>2</sub>C=SiH<sub>2</sub> from Millimeter-Wave Spectra and from Ab Initio Calculations**  
 S. Bailleux, M. Bogey, J. Demaison, H. Bürger, M. Senzlober, J. Breidung, W. Thiel, R. Fajgar, and J. Pola  
*J. Chem. Phys.* **106** (24), 10016 (1997)
3. **Silene H<sub>2</sub>C=SiH<sub>2</sub> : Millimeter-Wave Spectrum and Ab Initio Calculations**  
 S. Bailleux, M. Bogey, J. Breidung, H. Bürger, R. Fajgar, Y. Liu, J. Pola, M. Senzlober and W. Thiel  
*Angew. Chem., Int. Ed. Engl.* **35**, 2513 (1996)
2. **Microwave Measurements of J=2←1, K=0,1 Ammonia Transitions at 1.215 THz**  
 A.F. Krupnov, M. Yu. Tretyakov, M. Bogey, S. Bailleux, A. Walters, B. Delcroix, S. Civiš  
*J. Mol. Spectrosc.* **176**, 442 (1996)
1. **Millimeter-Wave Rotational Spectrum of H<sub>2</sub>SiO**  
 S. Bailleux, M. Bogey, C. Demuyneck, J.L. Destombes and A. Walters  
*J. Chem. Phys.* **101**, 2729 (1994)

# List of Communications

**31<sup>st</sup> International Symposium on Free Radicals: 24 – 29 July 2011, Port Douglas (Australia)**

51. Terahertz Spectroscopy of the Deuterated Methylene Radicals, CHD ( $X^3A''$ ) and CD<sub>2</sub> ( $X^3B_1$ )

**S. Bailleux**, H. Ozeki and G. Wlodarczak

50. High-Resolution Terahertz Spectroscopy of <sup>15</sup>NH and <sup>15</sup>NH<sub>2</sub> radicals. On the <sup>15</sup>N/<sup>14</sup>N Ratio Determination in the ISM with Herschel.

**S. Bailleux**, L. Margulès, G. Wlodarczak, O. Pirali, M.-A. Martin-Drumel, P. Roy, E. Roueff and M. Gerin

49. **66<sup>th</sup> International Symposium on Molecular Spectroscopy: 20 – 24 June 2011, Columbus (USA)**

<sup>15</sup>N/<sup>14</sup>N Ratio Determination in the ISM with Herschel from High Resolution Spectroscopy of Nitrogen Radicals

**L. Margulès**, S. Bailleux, G. Wlodarczak, O. Piralli, M.-A. Martin-Drumel, P. Roy, E. Roueff and M. Gerin

**The 21<sup>st</sup> International Conference on High Resolution Molecular Spectroscopy: 7 – 11 September 2010, Poznań (Poland)**

48. The Millimeter-wave Spectroscopy of H<sup>15</sup>NC, H<sup>15</sup>N<sup>13</sup>C, D<sup>15</sup>NC, D<sup>15</sup>N<sup>13</sup>C in their Ground Vibronic States

**P. Kania**, G. Wlodarczak, S. Bailleux

47. Rotational Spectrum and Nuclear Quadrupole Coupling Tensor of CH<sub>2</sub>ICl

**P. Kania**, **J. Štoviček**, **Š. Urban**, H. Ozeki and S. Bailleux

46. **Journées de la SF2A: 21 - 24 June 2010, Marseille (France)**

Preliminary work to ALMA, HERSCHEL, SOFIA: submillimeter wave spectroscopy of isotopic species of Methyl Formate

M. Goubet, L. Margulès, R. Motiyenko, S. Bailleux, T. Huet and G. Wlodarczak

**The 21<sup>st</sup> Colloquium on High-Resolution Molecular Spectroscopy: 31 August – 4 September 2009, Castellammare di Stabia (Italy)**

45. The Millimeter-Wave Spectroscopy of H<sup>15</sup>NC, H<sup>15</sup>N<sup>13</sup>C, D<sup>15</sup>NC, D<sup>15</sup>N<sup>13</sup>C in their ground vibronic states

**P. Kania**, G. Wlodarczak, and S. Bailleux

44. The Pure Rotational Spectrum of ICl: Rotational Parameters, Born-Oppenheimer Breakdown Corrections and Hyperfine Constants  
**P.Kania, J.Skřínský, S.Urban, H.Ozeki** and S.Bailleux, **Abstract/Poster N9.**
43. **30<sup>th</sup> International Symposium on Free Radicals** : 25 – 30 July 2009, Savonlinna (Finland)  
Fourier Transform Microwave and Millimeter-Wave Spectroscopy of the Iodomethyl Radical, CH<sub>2</sub>I ( $X^2B_1$ )  
**S. Bailleux**, H. Ozeki, T. Okabayashi, M. Tanimoto and **P. Kania**
- 20<sup>th</sup> International Conference on High Resolution Molecular Spectroscopy** : 2 – 6 September 2008, Prague (Czech Rep.)
42. Submillimeter-Wave Spectroscopy and Isotopically Invariant Analysis of Iodine Monochloride  
**P. Kania, J. Skřínský** and **S. Bailleux**
41. Detection in the Gas-Phase of the Monoiodomethyl Radical, CH<sub>2</sub>I, by Fourier Transform Microwave Spectroscopy Combined with Submillimeter-Wave Spectroscopy  
H. Ozeki, T. Okabayashi, M. Tanimoto, **J. Skřínský, P. Kania** and **S. Bailleux**
40. Rotational Transitions in the Interacting  $\nu_2$ ,  $\nu_3$ ,  $\nu_4$  and  $\nu_6$  Bands of Formaldehyde H<sub>2</sub><sup>12</sup>C<sup>16</sup>O in the Millimeter Range for Astrophysical Use  
**L. Margulès**, R. Janečková, S. Bailleux, **A. Perrin**, C. Endres, T. F. Giesen and S. Schlemmer
39. The Submillimeter-Wave Laboratory Spectrum of the CS<sup>+</sup> Radical Ion  
**S. Bailleux**, E. Grigorová, L. Margulès and A. Walters
38. Analysis of the Fourier Transform Infrared Spectrum of the  $\nu_4$  Band of the Fluoroformyloxyl Radical, FCO<sub>2</sub>, in the  $X^2B_2$  State  
**S. Bailleux**, **E. Grigorová, Z. Zelinger, H. Beckers** and H. Willner
37. **The Molecular Universe: an International Meeting on the Physics and Chemistry of the Interstellar Medium**: 5 – 8 May, 2008, Arcachon (France)  
The Submillimeter-Wave Laboratory Spectrum of the CS<sup>+</sup> Radical Ion  
S. Bailleux, **A. Walters**, E. Grigorová, and L. Margulès
- 19<sup>th</sup> International Conference on High Resolution Molecular Spectroscopy** : 29 August – 2 September 2006, Prague (Czech Rep.)
36. High Resolution Fourier Transform Spectroscopy of the FCO<sub>2</sub> Radical – First Analysis and Assignment of the  $\nu_4$  Band  
**Z. Zelinger, S. Bailleux, H. Beckers** and H. Willner

35. High Resolution Rotational Spectrum of the FCO<sub>2</sub> Radical; Extension to the Lower Frequency Region  
**Z. Zelinger**, **S. Bailleux**, L. Strítěská, P. Musil, P. Kania, S. Urban, H. **Beckers** and H. Willner
34. ***85<sup>th</sup> National Meeting of the Chemical Society of Japan***: 26 – 29 March 2005, Kanagawa (Japan)  
 Fourier Transform Microwave Spectroscopy of the CH<sub>2</sub>Br Radical  
**H. Ozeki**, T. Okabayashi, M. Tanimoto, S. Saito and S. Bailleux
33. ***19<sup>th</sup> Colloquium on High Resolution Molecular Spectroscopy***: 11 – 16 September 2005, Salamanca (Spain)  
 Fourier Transform Microwave Spectroscopy of the Bromomethyl Radical, CH<sub>2</sub>Br  
 H. Ozeki, T. Okabayashi, M. Tanimoto, S. Saito and **S. Bailleux**
- 18<sup>th</sup> International Conference on High Resolution Molecular Spectroscopy***: 8 – 12 September 2004, Prague (Czech Rep.)
32. First Observation of the Rotational Spectrum of the Bromomethyl Radical, CH<sub>2</sub>Br  
**S. Bailleux**, P. Dréan, M. Godon, **Z. Zelinger** and S. Civis
31. The Submillimeter-wave Spectrum of the Chloromethyl Radical  
**Z. Zelinger**, **S. Bailleux**, P. Dréan and M. Godon
- 18<sup>th</sup> Colloquium on High Resolution Molecular Spectroscopy***: 8 – 12 September 2003, Dijon (France)
30. Toward the Identification of the Submillimeter Wave Spectrum of the Bromomethyl Radical, CH<sub>2</sub>Br  
**S. Bailleux**, P. Dréan, C. Duan, M. Godon, M. Bogey and Z. Zelinger
29. Rotational Spectrum of Brominated Radicals produced by UV Photolysis  
 P. Dréan, C. Duan, H. Hassouna, A. Walters, M. Godon, M. Bogey and **S. Bailleux**
28. ***58<sup>th</sup> Ohio State University International Symposium on Molecular Spectroscopy***: 16 – 20 June 2003, Columbus (USA)  
 Rotational Spectrum of Brominated Radicals produced by UV Photolysis  
**P. Dréan**, C. Duan, M. Hassouna, A. Walters, M. Godon, M. Bogey and S. Bailleux
27. ***Pac Rim IV Conference*** (An International Conference on Advanced Ceramics and Glasses), 4 – 8 November 2001, Wailea, Maui, Hawaii (USA)  
 Recent Progress in Poling of Silica and Chalcogenide glasses  
**Y. Quiquempois**, G. Martinelli, H. Zeghlache, S. Bailleux, P. Niay

26. **Bragg Gratings, Photosensitivity and Poling in Glass Waveguides: 4 – 6 July**  
2001, Stresa (Italy)  
Influence of Sample thickness on the spatial distribution of the nonlinear susceptibility  $\chi_2$  induced in thermally poled silica glasses  
Y. Quiquempois, **G. Martinelli**, S. Bailleux, P. Bernage
25. **Journées Nationales d'Optique Guidée (JNOG 2000): 20 – 22 Novembre 2000,**  
*Toulouse (France)*  
Etude de l'influence des paramètres géométriques sur la répartition spatiale de la susceptibilité du second ordre induite par polarisation thermique dans des verres de silice  
**Y. Quiquempois**, G. Martinelli, S. Bailleux, P. Bernage
24. **5<sup>ème</sup> Colloque sur les sources Cohérentes et Incohérentes UV, VUV et X (UVX 2000): Applications et Développements Récents : 16 – 19 mai 2000, Porquerolles (France)**  
Etude comparée des photosensibilités des fibres optiques aux différents lasers UV. Application des lasers UV au "poling" des verres  
G. Martinelli, Y. Quiquempois, P. Bernage, **M. Douay**, **P. Niay**, **S. Bailleux**
23. **68<sup>ème</sup> Congrès de l'ACFAS. Session Optique Guidée et Photonique: 15 – 19 May 2000, Montréal (Canada)**  
Répartition spatiale de la non linéarité du second-ordre induite dans les verres SiO<sub>2</sub> et SiO<sub>2</sub>-GeO<sub>2</sub> par polarisation sous champ électrique  
P. Bernage, **Y. Quiquempois**, G. Martinelli, S. Bailleux, P. Niay, M. Douay
22. **54<sup>th</sup> International Symposium on Molecular Spectroscopy: 14 – 18 June 1999, Columbus (USA)**  
Observation of the van der Waals Bending Bands of the Ar-DCN Cluster by Millimetre-wave Spectroscopy in Supersonic Jet Expansion  
S. Bailleux, K. Harada, A. Mizoguchi and **K. Tanaka**
- 76<sup>th</sup> National Meeting of the Chemical Society of Japan: 28 – 30 March 1999, Yokohama (Japan)**
21. Millimeter-Wave Spectroscopy of the van der Waals Bending Vibration of Ar – HBr  
K. Harada, A. Mizoguchi, **S. Bailleux**, and K. Tanaka
20. Millimeter-Wave Spectroscopy of the van der Waals Bending Bands of Ar – DCN  
**S. Bailleux**, A. Mizoguchi, K. Harada and K. Tanaka
19. Millimeter-Wave Spectroscopy of the vdW Bending Mode ( $j=2-1$ ) of the Ar – HCN Complex  
A. Mizoguchi, **S. Bailleux**, K. Harada and K. Tanaka

18. **75<sup>th</sup> National Meeting of the Chemical Society of Japan: 16 – 19 September 1998, Matsuyama (Japan)**  
The Millimeter-Wave Spectrum of P<sub>2</sub>O in Vibrationally Excited States  
**S. Bailleux**, M. Bogey, C. Demuynck, Y. Liu and A. Császár
17. **15<sup>th</sup> International Conference on High Resolution Molecular Spectroscopy: 30 August – 03 Septembre 1998, Prague (Czech Rep.)**  
Fourier Transform Spectroscopy of H<sub>3</sub>Si<sup>37</sup>Cl : accurate constants for the ground state and for the  $\nu_2=1$ ,  $\nu_3=1-2$ ,  $\nu_5=1-2$  and  $\nu_6=1-2$  states  
**H. Bürger**, S. Bailleux, G. Graner, S. Bosc, and Y. Hennequin
16. **53<sup>rd</sup> Ohio State University International Symposium on Molecular Spectroscopy: 15 – 19 June 1998, Columbus (USA)**  
Submillimeter-Wave Spectroscopy of Negative Ions: SH<sup>-</sup> and SD<sup>-</sup>  
**S. Civiš**, M. Yu. Tretyakov, A. Walters, S. Bailleux and M. Bogey
15. **74<sup>th</sup> National Meeting of the Chemical Society of Japan: 27 – 30 March 1998, Kyoto (Japan)**  
The Equilibrium Structure of Silaethylene H<sub>2</sub>C=SiH<sub>2</sub>  
**S. Bailleux**, M. Bogey, H. Bürger, W. Thiel
- 15<sup>th</sup> Colloquium on High Resolution Molecular Spectroscopy: 7 – 11 Septembre 1997, Glasgow (Scotland)**
14. First Identified Submillimeter-Wave Spectral Lines of Negative Ions: SH<sup>-</sup> and SD<sup>-</sup>  
**S. Civiš**, S. Bailleux, M. Bogey, A. Walters and M. Yu Tretyakov.
13. Ab Initio Study and Millimeter-Wave Spectroscopy of P<sub>2</sub>O  
S. Bailleux, M. Bogey, **C. Demuynck**, **Y. Liu** and A.G. Császár.
- 14<sup>th</sup> International Conference on High Resolution Molecular Spectroscopy: 9 – 13 Septembre 1996, Prague (Czech Rep.)**
12. Oxidation of White Phosphorus : Millimeter-Wave Spectroscopy of Vibrationally Excited PO and Possible Detection of P<sub>2</sub>O  
**S. Bailleux**, M. Bogey, A.G. Császár, **C. Demuynck**, J.L. Destombes, N. Dujardin, Y. Liu
11. Detection of Silene CH<sub>2</sub>=SiH<sub>2</sub> in the Gas Phase by Millimeter-Wave Spectroscopy  
**S. Bailleux**, M. Bogey, J. Breidung, **H. Bürger**, R. Fajgar, Y. Liu, J. Pola, M. Senzlober and W. Thiel.
10. **XI<sup>th</sup> International Symposium on Organosilicon Chemistry: 1 – 5 Septembre 1996, Montpellier (France)**  
Millimeter-Wave Spectroscopy of Silene CH<sub>2</sub>=SiH<sub>2</sub>  
S. Bailleux, M. Bogey, **H. Bürger**, R. Fajgar, Y. Liu, J. Pola and **M. Senzlober**.

9. **12<sup>th</sup> International Symposium and School on High Resolution Molecular Spectroscopy: HighRus-96.** 1 – 5 July 1996, St Petersburg (Russia)  
Millimeter-Wave Spectroscopy of Silene CH<sub>2</sub>=SiH<sub>2</sub>  
S. Bailleux, **M. Bogey**, H. Bürger, R. Fajgar, Y. Liu, J. Pola and M. Senzlober.
8. **51<sup>st</sup> International Symposium on Molecular Spectroscopy:** 10 – 14 June 1996, Columbus (USA)  
Millimeter-Wave Spectrum of Silene: H<sub>2</sub>CSiH<sub>2</sub>  
S. Bailleux, M. Bogey, Y. Liu, **M. Cordonnier**, H. Bürger, M. Senzlober, R. Fajgar, J. Pola  
**Royal Society of Chemistry - Annual Meeting of the High Resolution Spectroscopy Group:** 17 – 19 December 1995, Reading University (UK)
7. Millimetre and Submillimetre-Wave Rotational Spectrum of Highly Vibrationally Excited PO  
**Y. Liu**, S. Bailleux, M. Bogey and C. Demuynck.
6. Submillimetre-Wave and Infrared Spectroscopy of P<sub>2</sub>O  
**Y. Liu**, S. Bailleux, M. Bogey, C. Demuynck, H.B. Qian and P.B. Davies.
5. **14<sup>e</sup> Colloque sur la Spectroscopie Moléculaire à Haute Résolution:** 11 – 15 Septembre 1995, Dijon (France)  
Structural Determination of H<sub>2</sub>SiO using Submillimeter-wave Rotational Spectroscopy  
S. Bailleux, **M. Bogey**, C. Demuynck, J.L. Destombes, B. Delcroix and A. Walters.
4. **XXIII<sup>rd</sup> International Symposium on Free Radicals:** 13 – 18 August 1995, Victoria (Canada)  
Determination of the Molecular Structure of H<sub>2</sub>SiO from its Millimeter-Wave Rotational Spectrum  
S. Bailleux, M. Bogey, B. Delcroix, **C. Demuynck**, J.L. Destombes and A. Walters.
3. **1<sup>ères</sup> Rencontres Franco-Britanniques sur la Physique et la Chimie du Milieu Interstellaire:** 10 – 12 July 1995, Lille (France)  
Recent Observations of Transient Species in the Laboratory: Carbon and Silicon Compounds  
**M. Bogey**, S. Bailleux, C. Demuynck, B. Delcroix, J.L. Destombes and A. Walters
2. **Royal Society of Chemistry - Annual Meeting of the High Resolution Spectroscopy Group:** 11 – 14 September 1994, Lille  
Millimetre-Wave Spectroscopy of Reactive Species in a Silane-Oxygene Plasma  
**A. Walters**, S. Bailleux, M. Bogey, B. Delcroix, J.L. Destombes and C. Demuynck
1. **Journées de Spectroscopie Moléculaire:** 18 – 19 July 1994, Albi (France)  
Molécules Réactives, Production par Décharge Electrique et Etude par Spectroscopie Millimétrique, Application à H<sub>2</sub>SiO  
S. Bailleux, M. Bogey, B. Delcroix et **A. Walters**

## Part 2

# Scientific Records

## INTRODUCTION

---

### 1.1 Motivation and scientific background

Transient species play a major role as intermediates in the chemistry of complex systems. Chemists already formulated their existence in the 19<sup>th</sup> century<sup>1</sup> to explain the obscure processes involved in chemical reactions. The discovery by Gomberg in 1900 of the first chemically stable intermediate,<sup>2</sup> the triphenyl-methyl radical,  $(\text{C}_6\text{H}_5)_3\text{-C}$ , established definitely their existence. During the course of the 20<sup>th</sup> century many others were discovered, in particular as numerous spectroscopic techniques appeared and developed, such as matrix isolation spectroscopy in 1954, free jet spectroscopy in the mid 1970's, laser magnetic resonance spectroscopy demonstrated by Evenson and his colleagues,<sup>3,4</sup> diode laser spectroscopy, microwave & (sub)millimetre-wave spectroscopy since 1946 with the

---

<sup>1</sup> G. Herzberg in: *The Spectra and Structure of Simple Free Radicals, an Introduction to Molecular Spectroscopy* (Cornell University Press, New-York, 1971).

<sup>2</sup> M. Gomberg, *J. Am. Chem. Soc.* **22**, p.757 (1900); M. Gomberg, *Chem. Rev.* **1**, 91 (1924).

<sup>3</sup> K. M. Evenson, H. P. Broida, J. S. Wells, R. J. Mahler and M. Mizushima, *Phys. Rev. Lett.* **21**, 1038 (1968)

<sup>4</sup> P. B. Davies, *J. Phys. Chem.* **85**, 2599 (1981).

advent of microwave oscillators, cavity ring down spectroscopy introduced in 1988, to cite but a few of them. The identification and characterization of reaction intermediates (radicals, ions or neutral molecules) are consequently indispensable to deeply understanding the reaction mechanisms occurring in a wide range of reactive and complex chemical environments. These include the Earth and non-terrestrial planetary atmospheres, combustion engines, atmospheric pollution, the interstellar medium and circumstellar shells, plasma etching of semiconductors in integrated circuits manufacturing<sup>5,6,7</sup> and optoelectronics. High-resolution spectroscopy has also been successfully used as non-intrusive diagnostics of silane<sup>8,9,10</sup> and methane plasma...<sup>10</sup>

Although the spectroscopic studies of transient species are complementary to those of stable molecules, the number of experimental data of the formers is still relatively scarce. Indeed, given their chemical reactivity, with typical lifetime scale in earth environments and in laboratory conditions ranging from microseconds for ions up to hundreds of milliseconds for the longest lived transients, the experimental investigations of reactive species have always been much more challenging<sup>11</sup> than compared with stable molecules. The experimentalist frequently has to face numerous difficulties to characterize elusive species due to the complexity of their preparation and their highly reactive nature. Their detection requires in

---

<sup>5</sup> R. J. Shul, S. J. Pearton in: *Handbook of Advanced Plasma Processing Techniques* (Springer, Berlin, 2000).

<sup>6</sup> Ç. Pak, L. Sari, J. C. Rienstra-Kiracofe, S. S. Wesolowski, L. Horný, Y. Yamaguchi and H. F. Schaefer III, *J. Chem. Phys.* **118**, 7256 (2003).

<sup>7</sup> Ç. Pak, J. C. Rienstra-Kiracofe and H. F. Schaefer III, *J. Phys. Chem. A* **104**, 11232 (2000).

<sup>8</sup> W. G. Breiland, B. S. Coltrin and P. Ho, *J. Chem. Phys.* **59**, 3267 (1986).

<sup>9</sup> J. M. Jasinski, B. S. Meyerson and B. A. Scott, *Ann. Rev. Phys. Chem.* **38**, 109 (1987).

<sup>10</sup> E. Hirota, *Pure & App. Chem.* **70**, 1145 (1998).

<sup>11</sup> A. M. Bass and H. P. Broida in: *Formation and Trapping of Free Radicals* (Academic Press, New York, 1960).

addition *sensitive* and *selective* techniques. High-resolution spectroscopy appears to be a technic well suited for that purpose since unambiguous identification of molecular species can be made through the analysis of their spectral signatures. From the theoretical point of view, even high-level quantum calculations still face difficulties in computing accurately the geometry of unstable species. For instance, non-classical structures and novel bonding in silicon-containing molecules have been reported, such as in the monobridged<sup>12</sup> and dibridged disilyne,<sup>13</sup> Si<sub>2</sub>H<sub>2</sub>, the formal all-silicon analogues of acetylene. The study of reactive molecules is intrinsically of high relevance to the spectroscopist, theoretician or experimentalist, for structural and bonding properties comparison between experiments and theory and between chemical elements of the same group. Yet quantum chemistry is an invaluable tool to the experimentalist to aid the spectroscopic identification of a new molecular species. The opposite holds as well, thus showing the necessity of close relations between experiment and theory.

Among the transient species, many belong to the category of free radicals, most often labile molecules (in typical terrestrial conditions) characterized by the presence at least of one unpaired electron, resulting in the ubiquitous occurrence of multiple low-lying electronic states in these complex systems. Free radicals are most frequently generated with the use of non-selective techniques such as in discharge and their reactions are characterised by the bright emission of visible light of many colours.<sup>14,15</sup> By virtue

---

<sup>12</sup> M. Cordonnier, M. Bogey, C. Demuyneck and J.-L. Destombes, *J. Chem. Phys.* **97**, 7984 (1994).

<sup>13</sup> M. Bogey, H. Bolvin C. Demuyneck and J.-L. Destombes, *Phys. Rev. Lett.* **66**, 413 (1991).

<sup>14</sup> A. M. Brass and H. P. Broida, *J. Res. Nat. Bur. Stand., Sect. A* **67A**, 379 (1963).

<sup>15</sup> E. E. Ferguson, F. C. Fehsenfeld and A. M. Schmeltekopf in: *Advances in Atomic and Molecular Physics*, Vol. 5 (Academic Press, New-York, London, 1969).

of the presence of unpaired electron(s), isolated radicals have many other unique properties that can be unravelled by high-resolution spectroscopy. The presence of electrons with unpaired spins in a molecule leads to the existence of magnetic interactions, not only within the molecule but with applied external fields as well, resulting in complications in its high-resolution spectra, the so-called fine- and hyperfine-structures. Amongst the other spectroscopic techniques, the advantage of microwave spectroscopy, in its broad sense (*i.e.* encompassing centimetre- and millimetre-wave radiations up to the THz range), is that many of these interactions are revealed even though their magnitude are often small.<sup>16</sup> The successful analysis of the fine and hyperfine structures yield to the determination of corresponding constants whose interpretation provide remarkable insights on the electronic and molecular structure.

More precisely, the interpretation of the fine- and hyperfine-structures implies the understanding how angular momenta couple with each other and with the end-over-end molecular rotation to produce the energy levels studied. The angular momenta involved in these couplings are the total electron spin angular momentum  $\mathbf{S}$ , the electronic orbital angular momentum  $\mathbf{L}$  (in diatomic and linear polyatomic molecules only, for which the projection of  $\mathbf{L}$  along the molecular axis is usually well defined), the nuclear spin angular momentum  $\mathbf{I}$  and the rotational angular momentum of the nuclei  $\mathbf{R}$ . The pairwise interactions can be summarized in Figure 1.1. It can be seen that three types of direct couplings may be encountered in analysing the fine-structure of a particular high-resolution molecular spectrum: the spin-orbit, the spin-rotation and the spin-spin interactions. As long as the orbital angular momentum is not quenched such as

---

<sup>16</sup> A. Carrington in: *Microwave Spectroscopy of Free Radicals* (Academic Press, London, New York, 1974).

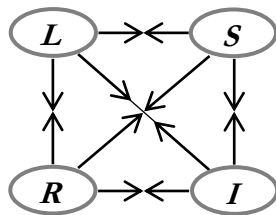


**Figure 1.1** Pairwise interactions of  $\mathbf{R}$ ,  $\mathbf{L}$ ,  $\mathbf{S}$  and  $\mathbf{I}$  (from Ref. 16).

in linear molecules, the spin-orbit coupling is the dominant one and the expression for the corresponding effective Hamiltonian may be written as:<sup>17</sup>

$$\mathbf{H}_{\text{SO}} = A_{\text{SO}} \mathbf{L} \cdot \mathbf{S} \quad (\text{Equation 1.1})$$

where  $A_{\text{SO}}$  denotes the spin-orbit coupling constant.

The next interaction represents the electron spin-rotation coupling which is the most important one in non-linear molecules. After combining  $\mathbf{L}$  and  $\mathbf{R}$  to form the total orbital angular momentum  $\mathbf{N}$ , the effective spin-rotation Hamiltonian takes the form:<sup>18,19</sup>

$$\mathbf{H}_{\text{SR}} = \frac{1}{2} \sum_{\alpha, \beta} \varepsilon_{\alpha\beta} (\mathbf{N}_{\alpha} \mathbf{S}_{\beta} + \mathbf{S}_{\beta} \mathbf{N}_{\alpha}) \quad (\text{Equation 1.2})$$

for asymmetric rotors ( $\alpha$  and  $\beta$  run independently over the  $x, y, z$  molecule-fixed coordinates). The parameters  $\varepsilon_{\alpha\beta}$  are the components of the electron spin-rotation tensor  $\boldsymbol{\varepsilon}$ . For linear molecules,  $\mathbf{N}$  is perpendicular to the molecular axis and the above expression simplifies<sup>20</sup> to give:

$$\mathbf{H}_{\text{SR}} = \gamma \mathbf{N} \cdot \mathbf{S} \quad (\text{Equation 1.3}).$$

<sup>17</sup> E. Hirota in: *High-Resolution Spectroscopy of Transient Molecules* (Springer-Verlag, Berlin, Heidelberg, New York, Tokyo, 1985).

<sup>18</sup> J. H. Van Vleck, *Rev. Mod. Phys.* **23**, 213 (1951).

<sup>19</sup> J. M. Brown and T. J. Sears, *J. Mol. Spectrosc.* **75**, 111 (1979).

<sup>20</sup> J. M. Brown and J. K. G. Watson, *J. Mol. Spectrosc.* **65**, 65 (1977).

It is well recognised that the dominant contributions to the spin-rotation parameters,  $\varepsilon_{\alpha\beta}$  and  $\gamma$ , arise from the second order mixing of electronic states by spin-orbit and Coriolis coupling.<sup>21</sup>

The last contribution, the spin-spin interaction, occurs only in free radicals involving two or more unpaired electrons (*i.e.* with  $S \geq 1$ ). The corresponding effective Hamiltonian may be cast into the form:<sup>22</sup>

$$\mathbf{H}_{SS} = \alpha_0 (3S_z^2 - S^2) + \beta_0 (S_x^2 - S_y^2) \quad (\text{Equation 1.4}).$$

In this case, it has been known that the second order contribution of the spin-orbit interaction has also to be taken into account for the interpretation of the spin-spin interaction constants  $\alpha_0$  and  $\beta_0$ .<sup>23</sup>

A nucleus which possesses non-zero nuclear spin angular momentum  $\mathbf{I}$  may interact with the electrons in a molecule through magnetic and/or electrostatic couplings giving rise to hyperfine structure. The nuclear magnetic moment associated to  $\mathbf{I}$  is proportional to the nuclear spin:

$$\boldsymbol{\mu}_I = g_I \mu_N \mathbf{I} \quad (\text{Equation 1.5}),$$

where  $g_I$  is the dimensionless  $g$  factor (also called the gyromagnetic ratio) of the nucleus involved in the interaction and  $\mu_N$  is the nuclear magneton. The magnetic couplings make important contribution in open-shell species and are caused by the dipolar interactions of the nuclear magnetic moment  $\boldsymbol{\mu}_I$  with the orbital electronic magnetic moment  $\boldsymbol{\mu}_L (=g_L \mu_B \mathbf{L})$  and/or with the electron spin magnetic moment  $\boldsymbol{\mu}_S (=g_e \mu_B \mathbf{S})$ , where  $\mu_B$  designate the Bohr magneton ( $\mu_B = e\hbar/2m_e c$ ),  $g_e \approx 2.0023$  (free electron

---

<sup>21</sup> R.F. Curl, *J. Chem. Phys.* **37**, 779 (1962); R.F. Curl, *Mol. Phys.* **9**, 585 (1965).

<sup>22</sup> W. T. Raynes, *J. Chem. Phys.* **41**, 3020 (1964).

<sup>23</sup> K. Kayama and J. C. Baird, *J. Chem. Phys.* **46**, 2604 (1967).

spin  $g$  factor) and  $g_L \simeq 1$  (orbital  $g$  factor). The first type of magnetic interaction dominates in linear radicals where there is a net orbital angular momentum and the effective Hamiltonian can be written as:

$$\mathbf{H}_{IL} = a \mathbf{I} \cdot \mathbf{L} \quad (\text{Equation 1.6}).$$

The second type of magnetic interaction involves the electron spin magnetic moment. The corresponding Hamiltonian contains two terms, one isotropic contribution:

$$\mathbf{H}_F = a_F \mathbf{I} \cdot \mathbf{S} \quad (\text{Equation 1.7}),$$

and one anisotropic contribution (nuclear – electron spin dipole-dipole coupling) well represented in an effective Hamiltonian of the form:

$$\mathbf{H}_{DD} = \mathbf{S} \cdot \mathbf{T} \cdot \mathbf{I} \quad (\text{Equation 1.8}),$$

where  $\mathbf{T}$  is a second-rank traceless tensor with five independent components in the most general case and  $a_F$  denotes the so-called Fermi contact term. This term was first introduced by Fermi to account for splittings observed in atomic spectra and requires that the unpaired electron has a non-zero spin density  $\psi^2(0)$  with an  $s$  character at the center of the nucleus with which it interacts, *i.e.* the unpaired electron must partially occupy an atomic  $s$  orbital. Its expression derived from quantum mechanics is given by:<sup>24</sup>

$$a_F = \frac{16\pi}{3} \frac{\mu_B \mu_I}{I} \psi^2(0) \quad (\text{Equation 1.9}).$$

In addition to the above-mentioned magnetic interactions, the nuclear quadrupole moment interacting with the electric field gradient produced by surrounding electronic charge distribution contributes to hyperfine structure in any molecule (radicals and close-shells) with  $I \geq 1$ . Indeed,  $2^{2I}$

---

<sup>24</sup> C. H. Townes and A. L. Schawlow in: *Microwave Spectroscopy* (Dover, New York, 1975).

is the highest pole order that can exist in a nucleus with spin  $I$ ,<sup>24</sup> but when they exist, higher order poles can be neglected. Furthermore, two other nuclear spin interactions can be observed, namely the nuclear spin-rotation interaction that correlates with the electron spin-rotation interaction and the spin-spin interaction between two nuclei. Both are usually small in magnitude compared with the previously described couplings and the latter one can rarely be detected, except maybe in  $\Sigma$  molecules<sup>24</sup>. The interactions described so far involved mainly one nucleus with spin  $I$  (Figure 1.1) and the situation becomes naturally more complicated if two or more nuclear spins have to be taken into account in the observed high-resolution spectra.

It should be noted that the interpretation of the coupling parameters associated with the *effective* Hamiltonians (both their magnitude and sign) to unravel intramolecular properties is clearly feasible, although not always trivial, since indirect couplings (second-order contributions) that involve mixing (admixture) of excited electronic states with the ground electronic state can occur, sometimes predominantly, even in close-shell molecules.<sup>16</sup> Care should accordingly be taken for the correct interpretation of the interaction constants. Accurate information in terms of electronic properties can nevertheless be obtained from the interpretation of the molecular constants related to the fine- and hyperfine-<sup>25</sup> structure. These include bonding properties (ionic character of a covalent bond), electron distribution within the molecule (spin density with  $s$  and  $p$  character), estimates of the energy levels of the lowest excited electronic states and the molecular structure.

---

<sup>25</sup> J. A. J. Fitzpatrick, F. R. Manby and C. Western, *J. Chem. Phys.* **122**, 084312 (2005) and references therein.

Since my PhD work on the characterisation by millimetre-wave spectroscopy of the unstable close-shells  $\text{H}_2\text{CSiH}_2$  and  $\text{P}_2\text{O}$  defended in 1997, with the exception of the analysis of the  $\nu_4$  vibration-rotation band of the  $\text{FCO}_2$  radical obtained by Fourier transform infrared spectroscopy, my investigations are devoted to a major extent to newly identified reactive molecules by millimetre-wave spectroscopy, a technique which is inherently high in resolution. Namely, they encompass the radicals PO, the halomethyls  $\text{CH}_2\text{X}$  ( $\text{X}=\text{Br}, \text{I}$ ), the molecular ion  $\text{CS}^+$ , CHD, the  $^{15}\text{N}$ -substituted radicals NH and  $\text{NH}_2$  in addition to the isotopologues of the  $\text{H}^{15}\text{NC}$  unstable, close-shell. The rotational spectra of the stable interhalogen species ICl and  $\text{CH}_2\text{ICl}$  have also been greatly extended, including in vibrational excited states in the case of ICl. All these species possess unpaired electron(s) and/or nuclear spin(s), and emphasis in this dissertation thesis is therefore given to their fine and/or hyperfine structures. More precisely, my contribution mostly deals with the characterization of radicals and other transient species. All the species studied are relevant either to atmospheric chemistry and/or to astrochemistry, and the laboratory detection, identification and characterization of transient and stable species in the gas-phase through the observation of their rotational or rovibrational spectra may help to confirm or invalidate chemical models of the environments inside which they are supposed to play important and unique roles. Halogen-containing species are known to participate in catalytic chain reactions perturbing tropospheric ozone levels, and they are presented in chap. 2. The second potential application developed in chap. 3 is the interstellar medium and circumstellar shells. As of December 2010, about a hundred and sixty molecular species have been identified in these complex environments. To a large extent, they have been identified by rotational spectroscopy and are presented in Ta-

ble 1.1.<sup>26</sup> It is interesting to point out that the very first molecular species to be conclusively detected outside Earth (in comets and interstellar medium) *via* one electronic transition was the methylidyne radical ( $\text{CH}$ ,  $X^2\Pi$ ).<sup>27</sup> The methylidyne ion ( $\text{CH}^+$ ,  $X^1\Sigma$ ) is one of the first molecules and the first ion to be found in space.<sup>28</sup> In the interstellar medium or in circumstellar envelopes, radicals and ionic species amount to twenty-five and fifteen percent, respectively. Overall, about fifty percent of the species identified in these environments are transient species under typical laboratory conditions. As a final comment, the linear isomer of propadienylidene ( $\text{C}_3\text{H}_2$ ) has been very recently (12/2010) proposed by J. P. Maier as a diffuse interstellar band (DIB) carrier,<sup>29</sup> a long-standing puzzle in spectroscopy and astronomy.<sup>30</sup> Although his group presents evidence of this discovery from two broad electronic band absorptions of  $\text{C}_3\text{H}_2$  at 4881 and 5450 Å that strongly correlate with DIBs, Oka and McCall remain skeptical.<sup>31</sup>

## 1.2 Characterizing reactive species by millimetre-wave spectroscopy

### 1.2.a Specificities, difficulties and...

Beside the difficulties encountered in analysing the spectrum of radicals arising from the numerous interactions described in the previous section, there are a wealth of challenges to overcome that are common among transient species (radicals, ions, and neutrals). The point of view adopted

---

<sup>26</sup> Compilation taken from the Cologne Database Molecular Spectroscopy: <http://www.astro.uni-koeln.de/cdms/molecules>

<sup>27</sup> P. Swings and L. Rosenfeld, *Astrophys. J.* **86**, 483 (1937).

<sup>28</sup> A. E. Douglas and G. Herzberg, *Astrophys. J.* **94**, 381 (1941).

<sup>29</sup> J. P. Maier, G. A. H. Walker, D. A. Bohlender, F. J. Mazzotti, R. Raghunandan, J. Fulara, I. Garkusha and A. Nagy, *Astrophys. J.* **726**:41 (2011).

<sup>30</sup> M. L. Heger, *Lick Obs. Bull.* **326** (1919).

<sup>31</sup> T. Oka and B. J. McCall, *Science* **331**, 293 (2011).

**Table 1.1** Molecules in the Interstellar Medium or Circumstellar Shells (as of 12/2010), ranked by number of atoms

2	3	4	5	6	7	8	9	10	11
H <sub>2</sub>	C <sub>3</sub>	<b>c-C<sub>3</sub>H</b>	C <sub>5</sub>	<b>C<sub>5</sub>H</b>	<b>C<sub>6</sub>H</b>	CH <sub>3</sub> C <sub>3</sub> N	CH <sub>3</sub> C <sub>4</sub> H	CH <sub>3</sub> C <sub>5</sub> N	HC <sub>9</sub> N
AlF	<b>C<sub>2</sub>H</b>	<b>/-C<sub>3</sub>H</b>	<b>C<sub>4</sub>H</b>	<b>/-H<sub>2</sub>C<sub>4</sub></b>	CH <sub>2</sub> CHCN	HC(O)OCH <sub>3</sub>	CH <sub>3</sub> CH <sub>2</sub> CN	(CH <sub>3</sub> ) <sub>2</sub> CO	CH <sub>3</sub> C <sub>6</sub> H
AlCl	C <sub>2</sub> O	<b>C<sub>3</sub>N</b>	C <sub>4</sub> Si	C <sub>2</sub> H <sub>4</sub>	CH <sub>3</sub> C <sub>2</sub> H	CH <sub>3</sub> COOH	(CH <sub>3</sub> ) <sub>2</sub> O	(CH <sub>2</sub> OH) <sub>2</sub>	C <sub>2</sub> H <sub>5</sub> OCHO
C <sub>2</sub>	C <sub>2</sub> S	C <sub>3</sub> O	<b>/-C<sub>3</sub>H<sub>2</sub></b>	CH <sub>3</sub> CN	HC <sub>5</sub> N	<b>C<sub>7</sub>H</b>	CH <sub>3</sub> CH <sub>2</sub> OH	CH <sub>3</sub> CH <sub>2</sub> CHO	
<b>CH</b>	C <sub>3</sub> S	C <sub>3</sub> S	<b>c-C<sub>3</sub>H<sub>2</sub></b>	CH <sub>3</sub> NC	CH <sub>3</sub> CHO	H <sub>2</sub> C <sub>6</sub>	HC <sub>7</sub> N		
<b>CH<sup>+</sup></b>	HCN	C <sub>2</sub> H <sub>2</sub>	<b>H<sub>2</sub>CCN</b>	CH <sub>3</sub> OH	CH <sub>3</sub> NH <sub>2</sub>	CH <sub>2</sub> OHCHO	<b>C<sub>8</sub>H</b>		<b>12</b>
<b>CN</b>	<b>HCO</b>	NH <sub>3</sub>	CH <sub>4</sub>	CH <sub>3</sub> SH	c-C <sub>2</sub> H <sub>4</sub> O	<b>/-HC<sub>6</sub>H</b>	CH <sub>3</sub> C(O)NH <sub>2</sub>		C <sub>6</sub> H <sub>6</sub>
CO	<b>HCO<sup>+</sup></b>	<b>HCCN</b>	HC <sub>3</sub> N	<b>HC<sub>3</sub>NH<sup>+</sup></b>	H <sub>2</sub> CCHOH	CH <sub>2</sub> CHCHO (?)	<b>C<sub>8</sub>H<sup>-</sup></b>		C <sub>2</sub> H <sub>5</sub> OCH <sub>3</sub> ?
<b>CO<sup>+</sup></b>	HCS <sup>+</sup>	<b>HCNH<sup>+</sup></b>	HC <sub>2</sub> NC	HC <sub>2</sub> CHO	<b>C<sub>6</sub>H<sup>-</sup></b>	CH <sub>2</sub> CCHCN	C <sub>3</sub> H <sub>6</sub>		<i>n</i> -C <sub>3</sub> H <sub>7</sub> CN
<b>CP</b>	<b>HOC<sup>+</sup></b>	HNCO	HCOOH	NH <sub>2</sub> CHO		H <sub>2</sub> NCH <sub>2</sub> CN			
<b>SiC</b>	H <sub>2</sub> O	HNCS	H <sub>2</sub> CNH	<b>C<sub>5</sub>N</b>					
HCl	H <sub>2</sub> S	<b>HOCO<sup>+</sup></b>	H <sub>2</sub> C <sub>2</sub> O	<b>/-HC<sub>4</sub>H</b>					<b>Above 12</b>
KCl	HNC	H <sub>2</sub> CO	H <sub>2</sub> NCN	<b>/-HC<sub>4</sub>N</b>					HC <sub>11</sub> N
<b>NH</b>	HNO	H <sub>2</sub> CN	HNC <sub>3</sub>	c-H <sub>2</sub> C <sub>3</sub> O					C <sub>60</sub>
<b>NO</b>	MgCN	H <sub>2</sub> CS	SiH <sub>4</sub>	H <sub>2</sub> CCNH (?)					C <sub>70</sub>
NS	MgNC	<b>H<sub>3</sub>O<sup>+</sup></b>	<b>H<sub>2</sub>COH<sup>+</sup></b>	<b>C<sub>5</sub>N<sup>-</sup></b>					
NaCl	<b>N<sub>2</sub>H<sup>+</sup></b>	c-SiC <sub>3</sub>	<b>C<sub>4</sub>H<sup>-</sup></b>						

<b>OH</b>	N <sub>2</sub> O	<b>CH<sub>3</sub></b>	HC(O)CN
PN	NaCN	<b>C<sub>3</sub>N<sup>-</sup></b>	
<b>SO</b>	OCS	PH <sub>3</sub> ?	
<b>SO<sup>+</sup></b>	SO <sub>2</sub>	HCNO	
<b>SIN</b>	c-SiC <sub>2</sub>	HOCN	
SIO	CO <sub>2</sub>	HSCN	
SIS	<b>NH<sub>2</sub></b>		
CS	<b>H<sub>3</sub><sup>+</sup></b>		
HF	<b>H<sub>2</sub>D<sup>+</sup>, HD<sub>2</sub><sup>+</sup></b>		
HD	<b>SiCN</b>		
FeO ?	AlNC		
<b>O<sub>2</sub></b>	<b>SINC</b>		
<b>CF<sup>+</sup></b>	HCP		
<b>SiH ?</b>	<b>CCP</b>		
<b>PO</b>	AlOH		
<b>AlO</b>	<b>H<sub>2</sub>O<sup>+</sup></b>		
<b>OH<sup>+</sup></b>	H <sub>2</sub> Cl <sup>+</sup>		
CN <sup>-</sup>			
<b>SH<sup>+</sup></b>			

Molecules with a question mark (?) are tentative detections. Those in bold, green font are radicals with at least one unpaired electron and those boxed in blue are molecular ions.

in this section is that of the experimentalist I am, and that of a theoretician I am not. Indeed, difficulties in the quantum chemical treatment of molecular properties of transient species still remain, such as in the computation of their accurate equilibrium geometry which is often vital to aid and confirm the spectroscopic identification of new species. This is particularly true for, but not limited to, open-shell species for which complications arise from the favourable coupling of low-lying electronic states induced for instance by vibration.<sup>32,33</sup> This is illustrated in chapt. 2, section 2.2 where the analysis of the  $\nu_4$  band of FCO<sub>2</sub> is presented.

By virtue of their short lifetimes, the main issue the experimentalist has to face is to *continuously* generate *in situ* chemically reactive (but thermodynamically stable) molecules in the highest possible number density to allow their detection in the gas-phase. The number density representative of transient species in an absorption cell of a millimetre-wave spectrometer ranges from 1ppm to a few percents<sup>17</sup>. High sensitivity (often limited by the stationary waves and noise of the millimetre-wave source) combined with efficient production methods are therefore indispensable for the spectroscopic investigation of labile species. Unless the transient molecule under investigation has previously been characterized by other spectroscopic techniques, the chemistry that enables its production is not known. In this case, the experimentalist might be forced to test several precursors (which may not be commercially available) and/or bond breaking techniques (such as dc discharge and photolysis). In addition the spectroscopic search requires the knowledge of important molecular parameters such as the rotational and centrifugal distortion constants, and the fine-structure coupling parameters if it is an open-shell. This

---

<sup>32</sup> J. F. Stanton and J. Gauss, *J. Chem. Phys.* **101**, 8938 (1994).

<sup>33</sup> R. G. Pearson in: *Symmetry Rules for Chemical Reactions* (Wiley, New York, 1976).

knowledge can be based either on high-level quantum calculations or on previous characterization from other spectral ranges. At the initial stage of the investigation the experimental conditions chosen, such as the partial pressures and the temperature of the gas mixture, can be far from best or even good. As a consequence, wide spectral range (several GHz) must be scanned while maintaining steady state conditions (such as the partial pressures and the temperature of the gas mixture...). In many cases, the inaccurate knowledge of the molecular parameters dictates repeating this procedure after tuning the conditions, until several candidate lines (*i.e.* transitions that match the prediction) are found. When introducing the precursors to the absorption cell, certain care must often be taken for several reasons: spontaneous reaction between them can occur and if required they should be introduced separately. It is also frequently necessary to cool the gas mixture by flowing liquid nitrogen through the outer jacket of a double-jacketed absorption cell. The main effects of the cooling consist in slowing the kinetics leading to the destruction of the reactive molecules and in increasing the population of lower energy levels. Even at low pressure (10 mTorr is representative of the total pressure maintained in the absorption cell of a millimetre-wave spectrometer), the reactants can rapidly be trapped to the liquid or solid phase onto the inner wall of the cell. The experimentalist should then conceive suitable means to circumvent phase condensation.

Furthermore, the production of short-lived molecules implies the cleavage of chemical bonds from one or more suitable precursors by means of techniques that are most often non-selective, such as electric discharges. As a result, it is often unavoidable to produce a number of undesirable and quite often unknown byproducts, short- or long-lived, that may recombine. They are likely to interfere in the spectrum, so do likewise the

reactants left intact in the reaction used to generate the desired molecule. This situation is rather frequently encountered and leads to the detection of spectrally dense “grass” of close-lying lines and this is also where high-resolution comes into play. The experimentalist is subsequently obliged to carry out various tests that consist in analyzing the measured spectra by setting the spectrometer to the frequency of the observed lines. These tests include for instance lifetime measurements. When possible, on/off modulation of the production of the labile species is carried out and the fundamental rate parameter (the lifetime) is determined by way of time-resolved analysis of the transient absorption signals. This invaluable technique has been successfully applied in the PhLAM laboratory to characterizing the millimetre-wave spectrum of  $\text{H}_2\text{SiO}$ , the silicon-analogue to formaldehyde.<sup>34</sup> Many other transitions belonging to at least two reactive molecules remain as yet unidentified in this experiment. Similarly, it was demonstrated about a decade ago that the analysis of the Doppler shifts, a standard technique used in infrared laser spectroscopy of ions developed in 1983,<sup>35</sup> could also be performed in the millimetre-wave region with the first identification in this frequency range of a negative ion,<sup>36</sup>  $\text{SH}^-$ . Recently Cazzoli and Puzzarini<sup>37</sup> have reported the second molecular anion observed by millimetre-wave spectroscopy,  $\text{OD}^-$ . Soon after, the Harvard-Smithsonian group reported a wealth of astrophysically important linear carbo-anions:  $\text{CN}^-$ ,<sup>38</sup>  $\text{C}_3\text{N}^-$ ,<sup>39</sup>  $\text{C}_{2n}\text{H}^-$ ,<sup>40</sup> with  $n = \{1 - 4\}$  de-

---

<sup>34</sup> S. Bailleux, M. Bogey, C. Demuynck, J. L. Destombes and A. Walters, *J. Chem. Phys.* **101**, 2729 (1994).

<sup>35</sup> C. S. Gudeman, M. H. Begemann, J. Plaff and R. J. Saykally, *Phys. Rev. Lett.* **50**, 727 (1983).

<sup>36</sup> S. Civiš, A. Walters, M. Yu Tretyakov, S. Bailleux and M. Bogey, *J. Chem. Phys.* **108**, 8369 (1998).

<sup>37</sup> G. Cazzoli and C. Puzzarini, *J. Chem. Phys.* **123**, 041101 (2005).

<sup>38</sup> C. A. Gottlieb, S. Brünken, M. C. McCarthy and P. Thaddeus, *J. Chem. Phys.* **126**, 191101 (2007).

<sup>39</sup> P. Thaddeus, C. A. Gottlieb, H. Gupta, S. Brünken, M. C. McCarthy, M. Agúndez, M. Guélin and J. Cernicharo, *Astrophys. J.* **677**, 1132 (2008).

tected by Fourier transform microwave and millimetre-wave spectroscopy. Amano subsequently extended the measurement of these anions up to 830 GHz using a new ion source, namely the *hollow anode* discharge.<sup>41</sup>

The above mentioned tests can also be complemented by inspection of the Zeeman effect on observed lines. Free radicals exhibit large Zeeman effect associated with their electronic angular momentum  $\mathbf{S}$  and  $\mathbf{L}$  and therefore belong to the class of *paramagnetic* species.<sup>17</sup> But the observation of a Zeeman effect, although usually characteristic of free radicals, are not specific to molecules with unpaired electrons. Indeed, in the presence of an external magnetic field, a similar effect may also appear in *diamagnetic* species whose ground electronic state is of  $^1\Sigma$  symmetry and hence have no electronic angular momentum. For such systems, the magnetic moment arises from the rotational angular momentum of the nuclei and as a consequence the magnetic moment is expected to be quite small in comparison with those found in free radicals possessing one or more unpaired electrons.<sup>16</sup> A few studies have reported a Zeeman effect in  $^1\Sigma$  molecular ions, namely in  $\text{ArH}^+$ ,<sup>42</sup> and very recently in  $\text{CH}^+$ .<sup>43</sup> The origin of the magnetic moment of close shell molecules is found to primarily arise from an admixture, induced by rotation, of paramagnetic excited electronic states with angular momentum  $\mathbf{L}$  and/or  $\mathbf{S}$  into the ground electronic state.<sup>17,44</sup>

---

<sup>40</sup> M. C. McCarthy, C. A. Gottlieb, H. Gupta, and P. Thaddeus, *Astrophys. J.* **652**, L141 (2006); S. Brünken, C. A. Gottlieb, H. Gupta, M. C. McCarthy and P. Thaddeus, *Astron. Astrophys.* **464**, L33 (2007); H. Gupta, S. Brünken, F. Tamassia, C. A. Gottlieb, M. C. McCarthy and P. Thaddeus, *Astrophys. J.* **655**, L57 (2007).

<sup>41</sup> T. Amano, *J. Chem. Phys.* **129**, 244305 (2008).

<sup>42</sup> K. B. Laughlin, G. A. Blake, R. C. Cohen, D. C. Hovde and R. J. Saykally, *Phys. Rev. Lett.* **46**, 2604 (1987).

<sup>43</sup> T. Amano, *J. Chem. Phys.* **133**, 244305 (2010).

<sup>44</sup> W. Gordy and R. L. Cook in: *Microwave Molecular Spectra* (Wiley-Interscience, New-York, 3<sup>rd</sup> Edition, 1984).

Other chemical tests rely on the analysis of the atomic elements contained in the species in order both to distinguish transitions belonging to the sought after species from other unwanted molecules. The detailed inspection finally yields to a classification of the observed transitions according to their chemical composition, lifetime and behavior. This is quite time-consuming and can prevent the identification the molecule when the precursors are expensive and/or available in limited amount, such as in deuterium- and <sup>15</sup>-nitrogen- substituted species.

Clearly, the above mentioned difficulties do not prevent the usual ones to be encountered during spectroscopic investigations of stable molecules. Large amplitude motions can occur in transient as well. For instance, the hydroxymethyl radical, CH<sub>2</sub>OH, has received considerable research interest due to practical and scientific considerations. It is involved in fuel combustion and plays some role in the chemistry of Earth's atmosphere.<sup>45</sup> In spite of the fact that a large body of theoretical and experimental research has been devoted to this radical, this open-shell has resisted so far the detection by high-resolution spectroscopy. Part of the reason can be ascribed to the large amplitude vibration of the OH and CH<sub>2</sub> moieties.<sup>46</sup> Additional complexity may arise from the possibility to observe several isotopologues of one transient species,<sup>47</sup> or unstable molecules in the ground and in vibrationally excited states as well.<sup>48</sup>

---

<sup>45</sup> S. Olivella, J. M. Bofill and A. Solé, *Chem. Eur. J.* **7**, 3377 (2001).

<sup>46</sup> L. Feng, J. Wei and H. Reisler, *J. Phys. Chem. A* **108**, 7903 (2004) and references therein.

<sup>47</sup> H. Ozeki, T. Okabayashi, M. Tanimoto, S. Saito and S. Bailleux, *J. Chem. Phys.* **127**, 224301 (2007).

<sup>48</sup> S. Bailleux, M. Bogey, C. Demuynck, J. L. Destombes, Y. Liu and A. Császár, *J. Chem. Phys.* **107**, 8317 (1997); S. Bailleux, M. Bogey, C. Demuynck, Y. Liu and a. Walters, *J. Mol. Spectrosc.* **216**, 465 (2002).

As a concluding remark, the firm identification of a new labile species, obtained by a least-squares analysis of the observed transitions, is *always* the outcome of a research project conducted with tenacity. At any rate, the gas-phase spectroscopic characterization of reactive molecules is a challenging and attractive project whose success is extremely rewarding.

### 1.2.b ... naturally, some of my research projects failed.

Taking the number of difficulties in detecting high-resolution spectra of transient species into consideration, a few experiments that I have conducted failed as the reader may have forecasted. Two molecular ions are concerned, namely the water cation  $\text{H}_2\text{O}^+$  and two of the deuterated isotopologues of the methyl cation:  $\text{CH}_2\text{D}^+$  and  $\text{CHD}_2^+$ . Interests for these studies are given together with some spectroscopic features, the reasons of the failure are inspected and some future prospects are also presented.

#### 1.2.b.i The case of $\text{H}_2\text{O}^+$

The water cation, also known as oxidaniumyl, has been the subject of intense research in the past decades because of its relevance in a wide variety of environments. It is mechanistically important in Earth's upper atmosphere<sup>49</sup>, in interstellar medium,<sup>50</sup> in oxygen-rich circumstellar shells<sup>51</sup> and more generally in chemistry. To illustrate its importance in space, it is worthwhile mentioning that Whipple postulated as early as 1950 that the heads of comets are primarily composed of solid water.<sup>52</sup> He anticipated that  $\text{H}_2\text{O}^+$  should therefore be generated in these systems by sunlight-induced photoionization of  $\text{H}_2\text{O}$ . It should be pointed out

---

<sup>49</sup> G. Herzberg, *Ann. Géophys. (C.N.R.S.)* **36**, 605 (1980).

<sup>50</sup> Y. P. Viala, *Astron. Astrophys. Suppl. Ser.* **64**, 391 (1986).

<sup>51</sup> G. A. Mamon, A. E. Glassgold and A. Omont, *Astrophys. J.* **323**, 306 (1987).

<sup>52</sup> F. L. Whipple, *Astrophys. J.* **111**, 375 (1950); F. L. Whipple, *Astrophys. J.* **113**, 464 (1951).

that the neutral species has no electronic *emission* spectrum because its excited electronic states predissociate. Detection of the cation is thus the only way, albeit indirect, of detecting indirectly water in visible emission.<sup>53</sup> The first high-resolution spectroscopic detection in emission of the water cation in the visible range (3500 – 6800 Å) in the laboratory came in 1973,<sup>54</sup> enabling to identify H<sub>2</sub>O<sup>+</sup> as the carrier of emission lines observed in the visible spectrum of the tail of comet Kohoutek in 1974.<sup>55</sup> The detailed analysis of the visible spectrum of H<sub>2</sub>O<sup>+</sup> was done later by Lew.<sup>56</sup> These observations conclusively provided evidence for Whipple’s conjecture on the presence of water in comets and therefore for the astrophysical importance of this ion. H<sub>2</sub>O<sup>+</sup> was subsequently discovered in the same visible range in many comets (References are given in 57). Very recently, pure rotational transitions have been detected in absorption by three groups with the HIFI instrument on board of the Herschel space observatory toward several star-forming regions.<sup>58</sup> Deep absorption signals of H<sub>2</sub>O<sup>+</sup> revealed that this ion is relatively abundant in these regions and strengthen the understanding of gas-phase formation of water in space.

The importance of the H<sub>2</sub>O<sup>+</sup> molecule has long since prompted a thorough number of theoretical studies.<sup>59</sup> The water cation is an open-shell

---

<sup>53</sup> B. Das and J. W. Farley, *J. Chem. Phys.* **95**, 8809 (1991).

<sup>54</sup> H. Lew and I. Heiber, *J. Chem. Phys.* **58**, 1246 (1973).

<sup>55</sup> P. A. Wehinger, S. Wycoff, G. H. Herbig, G. Herzberg and H. Lew, *Astrophys. J.* **190**, L43 (1974); G. Herzberg and H. Lew, *Astronom. Astrophys.* **31**, 123 (1974).

<sup>56</sup> H. Lew, *Can. J. Phys.* **54**, 2028 (1976).

<sup>57</sup> T. R. Huet, C. J. Pursell, W. C. Ho, B. M. Dinelli and T. Oka, *J. Chem. Phys.* **97**, 5977 (1992).

<sup>58</sup> a) M. Gerin, M. De Luca, J. Black *et al.*, *Astron. Astrophys.* **518**, L110 (2010) ;b) V. Ossenkopf, H. S. P. Müller, D. C. Lis *et al.*, *Astron. Astrophys.* **518**, L111 (2010);c) P. Schilke, C. Comito, H. S. P. Müller *et al.*, *Astron. Astrophys.* **521**, L11 (2010).

<sup>59</sup> M. Brommer, B. Weis, B. Follmeg, P. Rosmus, S. Carter, N. C. Handy, H. J. Werner and P. J. Knowles, *J. Chem. Phys.* **98**, 5222 (1993); M. Staikova, B. Engels, M. Perić and S.D. Peyerimhoff, *Mol. Phys.* **80**, 1485 (1993) and references therein.

species (isoelectronic to  $\text{NH}_2$ ) that exhibits a strong vibronic coupling, specifically the Renner-Teller effect which is an interaction between the orbital motion of the single unpaired electron and the bending vibration of the molecule ( $\nu_2$  mode).<sup>60</sup> As a result, oxidaniumyl presents a challenge to quantum chemists and to spectroscopists. The doubly degenerate state ( ${}^2\Pi_u$ ) in the fictitious linear equilibrium configuration of the molecule splits upon bending into the two Renner-Teller components: the sharply bent ground ( $X^2B_1$ ) and the quasilinear first excited ( $A^2A_1$ ) electronic states. The equilibrium geometry of the ionic ground state has been experimentally derived to be close to that of the neutral ground state, with slightly larger bond angle ( $109.30(10)^\circ$ ) and bond length ( $0.9992(6) \text{ \AA}$ ).<sup>57</sup>

The most important results for the millimetre-wave spectroscopic investigation of  $\text{H}_2\text{O}^+$  came with the measurements of pure rotational transitions (twenty-two in total) in the far-infrared region (between 25 and 200  $\text{cm}^{-1}$ ) by laser magnetic resonance spectroscopy, first in 1986 by Strahan, Mueller and Saykally<sup>61</sup> and later in 1998 by Mürtz, Zink, Evenson and Brown.<sup>62</sup> These experiments permitted the observation and analysis of the hyperfine structure due to the two equivalent protons. These measurements have been combined with optical as well as with infrared combination differences in a weighted least-squares analysis. It provided twenty-six molecular constants that can be used for zero-field prediction of millimetre-wave transitions. Although few spectroscopic investigations used a discharge in a flowing mixture composed of He,  $\text{O}_2$  and  $\text{H}_2$ , most of the experimental studies produced the  $\text{H}_2\text{O}^+$  radicals by applying a glow discharge through a flowing mixture of both highly purified water

---

<sup>60</sup> G. Herzberg and E. Teller, *Z. Phys. Chem. B* **21**, 410 (1933); R. Renner, *Z. Phys.* **92**, 172 (1934); J. A. Pople and H. C. Longuet-Higgins, *Mol. Phys.* **1**, 372 (1958).

<sup>61</sup> S.E. Strahan, R. P. Mueller and R. J. Saykally, *J. Chem. Phys.* **85**, 1252 (1986).

<sup>62</sup> P. Mürtz, L. R. Zink, K. M. Evenson and J. M. Brown, *J. Chem. Phys.* **109**, 9744 (1998).

vapour and helium, except in the second far-IR LMR work<sup>62</sup> where the water cation was generated by reacting ultrahigh purity helium (impurities >1 ppm) passed through a cw microwave discharge operating at 2450 MHz with purified water vapour. The chemistry with water as precursor is most favourable to the production of  $\text{H}_2\text{O}^+$  in the ground electronic state and some *ab initio* calculations support this experimental approach.<sup>63</sup> It involves one of the most fundamental processes in chemiionization, namely the Penning ionization reaction.<sup>64</sup> Briefly, metastable atoms of helium ( $\text{He}^*$ ) are produced in the discharge in excited states ( $2\ ^3\text{S}$ : 19.81 eV,  $\sim 90\%$ ;  $2\ ^1\text{S}$ : 20.61 eV,  $\sim 10\%$ )<sup>65</sup> and Penning ionization occurs through the electron exchange mechanism because the excitation energy of  $\text{He}^*$  is higher than the first vertical ionization energy of water (12.62 eV).<sup>66</sup> In both chemistries,  $\text{H}_2\text{O}^+$  is one of the primary ions formed (with  $\text{OH}^+$ ), and the terminal  $\text{H}_3\text{O}^+$  ion produced in secondary reactions is by far the dominant one.<sup>57,61</sup>

Given the fundamental importance of  $\text{H}_2\text{O}^+$  in various chemical environments, its millimetre-wave spectrum remains very attractive because previous high-resolution spectroscopic investigations lack microwave accuracy. For instance, the radio-detection in interstellar medium would be facilitated by the measurement of its millimetre-wave spectrum. Spectroscopically, the water cation is a *b*-type near symmetric prolate rotor (the Ray asymmetry parameter is  $\kappa = -0.62$ ) with a dipole moment appreciably larger than that of water:  $\sim 2.4\ \text{D}$ .<sup>67</sup> I have therefore conducted

---

<sup>63</sup> T. Ishida, *J. Chem. Phys.* **102**, 4169 (1995).

<sup>64</sup> F. M. Penning, *Naturwissenschaften* **15**, 818 (1925).

<sup>65</sup> P. A. Fleitz and C. J. Seliskar, *App. Spectrosc.* **43**, 293 (1989).

<sup>66</sup> K. Kimura, S. Katsumata, Y. Achiba, T. Yamazaki and S. Iwata in: *Handbook of HeI Photoelectron Spectra of Fundamental Organic Molecules* (Halsted, New York, 1981) and references therein; A. B. Trofimov and J. Schirmer, *J. Chem. Phys.* **123**, 144115 (2005).

<sup>67</sup> B. Weis, S. Carter, P. Rosmus, H. Werner and P. J. Knowles, *J. Chem. Phys.* **91**, 2818 (1989).

several attempts in order to detect its pure rotational spectrum, from the predictions based on the previously mentioned global analysis (it is unfortunate that the zero-field transitions frequencies were not reported, except for the fundamental transition of *ortho*-H<sub>2</sub>O<sup>+</sup>).<sup>61,62</sup> The rotational levels are described by the  $N$ ,  $K_a$  and  $K_c$  quantum numbers. Those with  $K_a > 0$  are split into two  $K_c$  sublevels:  $K_c = N - K_a$  and  $K_c = N + 1 - K_a$ . The presence of the unpaired electron ( $S = 1/2$ ) results in electron spin-rotation interaction that splits each rotational sublevel into two fine-structure levels:  $F_1$  ( $J = N + S$ ) and  $F_2$  ( $J = N - S$ ). The two identical hydrogen (with respect to the molecular  $b$ -axis) with nuclear spin  $I = 1/2$  requires that the molecular wave function obey the Fermi-Dirac spin statistics. The ground state of the cation being of  $b_1$  symmetry, the Pauli exclusion principle dictates that the rotational levels with  $K_a + K_c$  odd correspond to spin states with  $I_{\text{tot}} = 0$ , whilst those with  $K_a + K_c$  even correspond to states with  $I_{\text{tot}} = 1$ , where  $I_{\text{tot}}$  designates the total proton nuclear spin ( $I_{\text{tot}} = I_{\text{H1}} + I_{\text{H2}}$ ). The former case ( $K_a + K_c$  odd) must be associated with the *para*-species. In the latter one ( $K_a + K_c$  even), corresponding to the *ortho*-form of H<sub>2</sub>O<sup>+</sup>, each fine-structure level is further split into three sublevels giving rise to hyperfine structure. Strong lines are characterized by  $\Delta F = \Delta J = \Delta N$ , except the low quantum numbers where spin-flipping transitions have appreciable intensity, such as in the transitions searched during the spectroscopic campaigns (the following coupling scheme of angular momenta is adopted:  $J = N + S$  and  $F = J + I_{\text{tot}}$ ).

With this in mind, Z. Zelinger, S. Civiš and I undertook the detection of the four components of the  $N_{K_a, K_c} = 1_{1,0} \leftarrow 1_{0,1}$  rotational transition of *para*-H<sub>2</sub>O<sup>+</sup>, as early as 1995 and later in 2003. These are the strongest transitions occurring below 1 THz, and the energy of the lower levels is

about  $20 \text{ cm}^{-1}$  (corresponding to a temperature of 29 K) above the ground. The  $F_1 \leftarrow F_2$ ,  $F_1 \leftarrow F_1$ ,  $F_2 \leftarrow F_2$  and the  $F_2 \leftarrow F_1$  fine-structure components are accurately predicted to lie at 604684, 607227, 631732 and 634275 MHz, respectively (all  $\pm 2$  MHz,  $1\sigma$  uncertainty), *i.e.* in a frequency region where the spectrometer is most sensitive. For this purpose, a dedicated double-jacketted hollow cathode (made from copper) was especially built. Many scans were carried out, using a large number of different experimental conditions: discharge in a flowing mixture of Ar/H<sub>2</sub>O, or in Ar/O<sub>2</sub>/H<sub>2</sub>, either in positive column or in hollow cathode absorption cell, kept at room temperature or cooled by flowing either liquid nitrogen or refrigerated ethanol (down to about 200 K). Similar conditions were employed with He instead of Ar as buffer gas in order to make use of the Penning ionization mechanism. Very recently, these transitions were observed with the Herschel mission toward the massive star forming core Sg B2(M), respectively at the calculated frequencies (in MHz,  $1\sigma$  uncertainty given in units of the last significant figures):<sup>58c)</sup> 604678.6(25), 607227.3(19), 631724.1(37) and 634272.9(24). The small differences must mainly be imparted to the fact that hypothetical experimental zero-field frequencies and that their uncertainties were derived to perform the global analysis.<sup>61,62</sup> Although reasonable scanning regions were explored around the predictions ( $\pm 200$  MHz), we were not able to identify transitions to be ascribed to a paramagnetic species (in fact, no transition at all could be observed), and the failure of these exciting experiments must entirely be attributed to me.

Several reasons can be invoked. Not surprisingly, the most obvious one is related to production efficiency. Indeed, as stated previously, the Penning ionization mechanism is a fundamental process to produce ionic species. However, argon is generally used as buffer gas in millimetre-wave exper-

iments whilst He is preferred in infrared and LMR spectroscopy. The reason is that Ar has lower ionization energy (15.76 eV) than He (24.59 eV).<sup>68</sup> This combined with the fact that millimetre-wave experiments operate at lower pressures in order to avoid excessive line broadening (10 mTorr instead of 0.1 – 10 Torr) make it easier to initiate and maintain the discharge. In addition, the first metastable states of argon are  $^3P_2$  and  $^3P_0$  with energy of 11.55 eV and 11.72 eV, respectively.<sup>69</sup> These values are lower than the first vertical ionization energy of water (12.62 eV)<sup>66</sup> thus precluding the Penning ionization process of water in the plasma created by the discharge in an Ar/H<sub>2</sub>O mixture.

Another cause should be raised and is illustrated on Figure 1.2. The spectrum is very weak in the frequency region below 1 THz. The main

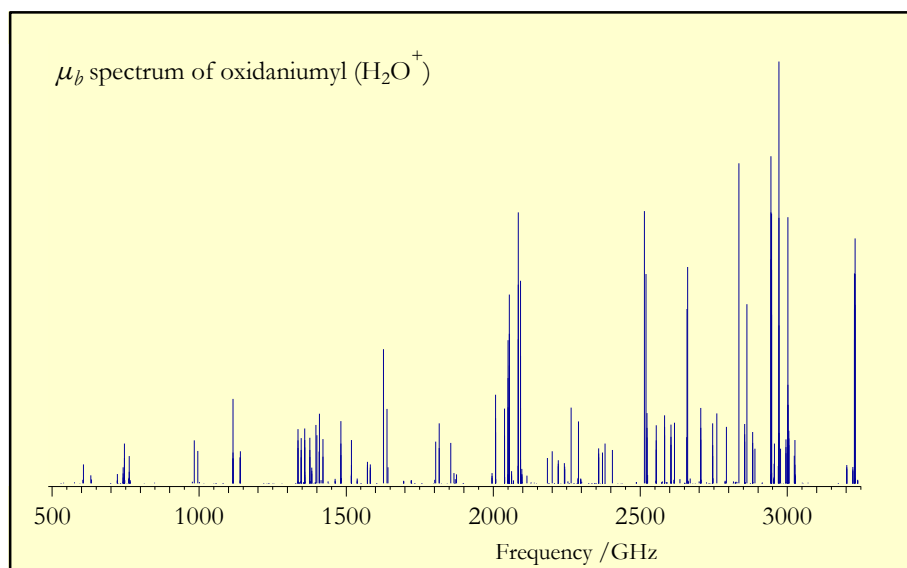


**Figure 1.2** Stick spectrum of  $H_2O^+$  predicted from the global least-squares analysis, using a temperature estimated at 225 K.

<sup>68</sup> [http://www.nist.gov/pml/data/ion\\_energy.cfm](http://www.nist.gov/pml/data/ion_energy.cfm) and references therein.

<sup>69</sup> L. G. Piper, M. A. A. Clyne and P. B. Monkhouse, *J. Chem. Soc. Far. Trans. 2* **78**, 1373 (1982).

argument arise from the fact that the corresponding energy levels involve low rotational quantum numbers ( $N=1, 2$  and  $3$  for the transitions occurring near  $600, 750$  and  $1000$  GHz, respectively). This domain is still not easily accessible and very few measurements carried out around  $1$  THz have been reported until now. In addition, it should be pointed out that the rotational temperature of the species in the plasma discharge often deviates from thermodynamic equilibrium,<sup>70</sup> and the Boltzmann population distribution among rotational energy levels (assumed in the predictions plotted in Figure 1.2) in such case is not obeyed.

In spite of this, I believe that the millimetre-wave detection of  $\text{H}_2\text{O}^+$  is promising in the near future. First of all, THz and sub-THz sources (BWO tubes from ISTOK company, Russia) delivering high-power (in the  $1 - 5$  mW range) in the THz range are being acquired. The search for stronger transitions will then be allowed (Figure 1.2) and their detection will be greatly enhanced with the use of a cyclotron resonance assisted InSb hot-electron bolometer that has increased detection sensitivity in the  $0.70 - 1.20$  THz frequency range. It might also be necessary to combine such an improved sensitivity with the design of a new absorption cell in order to gain production efficiency of the ionic radicals. One might think that  $\text{H}_2\text{O}$  is presumably the most suitable precursor for the production of  $\text{H}_2\text{O}^+$  ion. I did not try to produce metastable helium with a microwave discharge operating at  $2450$  MHz and such an experiment should be attempted. However, water has the major drawback of precluding cooling the plasma with liquid nitrogen. Therefore the use of the gaseous precursors can be retained as a second interesting alternative.

---

<sup>70</sup> V. Efimova, A. Derzsi, A. Zlotorowicz, V. Hoffmann, Z. Donkó and J. Eckert, *Spectrochim. Acta B* **65**, 311 (2010) and references therein.

### 1.2.b.ii The case of the deuterated isotopologues of $\text{CH}_3^+$

We next examine the mono- and di-deuterated isotopologues of the methyl cation, also known as methylium, namely the close-shells  $\text{CH}_2\text{D}^+$  and  $\text{CHD}_2^+$ .

$\text{CH}_3^+$  is a fundamental carbo-ion in many aspects. It was first discovered in the late 1920s in the mass spectrum of  $\text{CH}_4$  ionized by electron impact<sup>71</sup> and has since been found ubiquitous in hydrocarbon discharge chemistry. This property arises from its stability against hydrogen abstraction and thus makes it a pivotal ion in interstellar chemistry as well, since it is supposed to be involved in the formation of organic molecules.<sup>72</sup> The knowledge of its abundance is also essential for deriving the density of electrons in molecular clouds<sup>73</sup> but its direct radio astronomical observations are not permitted because  $\text{CH}_3^+$  is a symmetric planar molecule with no permanent dipole moment. However, deuteration breaks the overall symmetry and the deuterated forms of this ion possess a non-negligible permanent dipole (the 1:2 ratio of the atomic masses significantly shifts the center of mass from the center of charge). Hence both  $\text{CH}_2\text{D}^+$  and  $\text{CHD}_2^+$  have pure rotational spectra thus permitting their radio astronomical searches. Although efficient deuterium fractionation are known to occur in cold regions (<20 K) with a D:H ratio several orders of magnitude higher than the cosmic D:H ratio ( $1.5 \cdot 10^{-5}$ ), deuterated forms of  $\text{CH}_3^+$  are believed to be responsible for the deuterium fractionation in warmer environments (>50 K).<sup>74,75,76</sup> Indeed, deuteration need not stop at

---

<sup>71</sup> T. R. Hogness and H. M. Kvalnes, *Phys. Rev.* **32**, 942 (1928).

<sup>72</sup> M.-F. Jagod, C. M. Gabrys, M. Rösslein, D. Uy and T. Oka, *Can. J. Phys.* **72**, 1192 (1994).

<sup>73</sup> M. Guélin, W. D. Langer, R. L. Snell and H. A. Wootten, *Astrophys. J.* **217**, L165 (1977).

<sup>74</sup> B. E. Turner, *Astrophys. J. Suppl. S.* **136**, 579 (2001).

<sup>75</sup> E. Roueff, B. Parise and E. Herbst, *Astron. Astrophys.* **464**, 245 (2007).

<sup>76</sup> B. Parise, S. Leurini, P. Schilke et al., *Astron. Astrophys.* **508**, 737 (2009).

the singly-deuterated isotopologues, since *e.g.* doubly-deuterated formaldehyde presumably derives in part from  $\text{CHD}_2^+$ .<sup>75,77</sup>

Thus many theoretical and experimental studies have been devoted to  $\text{CH}_3^+$  and its deuterated counterparts. In particular, Oka in his ion factory succeeded in detecting by high-resolution infrared spectroscopy the  $\nu_1$  and  $\nu_4$  bands of  $\text{CH}_2\text{D}^+$  and the  $\nu_1$  band of  $\text{CHD}_2^+$  (in addition to the  $\nu_3$  band of  $\text{CH}_3^+$ ).<sup>78,72,79</sup> Several hundreds of lines were assigned and the analysis provided ground state molecular constants for the deuterated isotopologues, from which pure rotational transitions were calculated. These results entailed several groups in detecting rotational lines of  $\text{CH}_2\text{D}^+$  in the submillimetre-wave region, without success, including that of Lille.<sup>80</sup> Some recent searches for these species in space did not result in their firm identification,<sup>81,82</sup> thus demonstrating the urgent quest for their rotational spectrum.

From the spectroscopic point of view,  $\text{CH}_2\text{D}^+$  and  $\text{CHD}_2^+$  are planar, highly asymmetric light rotors with  $C_{2v}$  symmetry ( $\kappa = -0.231$  and  $-0.155$ , respectively). It should be pointed out that their rotational spectra exhibit significant disparities because of the different isotopic substitutions. The permanent dipole moment of  $\text{CH}_2\text{D}^+$  (0.329 D) lies along the  $C_{2v}$  molecular *a*-axis and the symmetric hydrogen nuclei (fermions with  $I = 1/2$ ) yield nuclear spin weights for the rotational levels of 3 for  $K_a$  odd (*ortho*) and of

---

<sup>77</sup> C. Vastel and T. G. Phillips, *Astrophys. J.* **606**, L127(2004), and references therein.

<sup>78</sup> M.-F. Jagod, M. Rösslein, C. M. Gabrys and T. Oka, *J. Mol. Spectrosc.* **153**, 666 (1992)

<sup>79</sup> M. W. Crofton, M.-F. Jagod, B. D. Rehfuss, W. A. Kreiner and T. Oka, *J. Chem. Phys.* **88**, 666 (1987).

<sup>80</sup> C. Demuyneck, *J. Mol. Spectrosc.* **168**, 215 (1994).

<sup>81</sup> A. Wootten and B. E. Turner in: *A Search for Interstellar  $\text{CH}_2\text{D}^+$* , *Proc. LAU Symp.* **252**, 33 (2008).

<sup>82</sup> D. C. Lis, P. E. Goldsmith, E. A. Bergin, E. Falgarone, M. Gérin and E. Roueff in: *Hydrides in Space: Past, Present and Future, Submillimeter Astrophysics and Technology*, *ASP Conf. Ser.* **417**, 23 (2009).

1 for  $K_a$  even (*para*). In  $\text{CHD}_2^+$ , the dipole moment (0.310 D) is oriented along the  $b$ -axis of symmetry, resulting in  $b$ -type rotational transitions. The two equivalent deuterium nuclei (bosons with  $I=1$ ) give a 1:2 nuclear spin statistics for the  $K_a + K_c$  odd and  $K_a + K_c$  even rotational states. In the infrared spectroscopic investigations, both these species were formed concurrently by ac discharging ( $\sim 150$  mA) a gas mixture of  $\text{CD}_4:\text{CH}_4:\text{H}_2:\text{He} = 120:10:100:7000$  mTorr in a liquid nitrogen cooled cell. These spectroscopic properties were used in combination with the reported molecular constants to predict the rotational spectra of the mono- and di-deuterated isotopologues of  $\text{CH}_3^+$ ; the stick spectra are depicted in Figure 1.3a and 1.3b, respectively. In collaboration with Z. Zelinger and S. Civiš under a two-year CNRS contract, the search for the millimetre-wave spectrum of  $\text{CHD}_2^+$  was carried out, at first in a negative glow discharge

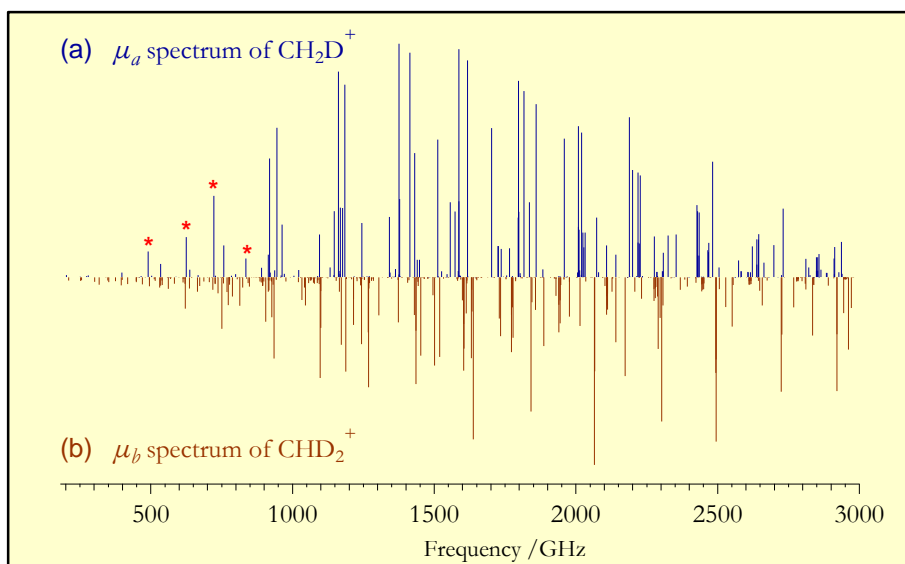


**Figure 1.3** Stick spectra of  $\text{CH}_2\text{D}^+$  (upward, (a)) and  $\text{CHD}_2^+$  (downward, (b)) calculated with a temperature of 150 K. The four lines marked with  $\star$  are those observed by Amano (Ref. 83).

extended with an axial magnetic field. I decided to discharge a mixture of helium and methane-D3 ( $\text{CHD}_3$ ). This deliberate choice was based on the fact that several groups failed in their attempt to detect  $\text{CH}_2\text{D}^+$  most probably by using the same combination of precursors as in Oka ion factory. Helium employed as buffer gas was preferred instead of argon for the same reason. Although several candidate lines were found near the predictions, we were not able to fit them in a global analysis using the combination differences derived from the transition wavenumbers for the  $\nu_1$  band of  $\text{CHD}_2^+$ .<sup>78</sup> In addition, during our investigation, Amano reported the detection of four millimetre-wave transitions of  $\text{CH}_2\text{D}^+$ , in the frequency range 490 – 840 GHz.<sup>83</sup> In an accompanying paper the Cologne group measured vibrational transitions of the same species (produced in a low-temperature ion trap) observed by high-resolution infrared spectroscopy and predicted low  $J$  rotational transitions up to 1.5 THz.<sup>84</sup> Amano succeeded in observing  $\text{CH}_2\text{D}^+$  in conditions very similar as those employed in Ref. 78. In particular, he found that helium was critical in producing this ionic species since no signal was detectable with argon. Although the complex mechanisms involved cannot be identified from his experiment, it is likely that Penning ionization process contributes importantly in forming primary ions like  $\text{CH}_3^+$  and  $\text{CD}_3^+$ . We have afterwards undertaken the detection of the same lines with the same gas mixture as Amano, but without success. Until now, I have not been able to clarify the reasons of these fruitless efforts. Since both spectrometers have similar sensitivities, it seems to me that the major rationale could lie in the specific and critical design in the absorption cell and/or electrodes of Amano’s spectrometer.

---

<sup>83</sup> T. Amano, *Astron. Astrophys.* **516**, L4 (2010).

<sup>84</sup> S. Gärtner, J. Krieg, A. Klemann, O. Asvany and S. Schlemmer, *Astron. Astrophys.* **516**, L3 (2010).

### 1.3 The Lille submillimetre-wave spectrometer

The salient features of the submillimetre-wave spectrometer devoted to the investigation and characterization of transient species studied are briefly described in this section. A block-diagram is shown in Figure 1.4.

The monochromatic millimetre-wave radiation is obtained from several backward wave oscillators (BWO from Thomson-CSF – now stopped – and from ISTOK Company, Fryazino, Russia) insuring broad frequency coverage in the 200-950 GHz region, with a gap between 650-800 GHz. The amount of power that is available ranges from several tens of milliwatt in the low frequency limit to a few milliwatt for the highest frequencies. Detection is achieved by a fast (relaxation time  $\sim 1\mu\text{s}$ ), liquid-helium-cooled InSb hot-electron bolometer (QMC Instruments, Cardiff, UK). The BWOs are phase-locked to a harmonic of a microwave radiation from a solid-state oscillator (12-18 GHz) which is referenced to a Rubidium atomic clock *via* the GPS system (Stanford Research Systems). For improved sensitivity, a 5 kHz phase modulation is applied to the BWO by modulating the 10 MHz reference frequency of the phase-lock synchronizer. Phase-sensitive detection at twice this frequency is accomplished with a lock-in amplifier, resulting in a second-derivative line shape. Adjusting the modulation depth to the spectral feature (linestrength and linewidth) provides optimization of signal detection. Whenever two or more lines are partially overlapped, the modulation depth is reduced until the best compromise between detection performance and resolution is found.

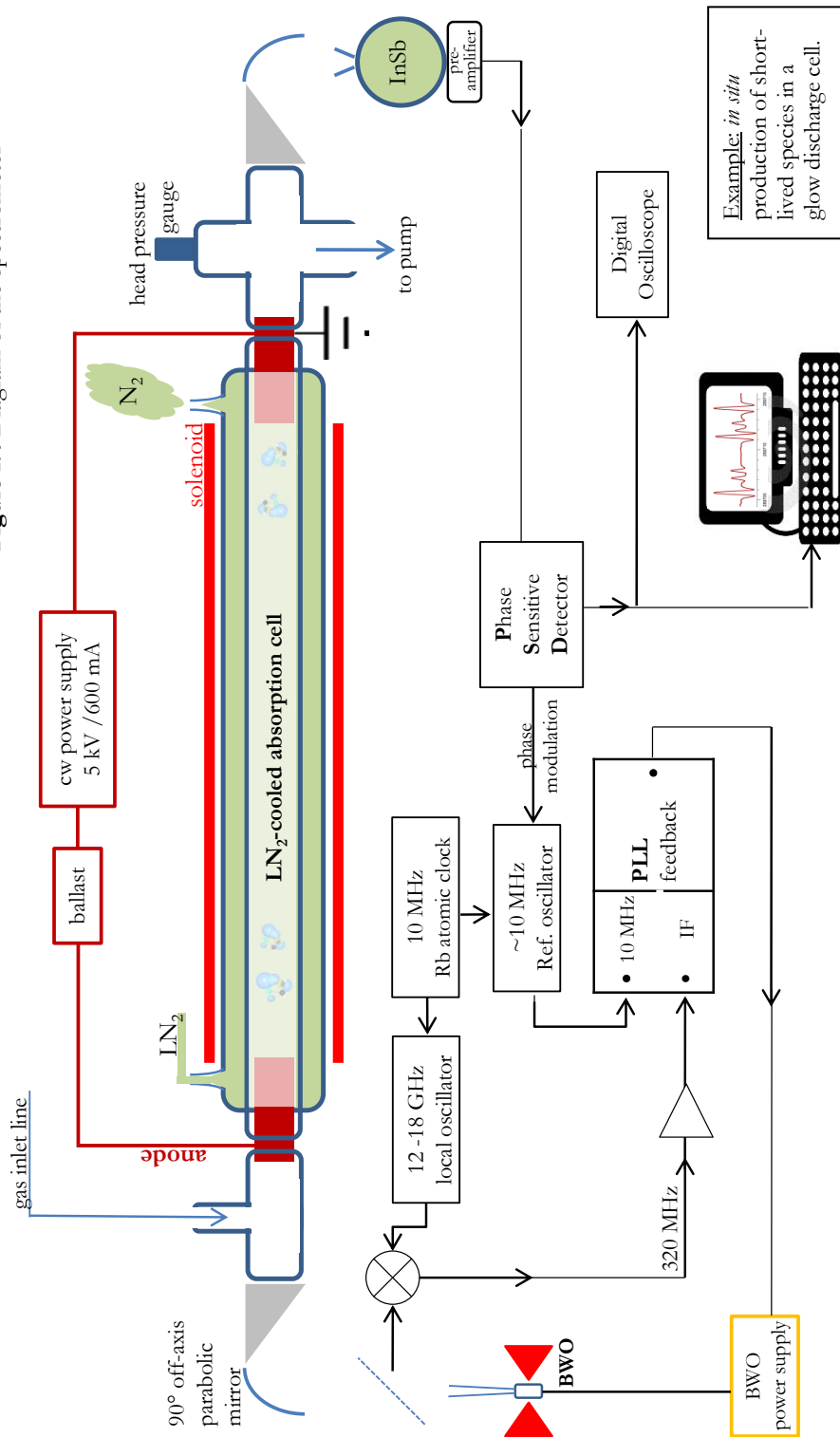
The 2-metre long, free space absorption cell is systematically designed for *in situ* production of the reactive molecules and is evacuated using a diffusion pump (Edwards Vacuum), the maximum pumping speed being

$\sim 800$  l/s for helium (a slide valve installed between the pump and the cell reduces the flow rate to  $\sim 50\%$  of the nominal pumping speed). The total pressure, measured downstream, usually does not exceed several tens of mTorr. As already mentioned, the cell is a double-jacketted Pyrex tubing so that the gas mixture can be cooled by flowing liquid nitrogen (77 K) between the two jackets. Both ends of the cell are sealed by Teflon windows mounted at Brewster angle in order to improve transmission of polarized millimetre-wave radiation. The standing waves that limit the sensitivity of the spectrometer are also reduced in this way. The cell is enclosed within a solenoid coil used for axial magnetic field generation (up to 250 Gauss) and allows to distinguish paramagnetic species through the observation of the Zeeman effect. The electrical characteristics of the solenoid (the inductance  $L \approx 460$  mH in particular is by far too large) as yet do not permit the use of the Zeeman modulation scheme. This double modulation technique, *i.e.* source- combined with Zeeman- modulation, is known to be very effective in reducing the standing waves and inherently results in the detection of paramagnetic species *only*.<sup>85</sup> Such a development is planned in the near future. Earth's magnetic field is not compensated for: although this could be easily done by a set of two (or three) pairs of Helmholtz coils mounted perpendicularly, its use was found so far to be unnecessary. Two off-axis parabolic mirrors are used, one to focus the radiation from the BWO on the cell, and the other one to collect and focus the radiation outcoming from the cell on the entrance window of the bolometer. Their use avoids the Teflon lenses that absorb millimetre-wave radiation, particularly in the high frequency limit of the spectrometer, and slightly reduces the standing-waves.

---

<sup>85</sup> T. Amano and A. Maeda, *J. Mol. Spectrosc.* **203**, 140 (2000) and references therein.

Figure 1.4 Diagram of the spectrometer



Various methods were employed to generate the labile molecules, such as microwave discharge operating at 2450 MHz, *in situ* flash-pyrolysis, dc discharge, and to a less extent photolysis. They are described in the papers associated to the species whose characterizations are given in the following chapters.

Given the number of parameters that most of the time a *single* operator has to *dynamically* adjust in order to *continuously* insure high sensitivity and optimal production of the transient species, the spectrometer obviously necessitates to be automatized and remotely controlled. This has first been carried out using object-oriented design and programming with Labview. Although it has the advantage of ease of programming for those new to computer programming like me, I find it heavy, thus slow, non-intuitive and difficult to read with the front and back windows. The major drawback I met is that Labview is not designed for data analysis (such as non-linear fit for lineshape deconvolution), and therefore a third-party software is required to perform such type of operations. Ergo, I recently developed several routines, written in a C-language making them very effective and fast to execute, under the all-in-one IgorPro software (Wavemetrics).<sup>86</sup> These computer-programmes allow data acquisition, fast and efficient data analysis, creation of user-defined menus together with excellent graphing capabilities *e.g.* for publishing.

In particular a nonlinear curve-fitting procedure, based on the Levenberg-Marquardt algorithm implemented in IgorPro, has been developed for lineshape deconvolution. This routine is chiefly useful when one wants to resolve lines that are partly overlapped. As stated previously in this section, the recorded line profiles approximately resemble the second-

---

<sup>86</sup> [www.wavemetrics.com](http://www.wavemetrics.com)

derivative of Voigt profile, and the computer code is based on an analytical expression that closely matches this profile: the second-derivative of the Pearson VII distribution.<sup>87</sup> The Pearson VII distribution is given by:

$$f(\nu) = -\frac{I}{\left\{1+\left(\frac{\nu-\nu_0}{\omega}\right)^2\right\}^M} \quad (\text{Equation 1.10}),$$

from which the second-derivative takes the form:

$$f''(\nu) = \frac{I_0}{\left\{1+\left(\frac{\nu-\nu_0}{\omega}\right)^2\right\}^{M+2}} \left\{1 - (1+2M)\left(\frac{\nu-\nu_0}{\omega}\right)^2\right\} \quad (\text{Equation 1.11}).$$

In these expressions,  $\nu_0$  denotes the resonance frequency (in MHz),  $I$  and  $I_0$  the peak intensities (in a.u.), and  $\omega$  (in MHz) represents the linewidth parameters.  $M$  is a dimensionless parameter corresponding to the lineshape. If  $M=1$ , the lineshape is Lorentzian whilst if  $M \rightarrow \infty$ , the profile is Gaussian. For intermediate  $M$  values, the lineshape is better described with a Voigt profile. From the expression of  $f''(\nu)$ , the full width at half maximum (FWHM, in MHz) of the recorded line is well approximated with the expression:

$$\text{FWHM} \approx \frac{2\omega}{\sqrt{(4+5M)}} \quad (\text{Equation 1.12}).$$

This formula shows that the parameters  $\omega$  and  $M$  are strongly correlated. Since the observed spectral lines are usually weak, the shape parameter  $M$  is fixed (at a value determined in a preliminary fit) and  $I_0$ ,  $\omega$  and  $\nu_0$  are the floating parameters. Try-and-error tests have shown that the influence of the value of  $M$  on the central frequency of the transition  $\nu_0$ , which is the parameter of primordial importance, is negligibly small. The routine

---

<sup>87</sup> K. Pearson, *Phil. Trans. R. Soc. Lond. A* **216**, 429 (1916).

employs an analytical expression to derive the lineshape and thus the least-squares method converges quickly. It is prevalently used to determine *accurately* the peak frequency of a single line but its full potential comes into play for consistent multipeak deconvolution in order to retrieve the main peaks of overlapped signals. An example of the results obtained on the deconvolution of the hyperfine structure owing to the iodine nucleus in  $\text{CH}_2\text{I}^{35}\text{Cl}$  (details on the spectral analysis of both chlorine isotopologues of  $\text{CH}_2\text{I}^{35}\text{Cl}$  are given in chapter 2) is illustrated in Figure 1.5. The spacings between the five spectral lines are nearly identical

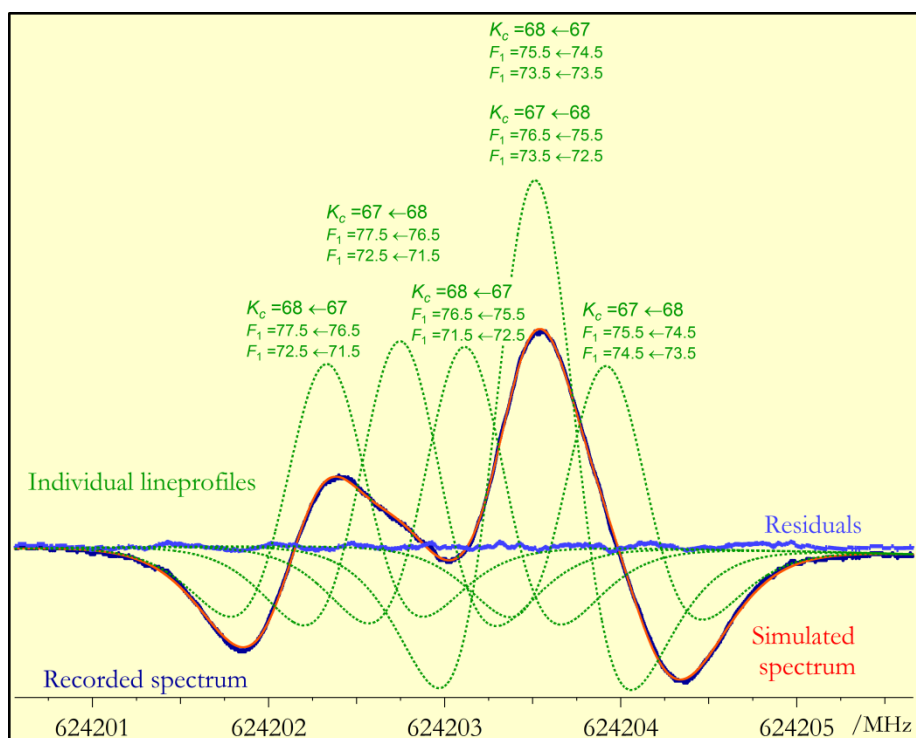


**Figure 1.5** Hyperfine structure arising from the iodine nuclear spin ( $I_I = 5/2$ ) in the  $b$ -type R-branch of the  $J = 75 \leftarrow 74$ ,  $K_a = 8 \leftarrow 7$  millimetre-wave transition of  $\text{CH}_2\text{I}^{35}\text{Cl}$  ( $\mathbf{F}_1 = \mathbf{J} + \mathbf{I}_I$ ): recorded spectrum (blue), individual line profiles (dotted, green) and the envelope corresponding to the convolution of the five spectral lines (red). The residuals are also displayed.

and vary from 375 to 420 kHz. The line frequencies were adjusted together with the peak frequencies with the same shape and width parameters for each hyperfine component. Since different species exhibit different pressure and Doppler broadenings, this method can be used to discriminate lines belonging to different species when searching for the rotational spectrum of a new molecule, for instance generated in a discharge (a non-selective technique). Although this example demonstrates the efficiency in resolving overlapped transitions, the major criticism that can be evoked resides in the fact that it is difficult to correlate the width parameter with a physical meaning. For instance, the translational temperature of the molecule can be estimated by fitting a line with a Gaussian.<sup>41</sup>

Finally, prediction of the spectra and least-squared analysis of the observed transition frequencies are carried out with the SPCAT and SPFIT routines, respectively, from the free CALPGM programme suite of Pickett.<sup>88</sup> This code is invaluable to spectroscopists since the spectra of molecules (possibly observed in many vibrational excited states) with up to 9 spins (regardless of whether they are electronic or nuclear) can be analyzed. Recently, the Euler approach has also been included to treat non-rigid species (such as water and the methylene bi-radical, CH<sub>2</sub>).<sup>89,90</sup>

---

<sup>88</sup> <http://spec.jpl.nasa.gov/>

<sup>89</sup> H. M. Pickett, J. C. Pearson and C. E. Miller, *J. Mol. Spectrosc.* **233**, 174 (2005).

<sup>90</sup> S. Brünken, H. S. P. Müller, F. Lewen and T. F. Giesen, *J. Chem. Phys.* **123**, 164315 (2005).

# ENVIRONMENTAL-RELATED SPECTROSCOPY OF HALOGEN- CONTAINING SPECIES

---

### 2.1 Introduction

Ozone is a tiny constituent of the Earth's atmosphere, approximately 90 percent of which is found in the stratosphere, the layer that extends from the troposphere up to ~51 km in altitude. Its concentration shows seasonal variations and peaks around the altitude of 30 km in tropics and around 20 km in polar regions, with volume mixing ratio of about 4-8 ppmv (parts per million by volume). The troposphere, the region of the atmosphere which begins at the surface (the atmospheric boundary layer) and extends to between 9 km at the poles and 17 km at the equator, makes up the remaining 10 percent of the ozone. Stratospheric ozone absorbs solar radiation at wavelengths shorter than 336 nm<sup>91</sup> that is not

---

<sup>91</sup> J. Malicet, D. Daumont, J. Charbonnier, C. Parrisé, A. Chakir and J. Brion, *J. Atmos. Chem.* **21**, 263 (1995).

absorbed by molecular nitrogen or molecular oxygen. *Stratospheric* ozone is accordingly crucial in maintaining life on Earth by shielding Earth's surface from biologically harmful, highly energetic ultraviolet (UV) radiation. In addition, ozone converts UV radiation into heat and is therefore responsible for a positive temperature gradient in the stratosphere. As a result, vertical circulation of chemicals and transport of energy are nearly suppressed in the stratosphere. This feature distinguishes the stratosphere from the troposphere where declining temperature with altitude promotes vertical migration mechanisms and affects the net *stratospheric* ozone balance through catalytic cycles.

In contrast to its beneficial role in the stratosphere, tropospheric ozone is hazardous to human health and has well-recognized adverse impacts *e.g.* on forest growth and crop yields.<sup>92,93,94</sup> Furthermore, ozone in the troposphere is a powerful greenhouse gas even if its contribution to the enhancement of greenhouse effect still needs to be quantified. Over the last few decades levels of stratospheric ozone have been declining globally over polar regions in the springtime and especially in Antarctica, whilst levels of tropospheric ozone have increased in the boundary layer.

The mechanisms that lead to the net stratospheric ozone loss have been largely studied and are well understood. Details of them can be found in the extensive review of Solomon<sup>95</sup> and are briefly summarized here. Chapman first proposed a photochemical theory for a steady state formation and destruction of ozone based on an oxygen-only chemical

---

<sup>92</sup> P. M. Vitousek, J. D. Aber, R. W. Howarth, G. E. Likens, P. A. Matson, D. W. Schindler, W. H. Schlesinger and D. G. Tilman, *Ecol. Appl.* **7**, 737 (1997).

<sup>93</sup> J. D. Aber, K. J. Nadelhoffer, P. Steudler and J. M. Melillo, *BioScience* **39**, 378 (1989).

<sup>94</sup> M. R. Ashmore, *Plant. Cell. Environ.* **28**, 949 (2005).

<sup>95</sup> S. Solomon, *Rev. Geophys.* **37**, 275 (1999), and references therein.

scheme.<sup>96</sup> He noted in his groundbreaking paper that ozone and atomic oxygen (considered together as an odd oxygen family, in contrast to the long-lived form of even oxygen, O<sub>2</sub>) rapidly interchange with each other in the stratosphere to produce molecular oxygen. In the following decades, it became clear that stratospheric ozone was chemically destroyed not solely by reaction with atomic oxygen, but also by hydrogen oxides (HO<sub>x</sub>,  $x=0, 1, 2$ ) and nitrogen oxides (NO<sub>y</sub>,  $y=1, 2$ ) chemistry. Both these oxides can destroy odd oxygen in catalytic cycles. Accordingly, the modeled profile of the ozone concentration has been remarkably improved if compared with the pure oxygen chemistry of Chapman. However, Molina and Rowland in 1974 first demonstrated that reactive chlorine radicals could also engage in catalytic cycles resulting in ozone destruction.<sup>97</sup> They showed that the manmade tropospheric chlorofluorocarbons (CFCs) reach the stratosphere where they are photolyzed, subsequently releasing reactive chlorine radicals. Stolarsky and Cicerone highlighted the same year that chlorine oxides (ClO<sub>y</sub>,  $y=1, 2$ ) of different origins (*i.e.* from solid fuel rocket and volcanic eruption) are involved in a photochemical scheme that sinks in two active catalytic cycles odd oxygen.<sup>98</sup> Later studies established that bromocarbons contribute similarly to ozone depletion. The resultant halogen chemistry couples one family of compounds to another (such as the formation of chlorine nitrate, ClONO<sub>2</sub>, through reaction of ClO with NO<sub>2</sub> and the coupling of bromine and chlorine chemistry). Bromine being less tightly bound than chlorine, this atom is more effective than chlorine, up to 100 times on an atom-per-atom basis.<sup>99</sup> In contrast, fluorine has a negligible impact on

---

<sup>96</sup> S. Chapman, *Philos. Mag.* **10**, 369 (1930).

<sup>97</sup> M. J. Molina and F. S. Rowland, *Nature* **249**, 810 (1974).

<sup>98</sup> R. S. Stolarsky and R. J. Cicerone, *Can. J. Chem.* **22**, 1610 (1974).

<sup>99</sup> R. R. Garcia and S. Solomon, *J. Geophys. Res.* **99**, 12937 (1994).

ozone since acid HF is quickly formed and so tightly bound that essentially all fluorine released from fluorine source gases in the stratosphere is irreversibly and rapidly neutralized. It should also be noted that enhanced ozone depletion over polar regions is linked to heterogeneous halogen chemistry that occurs on the surfaces of polar stratospheric clouds at cold temperatures. The partitioning of chlorine between active forms that destroy ozone and inert reservoirs that sequester it plays another significant role in our understanding of ozone depletion.

Increasing tropospheric ozone levels over the past 150 years have led to a significant air pollution and climate alteration.<sup>100</sup> It is more recently that halogenated compounds have been recognized to affect the chemistry of the tropospheric ozone as well,<sup>101</sup> although it has been postulated by numerical models more than a decade ago.<sup>102</sup> This is especially true in the marine boundary layer since oceans cover approximately 70 percent of the Earth's surface. The most recent photochemical reaction schemes not only take into account the role of chlorine and bromine chemistry, but also that of iodine.<sup>102</sup> It was afterwards found that intense chemical *interactions* between reactive chlorine, bromine and iodine compounds occur. In the marine boundary layer, Cl- and Br- compounds originate from sea-salts whilst photolabile iodocarbons (such as CH<sub>3</sub>I, the most abundant organic iodine compound, and CH<sub>2</sub>I<sub>2</sub> and CH<sub>2</sub>ICl among others), produced by marine algae, are released from the ocean surface because of

---

<sup>100</sup> S. Solomon, D. Qin, M. Manning, Z. Chen, M. Marquis, K. B. Averyt, M. Tignor and H. L. Miller in: *Climate Change 2007: The Physical Sciences Basis* (Contribution of Working Group I to the Fourth Assessment Report of the Intergovernmental Panel on Climate Change (IPCC), Cambridge University Press, Cambridge, New-York, 2007); <http://www.ipcc.ch>

<sup>101</sup> K. A. Read, A. S. Mahajan, L. J. Carpenter *et al.*, *Nature* **453**, 1232 (2008).

<sup>102</sup> R. Vogt, R. Sander, R. von Glasow and P. Crutzen, *J. Atmos. Chem.* **32**, 375 (1999) and references therein.

their low solubility. A set of chain reactions leading to ozone formation is initiated by chlorine atoms coupled with  $\text{HO}_x$  and  $\text{NO}_y$  radicals. In contrast, bromine atoms in the troposphere lead to ozone destruction. It should be pointed out that though oceans provide the largest source of halogens, halogen chemistry has also been observed in other locations, such as in plumes from burning oil wells, near alkaline dry lakes and volcanoes.<sup>103</sup> Although halogen gases are believed to play key roles in the chemistry of the lower atmosphere, many of them have not been detected or measured in ambient air.

Remote sensing using millimetre- and submillimetre-wavelength heterodyne spectroscopy from orbiting satellites is a powerful tool that can provide precise measurements of atmospheric trace species abundances from their thermal emission spectra. This technique started in the 1970s for monitoring changes and studying processes in the Earth's atmosphere, including the troposphere and the stratosphere.<sup>104,105</sup> Hence the laboratory investigation of halospecies by millimetre- and submillimetre-wave spectroscopy is essential to better understanding of atmospheric chemistry. Beside their key participation in atmospheric chemistry, their spectroscopic characterization is also interesting on their own, *e.g.* for structural comparison. In this chapter, the distinctive results of the studies of halogen-containing species by high-resolution spectroscopy are presented. They include the analysis of the  $\nu_4$  band of the fluoroformyloxyl radical ( $\text{FCO}_2$ ), the millimetre-wave investigations of the halomethyl radicals ( $\text{CH}_2\text{X}$ ,  $\text{X} = \text{Br}, \text{I}$ ) in addition to the laboratory stable interhalogen species  $\text{ICl}$  and  $\text{CH}_2\text{ICl}$ .

---

<sup>103</sup> B. J. Finlayson-Pitts, *Anal. Chem.* **82**, 710 (2010), and references therein.

<sup>104</sup> M. A. Janssen in: *Atmospheric Remote Sensing by Microwave Radiometry* (Wiley Interscience, New-York, 1993).

<sup>105</sup> J. W. Waters, *Proc. IEEE* **80**, 1679 (1992) and references therein.

## 2.2 The $\nu_4$ band of the FCO<sub>2</sub> radical analysed: evidence for the strong *pseudo* Jahn-Teller effect

This work has been carried out in collaboration with Z. Zelinger, E. Grigorová (J. Heyrovský Institute of Physical Chemistry, Academy of Science of the Czech Republic, Prague, Czech Republic) and H. Beckers (Bergische Universität Wuppertal, Germany).

At the time of writing this habilitation, although the paper is nearly completed, it has not yet been submitted. The main characteristics are briefly summarised here since details of this investigation are given in the concomitant paper.

The fluoroformyloxyl radical is one of the key intermediate species involved in the degradation of hydrofluorocarbons (HFCs) that came into replacements for the *stratospheric* ozone-depleting chlorofluorocarbons (CFCs) and the hydrochlorofluorocarbons (HCFCs). The importance of this radical occurs in a wide variety of chemical processes and accordingly has long stimulated a large number of theoretical and experimental studies. From the theoretical point of view, difficulties in the quantum chemical treatment arise from the favourable coupling of low-lying electronic states (often encountered in radicals) through the nuclear motion. These problems have been analysed in details:<sup>106</sup> when a nearby electronic state with a symmetry different from that of the ground state is present, *non-symmetric* distortions of the nuclear framework give rise to the *pseudo* Jahn-

---

<sup>106</sup> J. Breidung, W. Thiel, *J. Phys. Chem. A* **110**, 1575 (2006); W. F. Schneider, M. M. Maricq, J. S. Francisco, *J. Chem. Phys.* **103**, 6601 (1995).

Teller interaction. In particular, such a strong interaction is predicted to occur with the nearby  $B^2A_1$  state lying 1.630 eV above the ground state upon excitation of the  $\nu_4$  mode (C-O antisymmetric vibration). Experimentally, the millimetre-wave spectrum (first carried out at Lille) has been reported<sup>107</sup> and the high-resolution Fourier transform infrared spectrum has been recorded in the 600-1400  $\text{cm}^{-1}$  region. However, the analysis of the  $a$ -type  $\nu_2$  band (centred at 970.208  $\text{cm}^{-1}$ ) has been recently published.<sup>108</sup> The EPR spectra of this radical isolated in noble gas matrices have been investigated,<sup>109</sup> providing with the help of the accompanying millimetre-wave study<sup>110</sup> consistent fine- and hyperfine-structure parameters.

The molecular and spectroscopic properties of  $\text{FCO}_2$  in its ground electronic state ( $^2B_2$ ) are thus still insufficiently explored. Within this context, the unperturbed  $b$ -type  $\nu_4$  perpendicular band (the second strongest band) has been analysed. The  $\text{FCO}_2$  radical is a very asymmetric, oblate rotor ( $\kappa = +0.35$ ) belonging to the  $C_{2v}$  point group and possesses two indistinguishable oxygen nuclei ( $I_{\text{O}} = 0$ ). The unpaired electron is primarily located in an oxygen-centred in-plane orbital. Although half of the transitions are missing due to the nuclear spin statistics the whole spectrum is very congested and most of the lines are actually blended due to an overlap of

---

<sup>107</sup> Z. Zelinger, P. Dréan, A. Walters, J. R. Avilès Moreno, M. Bogey, H. Pernice, S. von Ahsen, H. Willner, J. Breidung, W. Thiel and H. Bürger, *J. Chem. Phys.* **118**, 1214 (2003); Z. Zelinger, S. Bailleux, D. Babánková, M. Šimečková, L. Strítěská, L. Kolesníková, P. Musil, P. Kania, Š. Urban, H. Beckers and H. Willner, *J. Mol. Spectrosc.* **243**, 292 (2007).

<sup>108</sup> A. Perrin M. Strižák, H. Beckers, H. Willner, Z. Zelinger, P. Pracna, V. Nevrlý and E. Grigorová, *Mol. Phys.* **108**, 723 (2010).

<sup>109</sup> H. Beckers, H. Willner, D. Grote, W. Sander and J. Geier, *J. Chem. Phys.* **128**, 224301 (2008).

<sup>110</sup> L. Kolesníková, J. Varga, H. Beckers, M. Šimečková, Z. Zelinger, L. N. Strítěská, P. Kania, H. Willner and Š. Urban, *J. Chem. Phys.* **128**, 224302 (2008).

several transitions. The transitions are split into two electron spin-rotation components corresponding to  $J = N \pm \frac{1}{2}$ . Since hyperfine interactions are not resolved in the spectrum, the total Hamiltonian was decomposed into two parts:

$$H = H_{Rot} + H_{SR},$$

where  $H_{Rot}$  and  $H_{SR}$  denote the Watson rotational Hamiltonian<sup>111</sup> and the electron spin-rotation Hamiltonian (see Equation 1.2), respectively. Both are set in the  $\mathcal{A}$  reduction,  $I'$  representation and include their quartic centrifugal distortion terms. A least-squares analysis that includes more than 3300 rovibrational lines has been carried out. It led to the accurate determination of 15 molecular parameters that account for all the observed spectral features (see accompanying paper). The significant change of the  $\epsilon_{aa}$  parameter (+114%) in addition to the unusual, large variations of the quartic centrifugal distortion constants  $\delta_K$ ,  $\Delta_K$  and  $\Delta_{NK}$  (-10%, +26% and -1463%, respectively) complicated the analysis to some extent. The latter features associated with the observed low excited state frequency  $\nu_4^0$  (1094.142210 (31)  $\text{cm}^{-1}$ ) and the unusual large variations of the centrifugal distortion constants  $\Delta_K$  and  $\Delta_{NK}$  support the predicted strong *pseudo* Jahn-Teller interaction that mixes the ground electronic state  ${}^2B_2$  with the low lying excited state  ${}^2A_1$  (1.630 eV) *via* the excitation of the  $\nu_4$  vibration.

---

<sup>111</sup> R. N. Zare in: *Angular Momentum* (Wiley-Interscience, New York, 1988) and references therein.

# Article in Preparation for *J. Mol. Spectrosc.*:

## Title

High-resolution FTIR study of the CO stretching band  $\nu_4$  of the fluoroformyloxy radical, FCO<sub>2</sub>; evidence for the strong pseudo Jahn-Teller effect.

## Authors

S. Bailleux<sup>a,\*</sup>, E. Grigorová<sup>a</sup>, Z. Zelinger<sup>b</sup>, H. Beckers<sup>c,\*</sup> and H. Willner<sup>c</sup>

<sup>a</sup> Laboratoire de Physique des Lasers, Atomes et Molécules, CERLA, UMR CNRS 8523, Université de Lille 1, F-59655 Villeneuve d'Ascq Cedex, France

<sup>b</sup> J. Heyrovský Institute of Physical Chemistry, Academy of Sciences of the Czech Republic, Dolejškova 3, 182 23 Prague 8, Czech Republic

<sup>c</sup> Bergische Universität Wuppertal, FB 9, Anorganische Chemie, Gaußstr. 20, 42097 Wuppertal, Germany

\* Corresponding authors. E-mail addresses: [stephane.bailleux@univ-lille1.fr](mailto:stephane.bailleux@univ-lille1.fr) (S. Bailleux); [beckers@uni-wuppertal.de](mailto:beckers@uni-wuppertal.de) (H. Beckers) – Fax : +33 3 2033 7020 (S. Bailleux) ; +49 202 439 3053

## Abstract

The  $\nu_4$  unperturbed, fundamental band ( $\text{CO}_2$  antisymmetric stretching mode) of the  $\text{FCO}_2$  radical in the ground electronic state  $\tilde{X}^2B_2$  has been recorded by Fourier-transform infrared spectroscopy at an effective resolution of  $0.003\text{ cm}^{-1}$  between  $1040\text{--}1130\text{ cm}^{-1}$ .  $\text{FCO}_2$  was generated by vacuum flash pyrolysis at about  $600^\circ\text{C}$  of  $\text{FC(O)OO(O)CF}$ . More than 3300 ro-vibrational transitions have been assigned, which involved levels with  $N'$  up to 56 and  $K'_a$  up to 38. The observed Doppler-broadened spectrum was analyzed to yield accurate values of the band origin ( $1094.142210(31)\text{ cm}^{-1}$ , one standard error in parentheses), the rotational constants, the quartic centrifugal distortion constants and electron spin-rotation interaction parameters in the  $\nu_4 = 1$  state. The unusual low vibrational frequency of this band, and the large variations of the centrifugal distortion parameters  $\Delta_K$  (+26 %),  $\Delta_{NK}$  (−1463 %) and  $\delta_K$  (−10 %) upon excitation of the  $\nu_4$  vibration are ascribed to a pseudo Jahn-Teller interaction that couples the ground electronic state with the low lying electronic state  $\tilde{B}^2A_1$  (1.630 eV) through the  $\text{CO}_2$  antisymmetric vibration.

### *Keywords:*

fluoroformyloxyl radical; high resolution Fourier-transform infrared spectrum; ro-vibrational analysis; pseudo Jahn-Teller interaction

## 1. Introduction

In recent years, the fluoroformyloxy radical has attracted much attention, particularly in the field of stratospheric chemistry, since it is one of the key intermediate species involved in the degradation of hydrofluorocarbons (HFCs) that came into replacements for the ozone-depleting chlorofluorocarbons (CFCs) and the hydrochlorofluorocarbons (HCFCs) [1]. Aside from atmospheric concerns, the study of fluorinated compounds, stable and reactive (radicals and non-radicals) as well, is also significant because they are involved in synthetic chemistry and in residual fumes of flames treated with fluorinated fire extinguishers [2].

$\text{FCO}_2$  is a very intriguing radical since in the series  $\text{XCO}_2$ , with  $X = \text{H, F, Cl, Br, and I}$ , only the fluorinated species is known experimentally. The parent formyloxy radical,  $\text{HCO}_2$ , has a negative C–H bond-dissociation energy [3] and other halogenated radicals ( $X = \text{Cl, Br or I}$ ) are very weakly bound van der Waals complexes, with C–X bond energies in the range  $0.5\text{--}1 \text{ kcal.mol}^{-1}$  [4]. Although the C–F bond dissociation energy of  $\text{FCO}_2$  ( $11.5 \text{ kcal.mol}^{-1}$ ) [4] is much smaller than other known C–F chemical bonds ( $\sim 100 \text{ kcal.mol}^{-1}$ ), its relative strengths makes  $\text{FCO}_2$  a rather long-lived radical with a half-life of at least 3 s with respect to dissociation at room temperature and in 700 Torr of air [5].

The importance of the fluoroformyloxy radical in various chemical processes [2,6,7] has stimulated a number of experimental studies. Maricq *et al.* have recorded [8] the visible absorption spectrum of  $\text{FCO}_2$  which was assigned to the  $\tilde{B}^2 A_1 \leftarrow \tilde{X}^2 B_2$  transition. Argüello *et al.* have reported [9] the analysis of the visible and IR spectra of  $\text{FCO}_2$  isolated in inert gas matrices, leading to the assignment of all six fundamental vibrations on the basis of  $C_{2v}$  symmetry. This radical has only recently been detected by high-resolution millimetre wave and infrared spectroscopy in the gas-phase [10,11,12]. The latter millimetre wave study [12] includes details on the fine and hyperfine structures that are supported by the recent analysis of the electron paramagnetic resonance (EPR) spectrum of  $\text{FCO}_2$  [13]. From the theoretical point of view, difficulties in the quantum chemical treatment arise from the favourable coupling of low-lying electronic states (often encountered in radicals) through the nuclear motion. These problems have been analyzed in details [14,15]. Briefly, when a nearby electronic state with a symmetry different from that of the ground state is present, non-symmetric distortions of the nuclear framework give rise to the pseudo Jahn-Teller interaction

[16,17,18,19,20]. In particular, these studies [14,15] revealed that such a strong interaction is susceptible to occur with the nearby  $\tilde{B}^2A_1$  state lying 1.630 eV above the ground state [8] upon excitation of the  $\omega_4$  mode (C–O antisymmetric vibration).

As part of the effort to understand the environmental impact of the degradation of HFCs, and since the knowledge on FCO<sub>2</sub> and other oxyradicals is rather scarce, this work is devoted to the analysis of the  $\nu_4$  unperturbed fundamental band (antisymmetric C–O stretching vibration) measured by Fourier-transform infrared spectroscopy. It is believed that this work will favour its spectroscopic detection in the upper atmosphere in the near future. This analysis awaited the accurate determination of the molecular constants of the radical in the  $\tilde{X}^2B_2$  ground electronic state that are now available [10,11,12].

## 2. Experimental details

The fluoroformyloxyl radical was generated by vacuum flash pyrolysis of the FC(O)OO(O)CF precursor [10] at a temperature of about 600°C. As described earlier [10], the gas phase infrared spectrum of flowing FCO<sub>2</sub> radical in N<sub>2</sub> was investigated, with a backing pressure of 0.6 bar and a total cell pressure of 1.34 mbar. Several fundamental and combination bands ( $\nu_6 \sim 735 \text{ cm}^{-1}$ ,  $2\nu_5 \sim 948 \text{ cm}^{-1}$ ,  $\nu_2 \sim 970 \text{ cm}^{-1}$  and  $\nu_4 \sim 1094 \text{ cm}^{-1}$ ) were recorded between 600 and 1500  $\text{cm}^{-1}$  with the Brüker 120 HR interferometer at Wuppertal. A multipass cell outfitted with BaF<sub>2</sub> windows and adjusted to a path length of 32 m was employed. The achieved resolution (1/maximum optical path difference) was about the Doppler width (0.003  $\text{cm}^{-1}$ ) and altogether 60 scans were co-added to obtain the final spectrum. The signal to noise ratio of the power spectrum was ca. 20:1. Calibration was done by comparison with CO<sub>2</sub> lines [21] applying the corrections according to Ref. [22].

## 3. Description of the spectrum

The  $\nu_4$  perpendicular band (reproduced in Fig. 1), associated to the antisymmetric C–O stretching mode, covers the 1050–1122  $\text{cm}^{-1}$  spectral range with a band origin near 1094  $\text{cm}^{-1}$ . It is the second strongest absorption band of FCO<sub>2</sub>.

*P*- and *R*-branch transitions of medium intensity (about 30 percent absorption at maximum) dominate the spectrally dense regions of close-lying lines of

the  $^{p,r}Q$ -branches (mainly within  $\pm 10 \text{ cm}^{-1}$  of the band origin). These transitions reveal regular cluster structures spaced with an interval of  $0.41\text{--}0.48 \text{ cm}^{-1}$ . The apparent random intensity distribution of the lines within each cluster is ascribed i) to the electron spin-rotation interaction causing accidental overlaps and ii) to the fact that each cluster is blue-shaded in both  $P$ - and  $R$ - branches, featuring a cluster head at the low wavenumber limit.

Indeed, rotational analysis reveals that each cluster is made up of a series of low  $K_a''$  lines corresponding to a constant  $2N'' - K_c''$  value with  $K_c''$  being either even or odd in two consecutive clusters. The transitions then originate from the following ground state vibrational levels (denoted  $N''_{K_a'', K_c''}$ ):

$$\begin{aligned} & (2N'' - K_c'')_{1, N''}, (2N'' - K_c'' - 1)_{1, N''-1}, (2N'' - K_c'' - 2)_{3, N''-2}, \\ & (2N'' - K_c'' - 3)_{3, N''-3} \text{ etc.} \end{aligned}$$

Each of these transitions is actually a doublet because of the electron spin-rotation interaction. While the fine splitting increases with  $N''$ , the lines pile up to the lower wavenumbers and turn around at the cluster head. A sample region of the  $P$ -branch comprising two clusters is shown in Fig. 2. The strongest line is the  $K_c'' = N''$  doublet and line strengths fade as  $N'' - K_c''$  increases. As  $N''$  further increases the fine splitting grows substantially and the lines then lie to the red, as is shown in Fig. 3 for the  $2N'' - K_c'' = 35$  (expanded region of Fig. 2). The partly resolved, complex pattern of the clusters could not be understood until the rotational constants, the quartic centrifugal distortion parameter  $\Delta_{NK}$  and the electron spin-rotation interaction parameters were precisely obtained by least-squares analysis. In the rigid rotor approximation, the series of clusters is expected to run with [23]  $\nu_{N''} \approx \nu_0 + (C' - C'')N''^2 \pm C'(2N'' \pm 1) \pm A'$  (+/- for the  $R$ - and  $P$ -branches, respectively). The spacing between two clusters is then given by  $\nu_{N''+1} - \nu_{N''} \approx (C' - C'')(2N'' + 1) \pm 2C'$ , and equals  $-0.452 \text{ cm}^{-1}$  for  $N'' = 34$  in the  $P$ -branch, which compares very well with the observed interval ( $-0.454 \text{ cm}^{-1}$ , Fig. 2).

In addition, series of relatively strong doublets unrelated to the  $2N'' - K_c''$  clusters run through the  $P$ - and  $R$ -branches and constitute another striking feature of the  $\nu_4$  band. These series are composed of evenly spaced doublets (by about  $0.58$  and  $0.68 \text{ cm}^{-1}$  in the  $P$ - and  $R$ -branches, respectively) arising from the fine

splittings of the energy levels. The transitions correspond to levels with  $K_a'' \approx N''$ ,  $K_c'' \approx 0$  and continue to have noticeable intensity in the far wings of the band where the clusters vanish. For a given series, as  $N''$  increases,  $K_a''$  is a constant (with odd values, see next section) and the line strengths decrease. Each component of the doublets is actually made up from the overlap of two nearly degenerate transitions ( $K_c$  degeneracy) which are resolved for  $K_c'' \geq 4$ . The two

doublets designated  ${}^p P_{15, (1,2)}$  (16) ( $1078.8940 \text{ cm}^{-1}$ ,  $1078.9364 \text{ cm}^{-1}$ ), and

${}^p P_{15, (0,1)}$  (15) ( $1079.4769 \text{ cm}^{-1}$ ,  $1079.5188 \text{ cm}^{-1}$ ) in Fig. 2 belong to such a series with  $K_a'' = 15$ . The generally adopted notation for individual transitions is

$\Delta K_a \Delta N_{K_a'', K_c''} (N'')$  where  $\{\Delta K_a, \Delta N\} = -1, 0, +1$  are represented by  $p, q$  and  $r$  for  $\Delta K_a$  and by  $P, Q$  and  $R$  for  $\Delta N$ . These doublets derive their intensity from the fact that, for low  $K_c''$  values, the regular cluster structure collapses as the energy levels  $N''_{N''-K_c'', K_c''}$  and  $N''_{N''-K_c'', K_c''+1}$  with a given value of  $K_a'' = N'' - K_c''$  become systematically degenerate. These lines constitute 20 percent of the number of lines included in the fit. The transition frequencies of this series follows [23]

$$\nu_{N'', K_c''} \approx \nu_0 + (A' - A'')N''^2 + 2A'(N'' + 1) - (A' - 2C')(2K_c'' + \lambda) - C' \text{ and}$$

$$\nu_{N'', K_c''} \approx \nu_0 + (A' - A'')N''^2 - 2A'N'' + (A' - C')(2K_c'' + \lambda) \text{ for the } R\text{- and } P\text{-}$$

branches, respectively, where  $\lambda = \Delta K_c = \pm 1$  ( $\Delta K_c = +1$  and  $-1$  correspond to levels with  $K_a'' + K_c'' = N''$  and  $K_a'' + K_c'' = N'' + 1$ , respectively). The spacing

between two consecutive series is then given by  $\nu_{N''+2, K_c''} - \nu_{N'', K_c''} \approx$

$$4[(A' - A'')(N'' + 1) \pm A'] \text{ while that between two consecutive doublets is}$$

$$\text{equal to } \nu_{N''+1, K_c''+1} - \nu_{N'', K_c''} \approx (A' - A'')(2N'' + 1) \pm \zeta C', \text{ with } \zeta = 4 \text{ and } 2 \text{ for}$$

the  $R$ - and  $P$ - branches, respectively. In the  $P$ -branch, the intervals between two series and between two doublets have been calculated for  $N'' = 15$ . They are equal to  $-2.16$  and  $-0.58 \text{ cm}^{-1}$ , respectively, again in good agreement with the observed values (see Fig. 2 for the spacing between two doublets).

The somewhat weaker  ${}^{p,r} Q$ -branches extend widely on the  $P$ - and  $R$ -branches and the region between  $1088$  and  $1102 \text{ cm}^{-1}$  is much more congested than the  $P$ - and  $R$ -branch regions. A part of the  ${}^r Q$ -branch is plotted in Fig. 4.

Nonetheless, in the initial stages of the least-squares analysis, we proceeded the assignment of the spectrum with weak, but well isolated  $^{p,r}Q$ -branches lines located near the band origin as described in the following section.

#### 4. Assignments and analysis

The FCO<sub>2</sub> radical is a very asymmetric, oblate rotor ( $\kappa = +0.35$ ) belonging to the  $C_{2v}$  point group. The presence of the two indistinguishable oxygen nuclei ( $I_{^{16}O} = 0$ ) requires that the molecular wave function ( $\psi_{elec} \times \psi_{rot} \times \psi_{vib} \times \psi_{ns}$ ) obeys the Bose-Einstein statistics. The ground vibronic component of the wavefunction has  $b_2 \times a_1 = b_2$  symmetry. Therefore, according to the Pauli exclusion principle (the total wavefunction must have even parity with respect to the molecular  $a$ -axis), only rovibrational levels with odd  $K_a$  values have nonzero spin statistical weight. This statement is just reversed for the first excited state of the antisymmetric stretching vibration, i.e., since the  $\nu_4 = 1$  level has  $b_2$  vibrational symmetry, only rovibrational levels with even  $K_a$  values are allowed. Thus, a pure  $b$ -type infrared spectrum is expected and all transitions are of the type  $\{\Delta K_a, \Delta K_c\} = \pm 1$ .

The  $\nu_4$  band is well separated from other bands and revealed no perturbation. Many of the observed transitions showed relatively clear evidence of electron spin-rotation splittings. Although half of the transitions are missing due to the nuclear spin statistics the whole spectrum remains very congested (except on the far wings of the  $P$ - and  $R$ - branch regions), and most of the lines are actually blended due to an overlap of several transitions. Hyperfine interactions are not resolved in the spectrum, thus the total Hamiltonian was decomposed into :

$$\mathcal{H} = \mathcal{H}_{Rot} + \mathcal{H}_{SR}$$

where  $\mathcal{H}_{Rot}$  and  $\mathcal{H}_{SR}$  denote the Watson rotational Hamiltonian [24,25] and the spin-rotation Hamiltonian [24,26], respectively. Both are set in the  $A$  reduction and  $I'$  representation and include their quartic centrifugal distortion terms.

Hund's case  $b$  like coupling scheme (the rotational  $N$  and the electron spin  $S$  are coupled to form the resultant total angular momentum  $J$ ) is appropriate to describe the spectrum. The majority of the observed transitions are the strongest of the allowed  $\Delta J = \Delta N$  transitions.

To carry out the analysis, all calculations were implemented using Pickett's CALPGM spectroscopy package [27]. Initial simulation of the  $\nu_4$  band was done using molecular parameters in the  $\nu_4 = 1$  state identical to those of the vibrational

ground state, but the obtained calculated spectrum bore only a poor resemblance to the observed one. The high density of lines combined with the complex patterns of the recorded clusters and the uncertainty as to absolute  $N''$  prohibited the assignment of  $P$ - and  $R$ -branch transitions at this initial step. As mentioned in the previous section, the  $^{p,r}Q$ -branches exhibit also a complex nature, preventing again straightforward assignments of  $^{p,r}Q$ -branches transitions. However around the band origin  $^{p,r}Q$ -branches transitions are scarce. Therefore, we focused our initial assignments exclusively on weak but well identified rovibrational doublets of transitions frequencies occurring near the band origin. Nonetheless, the analysis required many iterations that consisted of enlarging the number of assignments based on the predicted line positions and intensities, and molecular constants optimizations followed with simulations until a good correspondence between the calculated and experimental spectra was found.

A weighted nonlinear least-squares fit was performed, with vibrational ground state constants fixed at previously determined millimetre wave values [12]. Unitary weights were given to isolated lines, whereas for lines with multiple assignments, the transitions were intensity-weighted. Experimental uncertainties of  $0.5 \times 10^{-3} \text{ cm}^{-1}$  were attributed to single, well isolated lines and the wave-number accuracy of non resolved, blended lines were adjusted according to the observed linewidth. Almost all  $\nu_4$  transitions of  $\text{FCO}_2$  that could be unambiguously identified in the spectrum were assigned. In cases where the two  $K_c''$  components of a transition coincide, both were included in the data set with unitary weight. In total, 3310 infrared transitions were subjected to the least-squares analysis using 15 adjustable parameters in the  $\nu_4 = 1$  state, while 18 lines, whose transitions frequencies deviated from their calculated values more than 3.3 times their experimental uncertainty, were discarded. All assigned lines obey  $b$ -type selection rules. The absolute  $N''$  assignments were confirmed by ground state combination differences. The quantum numbers of the assigned transitions span the range  $N' = 0 - 56$ ,  $K'_a = 0 - 38$  ensuring a precise determination of all quartic centrifugal distortion constants. The standard deviation of the fit is  $0.00046 \text{ cm}^{-1}$ , which is slightly below the experimental error. Inclusion of higher order centrifugal distortion parameters did not reduce the standard deviation of the fit. The obtained parameters are relatively well uncorrelated, most of the correlation coefficients being under 0.6.

## 5. Results and discussion

Essentially, all the spectral features were reproduced, with Fig. 2 and Fig. 4 showing as examples the high fidelity with which the experimental spectra were simulated. The rotational and quartic centrifugal distortion constants together with the band origin for the  $\nu_4$  fundamental band of FCO<sub>2</sub> determined in this work are listed in Table 1. They are generally consistent with those of the vibrational ground state [12] which are also given in Table 1. The inertial defects  $\Delta$  ( $= I_c - I_a - I_b$ ) for the two states (Table 1) are both small and positive with the value in the vibrationally excited state (+0.061 amu Å<sup>2</sup>) being almost three times smaller than that in the ground state (+0.176 amu Å<sup>2</sup>).

Inspection of Table 1 reveals that the ( $B + C$ ) rotational constants in the ground and in the  $\nu_4 = 1$  states are almost identical ( $0.58395 \text{ cm}^{-1}$ ,  $\Delta_{B+C} \approx +0.018\%$ ) and that the  $A$  rotational constant decreases significantly ( $-1.2\%$ ) upon excitation of the antisymmetric stretching mode. In contrast, it is worth noting that the quartic centrifugal distortion constant  $\Delta_K$  increases substantially by  $135 \cdot 10^{-9} \text{ cm}^{-1}$  ( $+26\%$ ) while  $\Delta_{NK}$  decreases by a similar amount,  $-146 \cdot 10^{-9} \text{ cm}^{-1}$  ( $-1463\%$ ). The difference of  $\delta_K$  is smaller but still amounts to about  $-10\%$ . For comparison, the corresponding differences of  $\Delta_K$  ( $+16 \cdot 10^{-9} \text{ cm}^{-1}$ ) and  $\Delta_{JK}$  ( $-17 \cdot 10^{-9} \text{ cm}^{-1}$ ) of the related molecule FNO<sub>2</sub> were found to be one order of magnitude smaller (note that the III<sup>l</sup> representation was used in this work) [28].

The distortion coefficients obtained for the ground vibrational state are known to be effective values which contain contributions from a vibrational averaging primarily of the lower frequency vibrational modes, and their vibrational dependences have well been studied. For a planar asymmetric rotor molecule such as FCO<sub>2</sub>, the five quartic distortion coefficients obtained with the  $A$  reduction may be expressed in terms of seven distortion constants  $\tau_{\alpha\beta\gamma\delta}$ , where the subscripts  $\alpha, \beta$ , and  $\gamma, \delta$  denote pairs of the molecular principal axes  $a, b$ , and  $c$ . Appropriate planarity relations reduce the number of independent  $\tau$ 's to four, e. g.  $\tau_{aaaa}$ ,  $\tau_{bbbb}$ ,  $\tau_{aabb}$ , and  $\tau_{abab}$  [23,29]. Because of symmetry, only  $\tau_{abab}$  is expected to carry a vibrational dependence on  $\nu_4$  ( $b_2$ ) implying that i) only  $\Delta_{NK}$ ,  $\Delta_K$  and  $\delta_K$  are affected and ii)  $\Delta_{NK}$  and  $\Delta_K$  change by a similar magnitude, but with opposite signs [23,29]. These relations are well satisfied by the observed variations in the distortion constants with excitation of  $\nu_4$ .

In addition, two possible explanations may account for the particular large amplitude variation of these distortion constants when the  $\nu_4$  mode is excited: i) a

$c$ -type Coriolis interaction between  $\nu_4$  and  $2\nu_3$  where the wavenumber of  $2\nu_3$  is estimated from a matrix IR study [9] to be about  $2 \times 519 = 1038 \text{ cm}^{-1}$  and ii) a vibronic interaction [16,17,18,19,20] of the ground electronic state with the nearby  $\tilde{B}^2A_1$  electronic state [8] (1.630 eV,  $13150 \text{ cm}^{-1}$ ).

During our assignment procedure, no local perturbation was detected and the  $\nu_4$  level appeared to be unperturbed. On the other hand, recent *ab initio* studies [14,15] revealed a strong vibronic interaction between the ground  $^2B_2$  and the lowest excited  $^2A_1$  electronic states of FCO<sub>2</sub> through the antisymmetric C–O stretching deformation. When the radical is distorted along the  $b_2$  stretching coordinate the molecular symmetry reduces from  $C_{2v}$  to  $C_s$  and both these electronic states have  $^2A'$  symmetry. Such a vibronic perturbation of the ground state  $\nu_4$  level is in accord with the unusual low wavenumber  $\nu_4^0$  compared to  $\nu_1^0$  ( $1475 \text{ cm}^{-1}$ ) [9]. The matrix-isolation study [9] also revealed a negative anharmonicity of this vibration, i. e.  $2\nu_4$  appeared at a higher wavenumber ( $2233 \text{ cm}^{-1}$ ) than twice the fundamental ( $1098 \text{ cm}^{-1}$ ), and a rather high intensity of this overtone of about 18% of the fundamental was observed. These experimental observations support the predicted strong pseudo Jahn-Teller interaction with the nearby  $\tilde{B}^2A_1$  electronic state. As  $\tau_{\text{abab}}$  is related to the quadratic force constant of the antisymmetric  $b_2$  vibrations, it is thus consistent to conclude that the large changes observed for  $\Delta_{NK}$  and  $\Delta_K$  can predominantly be attributed to this strong vibronic interaction.

The three electron spin-rotation constants  $\varepsilon_{\alpha\alpha}$  of the  $\nu_4$  state in the principal inertial axis system have also been accurately determined together with the three parameters describing their centrifugal distortion correction  $\Delta_N^S$ ,  $\Delta_{NK}^S$ , and  $\Delta_K^S$ . [Table 2](#) provides the values obtained in this study and those in the ground state as well for comparison. The reduced electron spin-rotation parameters with the corresponding rotational constants are also given ([Table 2](#)). The spin-rotation terms  $\varepsilon_{\alpha\alpha}$  and their quartic centrifugal distortion corrections are consistent with those of the ground vibrational state. More precisely, when the  $\nu_4$  vibration is excited, the magnitude of  $\varepsilon_{cc}$  increases slightly ( $+0.11 \cdot 10^{-3} \text{ cm}^{-1}$ , +8%) and both  $\varepsilon_{aa}$  and  $\varepsilon_{bb}$  decrease by a similar magnitude,  $3.2 \cdot 10^{-3}$  and  $2.0 \cdot 10^{-3} \text{ cm}^{-1}$ , respectively (corresponding to the relative variations  $-114\%$  and  $-7.5\%$ ). The same

observation can be made (Table 2) for  $\varepsilon_{aa}/A$  and  $\varepsilon_{bb}/B$ , whose magnitudes decrease by  $7.1 \cdot 10^{-3}$  and  $5.1 \cdot 10^{-3}$ , respectively (corresponding to the relative variations  $-117\%$ , and  $-7\%$ ). It is tempting to explain, at least qualitatively, the observed values and their changes. It is well known that the dominant contributions to the spin-rotation parameters arise from the second order mixing of electronic states by spin-orbit and Coriolis couplings [26,30]; they are expressed with the following formula:

$$\varepsilon_{\alpha\alpha} \approx -4 \sum_n \frac{k_n \langle 0 | A_{\text{SO}} L_\alpha | n \rangle \langle n | B_\alpha L_\alpha | 0 \rangle}{E_0 - E_n} \quad (1)$$

in which  $|0\rangle$  and  $|n\rangle$  are ground- and excited-state vibronic wave functions at energies  $E_0$  and  $E_n$ , respectively.  $L_\alpha$  stands for the  $\alpha$  component of the orbital angular momentum about the molecular center of gravity,  $B_\alpha$  denotes the rotational constant along the  $\alpha$  inertial molecular axis, and  $k_n$  is either  $+1$  or  $-1$  according to whether the  $|0\rangle \rightarrow |n\rangle$  excitation occurs to an unoccupied orbital or to a singly occupied orbital [30]. The effective spin-orbit coupling constant of  $\text{FCO}_2$ ,  $A_{\text{SO}}$ , can reasonably be approximated by the experimental fine-structure splitting between the  $^3P_2$  and  $^3P_1$  states of atomic oxygen,  $158.3 \text{ cm}^{-1}$  [31], because the unpaired electron is shared equally between the two oxygen atoms [14]. Eq. (1) then predicts the  $\varepsilon_{\alpha\alpha}$  constants to be proportional to the rotational constants when the  $B_\alpha$  are independent of the vibronic coordinates. The ground electronic state has symmetry  $B_2$  under the group  $C_{2v}$  and the operator  $L_\alpha$  belongs to the representation  $A_2$ , therefore excited states which contribute to  $\varepsilon_{aa}$  must be of  $B_1$  symmetry. Similar symmetry considerations (the  $b$  and  $c$  components of the orbital angular momentum belong to  $B_1$  and  $B_2$  species, respectively) show that the  $\varepsilon_{bb}$  and  $\varepsilon_{cc}$  constants can only receive contributions from excited electronic states of  $A_2$  and  $A_1$  symmetry, respectively.

The  $\varepsilon_{\alpha\alpha}$  constants can then be calculated with the assumption that the matrix element of the orbital angular momentum is  $1/\sqrt{2}$  because the single occupied molecular orbital is described as a linear combination of the oxygen in-plane  $p_z$  and  $p_y$  orbitals (see Eq. (8) of Ref. [13]). They are presented in Table 2, when only one excited state is taken into account in Eq. (1). The  $E_n$  experimental values  $13150 \text{ cm}^{-1}$  (1.630 eV) for the  $\tilde{B}^2A_1$  [8] and  $4670 \text{ cm}^{-1}$  (0.579 eV) for the

$\tilde{A}^2 A_2$  [4] states have been employed while the calculated value  $47600 \text{ cm}^{-1}$  (5.90 eV) for the  ${}^2 B_1$  [4] state has been used. While the derived values for the  $\varepsilon_{aa}$  and  $\varepsilon_{bb}$  constants are in good agreement with the experimental ones, that for  $\varepsilon_{cc}$  is about 3.4 times that of the experimental one. The  $\varepsilon_{aa}$  and  $\varepsilon_{cc}$  constants are of similar magnitude and Eq. (1) shows that the large magnitude of  $\varepsilon_{bb}$  can mainly be attributed to the admixture with the low-lying  $\tilde{A}^2 A_2$  state at  $4670 \text{ cm}^{-1}$  [4].

The following vibrational dependence of the  $\varepsilon_{aa}$  and  $\varepsilon_{bb}$  constants with excitation of  $\nu_4$  is suggested. According to Eq. (1) the variation of these constants can be due to i) a change in the electronic excitation energy  $E_0 - E_n$ , and/or ii) a variation of the nature of the single occupied molecular orbital in the two states involved. The influence of the first change is obvious, and the latter variation may change the matrix element of the orbital angular momentum from  $1/\sqrt{2}$  up to 1.0. The important point is that the matrix elements for  $\varepsilon_{aa}$  and  $\varepsilon_{bb}$  involve a promotion of an electron from the oxygen  $p_\pi$  orbitals ( $p_x^1 + p_x^2$ ) ( $b_1$ ), and ( $p_x^1 - p_x^2$ ) ( $a_2$ ), respectively, into the half-filled  $b_2$  orbital (atomic orbitals for the two oxygens are distinguished by superscripts). When the molecular symmetry is reduced from  $C_{2v}$  to  $C_s$  upon excitation of the  $\nu_4$  vibration, the corresponding electronic excited states  ${}^2 B_1$  and  ${}^2 A_2$  both have  ${}^2 A''$  symmetry and may repel each other. Furthermore, the oxygen  $p_\pi$  orbitals ( $p_x^1 + p_x^2$ ) ( $a''$ ) and ( $p_x^1 - p_x^2$ ) ( $a''$ ) in these states will also mix and these orbitals will be polarized, with the result that the unpaired electron in the electronic states involved is more localized at the oxygen atom with the longer CO bond. Thus, both these excitation energies and the nature of the molecular orbitals are changed upon the antisymmetric vibration, and it is hard to predict even qualitatively these effects on the  $\varepsilon_{aa}$  and  $\varepsilon_{bb}$  constants.

## 6. Conclusion

The first analysis of the  $\text{CO}_2$  asymmetric stretching mode of the  $\text{FCO}_2$  radical has been performed and the inclusion of more than 3300 rovibrational lines in the least-squares analysis led to the determination of the band origin together with the rotational constants, including their quartic centrifugal distortion effects as well as the electron spin-rotation interaction parameters. In total, 15 molecular parameters have been precisely obtained that account for all of the observed

spectral features. A low excited state frequency  $\nu_4^0$  and the unusual large variations of the centrifugal distortion constants  $\Delta_{NK}$ , and  $\Delta_K$  support the predicted strong pseudo Jahn-Teller interaction that mixes the ground electronic state  ${}^2B_2$  with the low lying excited state  ${}^2A_1$  (1.630 eV) via the excitation of the  $\nu_4$  vibration.

A similar vibronic interaction is expected to occur upon excitation of the  $\text{CO}_2$  wag mode ( $\omega_6$  out-of-plane vibration) arising from the coupling of the ground electronic state with the low-lying  ${}^2A_2$  excited electronic state (0.579 eV). The analysis of the  $\nu_6$  band ( $735\text{ cm}^{-1}$ ) will be the subject of another publication.

### **Acknowledgments**

S. B. gratefully acknowledges the support for this work by the INTROP program via the Grant No. 1051 and the ARCUS (Actions en Régions de Coopération Universitaire et Scientifique) 2005 program. The work was also supported through the QUASAAR network. The CERLA (FEDER 2416) is partly supported by the French Research Ministry, the Nord-Pas-de-Calais Region, and the European Funds for Regional Economic Development.

### **Appendix A. Supplementary data**

Supplementary data for this article are available on ScienceDirect (<http://www.science.direct.com>) and as part of the Ohio State University Molecular Spectroscopy Archives ([http://msa.lib.ohio-state.edu/jmsa\\_hp.htm](http://msa.lib.ohio-state.edu/jmsa_hp.htm)).

**Table 1**

Band origin, rotational and quartic centrifugal distortion constants (in  $\text{cm}^{-1}$ , except otherwise stated) for the ground vibrational and the  $\nu_4 = 1$  states of  $\text{FCO}_2$  in  $\tilde{X}^2B_2$  ( $A$  reduction,  $I^r$  representation).

<i>constants</i>	<i>G.S.</i> <sup>a</sup>	$\nu_4 = 1$
$\nu_0$		1094.142210 (31) <sup>b</sup>
$A$	0.458 724 842 (58) <sup>b</sup>	0.453 327 285 (210)
$B$	0.377 271 605 (39)	0.377 979 826 (217)
$C$	0.206 569 549 (6)	0.205 965 743 (67)
$10^6 \times \Delta_N$	0.26074 (15)	0.25915 (12)
$10^6 \times \Delta_{NK}$	-0.00992 (61)	-0.15509 (43)
$10^6 \times \Delta_K$	0.51763 (62)	0.65278 (36)
$10^6 \times \delta_N$	0.11263 (7)	0.11948 (6)
$10^6 \times \delta_K$	0.35841 (17)	0.32396 (11)
<i>Inertial defect</i> (amu $\text{\AA}^2$ )	+0.176	+0.061
<i>Number of data</i>		3310
$10^3 \times \sigma(\text{fit})$		0.46

<sup>a</sup> Ref [12].

<sup>b</sup> One standard deviation between parentheses.

**Table 2**

Electron spin interaction parameters (in  $\text{cm}^{-1}$ , except for the reduced spin-rotation constants) for the ground vibrational and the  $\nu_4 = 1$  states of  $\text{FCO}_2$  in  $\tilde{X}^2B_2$  (A reduction,  $\Gamma^r$  representation).

<i>parameter</i>	<i>G.S.</i>	<i>Calc.</i>	<i><math>\nu_4 = 1</math></i>
	<i>Obs.</i> <sup>a</sup>		<i>Obs.</i>
$\varepsilon_{aa}$	−0.002 7801 (27) <sup>b</sup>	−0.0031	−0.005 9540 (80) <sup>b</sup>
$\varepsilon_{aa}/A$	−0.006 0605		−0.013 1340
$\varepsilon_{bb}$	−0.026 5055 (20)	−0.0256	−0.028 5027 (48)
$\varepsilon_{bb}/B$	−0.070 2557		−0.075 4080
$\varepsilon_{cc}$	−0.001 4733 (3)	−0.0050	−0.001 5845 (44)
$\varepsilon_{cc}/C$	−0.007 1322		−0.007 6930
$10^6 \times \Delta_N^S$	0.1370 (34)		0.1362 (18)
$10^6 \times \Delta_{NK}^S$	0.299 (61)		0.299 <sup>c</sup>
$10^6 \times \Delta_{KN}^S$	−0.389 (57)		−0.245 (14)
$10^6 \times \Delta_K^S$	0.549 (18)		0.437 (18)
$10^6 \times \delta_N^S$	0.0685 (18)		0.0685 <sup>c</sup>
$10^6 \times \delta_K^S$	−0.1034 (61)		−0.1034 <sup>c</sup>

<sup>a</sup> Ref [12].

<sup>b</sup> One standard deviation between parentheses.

<sup>c</sup> Fixed to the ground state value.

**Fig. 1.**

Overview of the  $b$ -type band  $\nu_4$  of  $\text{FCO}_2$ .

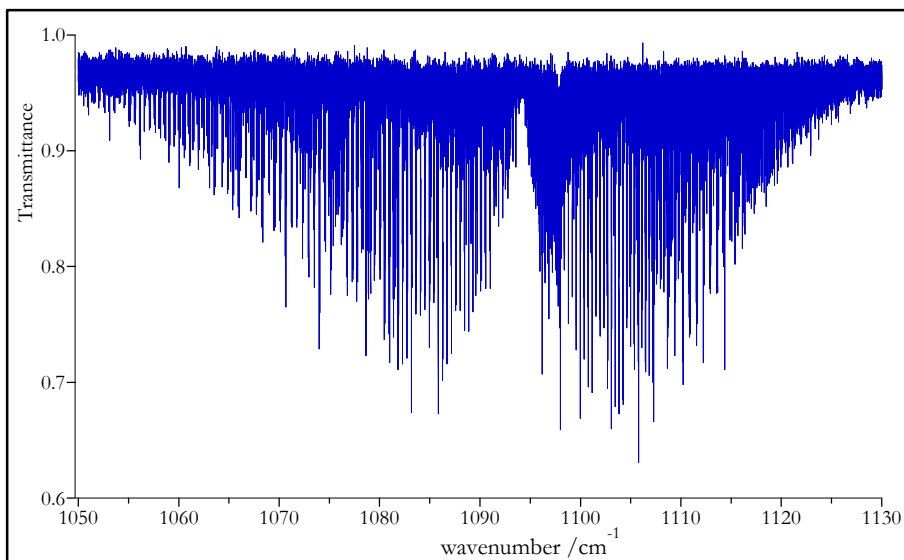


**Fig. 2.**

Part of the  $\nu_4$   $^pP$ -branch region of the  $\nu_4$  fundamental band of  $\text{FCO}_2$ . Experimental (upward) and simulated spectra (downward). The figure shows clusters for  $2N'' - K_c'' = 34$  and  $35$ , and selected doublets for  $K_a'' = 13$  and  $15$ . For these doublets the  $J''$  components are given, and for low  $K_c''$  the  $K$  components are pairwise coincident giving rise to particular strong lines in the spectrum. The splitting of the  $^pP_{15,(0,1)}(15)$  and  $^pP_{15,(1,2)}(16)$  doublets arises from electron spin-rotation interaction whereas the splittings of the  $^pP_{13}(17)$  transitions are due to both the  $K$ -type and the fine splitting.

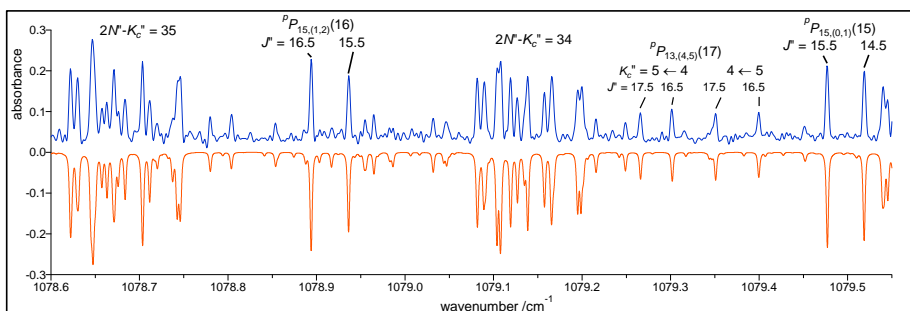


**Fig. 3.**

Experimental spectrum (downward) and calculated stick diagram (upward) showing an expanded view of the  $2N'' - K_c'' = 35$  cluster. The quantum number  $N''$  and the spin-rotation splittings within the cluster are indicated.

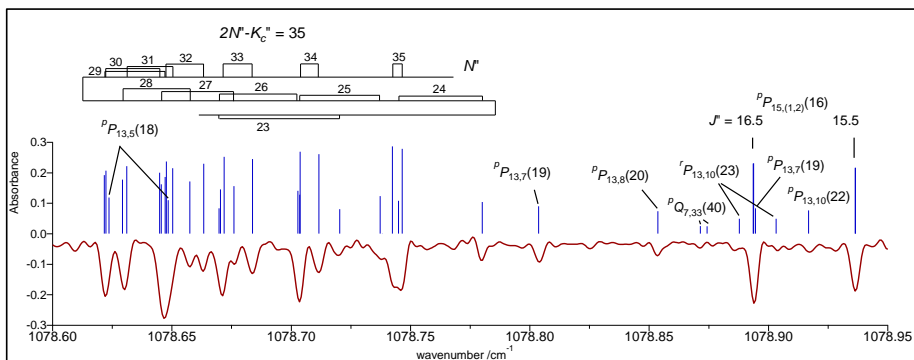
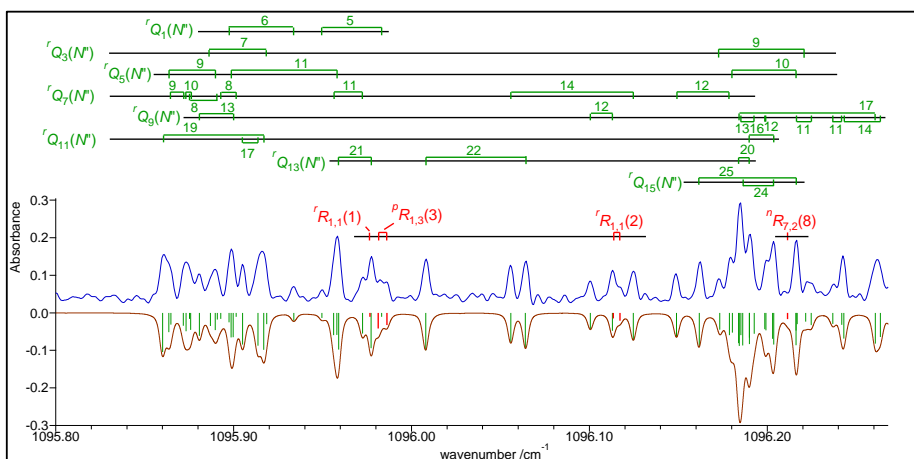


**Fig. 4.**

Part of the  $^r Q$ -branch region between 1095.80 and 1096.25  $\text{cm}^{-1}$  with the experimental spectrum upward (upper trace), and the calculated stick diagram downward (lower trace). The simulated spectrum (downward) is also shown.



## References

---

- [1] see <http://www.afeas.org>
- [2] S. von Ahsen, H. Willner, G.A. Argüello, *J. Flu. Chem.* 125 (2004) 1057–1070 and reference [7] of this paper: Emission of Greenhouse Gases in the United States 2005 – Executive Summary available at <http://www.eia.doe.gov/oiaf/1605/ggrpt/summary/index.html>, Energy Information Administration of the United States.
- [3] E.H. Kim, S.E. Bradford, D.W. Arnold, R.B. Metz, D.M. Neumark, *J. Chem. Phys.* 103 (1995) 7801–7814.
- [4] D.W. Arnold, S.E. Bradford, E.H. Kim, D.M. Neumark, *J. Chem. Phys.* 102 (1995) 3493–3509.
- [5] T.J. Wallington, M.D. Hurley, M.M. Maricq, *Chem. Phys. Lett.* 205 (1993) 62–68.
- [6] J.S. Francisco, M.M. Maricq, *Acc. Chem. Res.* 29 (1996) 391–397; J.S. Francisco, A.N. Goldstein, Z. Li, Y. Zhao, I.H. Williams, *J. Phys. Chem.* 94 (1990) 4791–4795.
- [7] T.J. Wallington, T. Ellerman, O.J. Nielsen, J.J. Sehested, *J. Phys. Chem.* 98 (1994) 2346–2356; M.M. Maricq, J.J. Szente, T.S. Dibble, J.S. Francisco, *J. Phys. Chem.* 98 (1994) 12294–12309; V. Mörs, G.A. Argüello, A. Hoffmann, W. Malms, E.P. Röth, R. Zellner, *J. Phys. Chem.* 99 (1995) 15899–15910.
- [8] M.M. Maricq, J.J. Szente, Z. Li, J.S. Francisco, *J. Chem. Phys.* 98 (1993) 784–790.
- [9] G.A. Argüello, H. Grothe, M. Kronberg, H. Willner, H.G. Mack, *J. Phys. Chem.* 99 (1995) 17525–17531.
- [10] Z. Zelinger, P. Dréan, A. Walters, J.R. Avilès Moreno, M. Bogey, H. Pernice, S. von Ahsen, H. Willner, J. Breidung, W. Thiel, H. Bürger, *J. Chem. Phys.* 118 (2003) 1214–1220.
- [11] Z. Zelinger, S. Bailleux, D. Babánková, M. Šimečková, L. Stříteská, L. Kolesníková, P. Musil, P. Kania, Š. Urban, H. Beckers, H. Willner, *J. Mol. Spectrosc.* 243 (2007) 292–295.
- [12] L. Kolesníková, J. Varga, H. Beckers, M. Šimečková, Z. Zelinger, L. Nová Stříteská, P. Kania, H. Willner, Š. Urban, *J. Chem. Phys.* 128 (2008) 224302.
- [13] H. Beckers, H. Willner, D. Grote, W. Sander, J. Geier, *J. Chem. Phys.* 128 (2008) 224301.
- [14] W.F. Schneider, M.M. Maricq, J.S. Francisco, *J. Chem. Phys.* 103 (1995) 6601–6607.
- [15] J. Breidung, W. Thiel, *J. Phys. Chem. A* 110 (2006) 1575–1585.

- 
- [16] G. Herzberg, E. Teller, *Z. Phys. Chem.* B21 (1933) 410; H.A. Jahn, E. Teller, *Proc. Roy. Soc. London Ser. A* 161 (1937) 200–235; R.G. Pearson, *J. Am. Chem. Soc.* 91 (1969) 4947–4955; R.G. Pearson, *Acc. Chem. Res.* 4 (1971) 152–160.
- [17] R.G. Pearson, *Symmetry Rules for Chemical Reactions*, Wiley-Interscience, New-York, 1976.
- [18] E.R. Davidson, W.T. Borden, *J. Phys. Chem.* 87 (1983) 4783–4790.
- [19] H. Köppel, L.S. Cederbaum, W. Domcke, S.S. Shaik, *Angew. Chem. Int. Ed. Eng.* 22 (1983) 210–224.
- [20] J.F. Stanton, J. Gauss, *Adv. Chem. Phys.* 125 (2003) 101–146.
- [21] G. Guelachvili, K. Narahari Rao, *Handbook of Infrared Standards*, Academic Press, San Diego, 1986.
- [22] G. Guelachvili, M. Birk, Ch.J. Bordé, J.W. Brault, L.R. Brown, B. Carli, A.R.H. Cole, K.M. Evenson, A. Fayt, D. Hausamann, J.W.C. Johns, J. Kauppinen, Q. Kou, A.G. Maki, K. Narahari Rao, R.A. Toth, W. Urban, A. Valentin, J. Vergès, G. Wagner, M.H. Wappelhorst, J.S. Wells, B.P. Winnewisser, M. Winnewisser, *Pure Appl. Chem.* 68 (1996) 193–208.
- [23] W. Gordy, R.L. Cook, in: A. Weissberger (Ed.), *Microwave Molecular Spectra*, 3rd ed., *Techniques of Chemistry* vol. XVIII, Wiley-Interscience, New-York, 1984, Chap 8.
- [24] R.N. Zare, *Angular Momentum*, Wiley-Interscience, New York, 1988.
- [25] J.M. Brown, T.J. Sears, *J. Mol. Spectrosc.* 75 (1979) 111–133.
- [26] J.H. Van Vleck, *Rev. Mod. Phys.* 23 (1951) 213–227; W.T. Raynes, *J. Chem. Phys.* 41 (1964) 3020–3032; R.F. Curl, J.L. Linsey, *J. Chem. Phys.* 35 (1961) 1758–1765; A. Carrington, B.J. Howard, *Mol. Phys.* 18 (1970) 225–231; X. Q. Tan, J.M. Williamson, S.C. Foster, T.A. Miller, *J. Phys. Chem.* 97 (1993) 9311–9316; J.M. Brown, T.J. Sears, J.K. Watson, *Mol. Phys.* 41 (1980) 173–180.
- [27] H.M. Pickett, *J. Mol. Spectrosc.* 148 (1991) 371–377; see also the website <http://spec.jpl.nasa.gov/>
- [28] C.E. Miller, S.P. Sander, *J. Mol. Spectrosc.* 181 (1997) 18–23.
- [29] L. Hedberg, I.M. Mills, *J. Mol. Spectrosc.* 160 (1993) 117–142.
- [30] R.F. Curl, *J. Chem. Phys.* 37 (1962) 779–784; R.F. Curl, *Mol. Phys.* 9 (1965) 585–597.
- [31] L.R. Zink, K.M. Evenson, F. Matsushima, T. Nelis, R.L. Robinson, *AstroPhys. J.* 371 (1991) L85-L86. See also the webpage of the National Institute of Standards and Technology on the Handbook of Basic Atomic Spectroscopic Data: [http://physics.nist.gov/PhysRefData/Handbook/element\\_name.htm](http://physics.nist.gov/PhysRefData/Handbook/element_name.htm) and the reference therein.



### 2.3 The rotational spectrum of the $\text{CH}_2\text{X}$ radicals, with $\text{X}=\text{Br, I}$

The investigations of these radicals have been performed in collaboration with H. Ozeki (Department of Environmental Science, Faculty of Science, Toho University, Japan) and P. Kania (Department of Analytical Chemistry, Institute of Chemical Technology, Prague, Czech Republic). Other collaborators include Z. Zelinger, J. Skřinský and S. Civiš (J. Heyrovský Institute of Physical Chemistry, Academy of Science of the Czech Republic, Prague), and to a minor extent D. Duflot and J.-P. Flament (theoretical molecular physical chemistry group, PhLAM Laboratory).

A quasi simultaneous but independent study on the  $\text{CH}_2\text{Br}$  radical led by H. Ozeki and me in 2004 resulted in a very fruitful collaboration since then. In particular, the Fourier transform microwave spectra of  $\text{CH}_2\text{Br}$  and  $\text{CH}_2\text{I}$  obtained in Japan combined with their millimetre-wave spectra investigated in Lille provided a detailed understanding of both their electronic and molecular structures through the analysis of the observed fine and hyperfine structures.

These studies led to the publication of five articles: one on the extended measurement of the rotational spectrum of  $\text{CH}_2\text{Cl}$  first measured by Endo, Saito and Hirota in 1984,<sup>112</sup> three on  $\text{CH}_2\text{Br}$  and one on  $\text{CH}_2\text{I}$ . A brief summary related to the interest, previous studies and results is given here. The references related to these research projects can be found in the corresponding papers and primarily in the article on  $\text{CH}_2\text{I}$  since this report concludes the millimetre-wave spectroscopic studies of the halogen-substituted  $\text{CH}_2\text{X}$  derivatives.

---

<sup>112</sup> Y. Endo, S. Saito and E. Hirota, *Can. J. Phys.* **62**, 1347 (1984).

As stated in the preamble of this chapter the  $\text{CH}_2\text{X}$  halo-species, with  $\text{X} = \{\text{F}, \text{Cl}, \text{Br}, \text{I}\}$ , are transient intermediates that play key role in atmospheric chemistry (except maybe for the  $\text{X} = \text{F}$  case). They are susceptible to release halogen atoms that can initiate catalytic cycles involved in the perturbation of atmospheric ozone concentration. They are also relevant to a variety of chemical environments, since their precursors are widely used in industrial applications such as halocarbon-based fire extinguishing agents and organic chemistry.

The spectroscopic studies of this series of radicals are also very much stimulating. Indeed, a progressive change in the variety of some chemical properties (such as chemical speciation or reactivity) of halogen-substituted compounds, on going from fluoro-, through chloro-, bromo-, and to iodo-containing molecules, has long been established, with the difference between two successive halogen atoms being most pronounced for fluorine and chlorine. Similarly, in the case of the fluorine-substituted analogues,  $\text{CH}_n\text{F}_{3-n}$  with  $n = 0 - 3$ , deviations from planarity with increasing fluorine substitution have been revealed:  $\text{CH}_3$  is well-known to be planar,  $\text{CH}_2\text{F}$  is quasiplanar while  $\text{CHF}_2$  and  $\text{CF}_3$  exhibit an increasing pyramidal structure. In contrast, our studies showed that  $\text{CH}_2\text{Br}$  and  $\text{CH}_2\text{I}$  are planar radicals, like  $\text{CH}_2\text{Cl}$ . The differences have been interpreted in terms of the much larger difference in the electronegativities between carbon and fluorine than between carbon and the heavier halogens. A limited number of experimental spectroscopic investigations have been performed on this series of halogen-bearing species. In 1983 and 1984, Endo *et al.* reported the microwave spectra of  $\text{CH}_2\text{F}$  and  $\text{CH}_2\text{Cl}$ , respectively.<sup>113,114</sup> Their studies were primarily aimed at exploring

---

<sup>113</sup> Y. Endo, C. Yamada, S. Saito and E. Hirota, *J. Chem. Phys.* **79**, 1605 (1983).

the molecular structure of this series of radicals. In 1993, Davies *et al.* reported the detection of the CH<sub>2</sub>Br radical in the gas-phase by far infrared laser magnetic resonance.<sup>115</sup> They observed congested and irregular spectra that prevented them to make a *complete* rotational assignment. Smith and Andrews carried out in the early 1970s low temperature matrix infrared studies of CH<sub>2</sub>Br and CH<sub>2</sub>I radicals.<sup>116,117</sup> They assigned the  $\nu_2$ ,  $\nu_3$  and  $\nu_6$  (out-of-plane hydrogen inversion) modes. Based on the sense of anharmonicity of the latter mode, they suggested that these radicals should be planar, too. The planarity in their equilibrium configuration was firmly confirmed from the observed proton hyperfine structure. The proton hyperfine structure, not observable in the millimetre-wave region, was fully resolved with the Fourier-transform microwave spectrometer available at Shizuoka University.

In the millimetre-wave spectrometer, the radicals were mainly generated *in situ* by hydrogen abstraction from CH<sub>3</sub>X precursor by chlorine atoms that were produced in a 2450 MHz microwave discharge (delivering a power of about 20 W) in molecular chlorine diluted with helium (5 %). The *a*-type spectra were predicted using rotational constants obtained from *ab initio* calculations. Experimental conditions were first optimised on transitions of CH<sub>2</sub>Cl and led to the publication of a note. The photolytic generation of CH<sub>2</sub>Cl and CH<sub>2</sub>Br at 248 nm from CH<sub>2</sub>BrCl and CH<sub>2</sub>Br<sub>2</sub>, respectively, led to their  $1/e$  lifetime measurement: 146(2) and 45(1)ms, respectively. In the case of CH<sub>2</sub>Br, the assignment was complicated because of the presence of two Br-isotopologues that exist in nearly

---

<sup>114</sup> Y. Endo, S. Saito and E. Hirota, *Can. J. Phys.* **62**, 1347 (1984).

<sup>115</sup> P. B. Davies, Y. Liu and Z. Liu, *Chem. Phys. Lett.* **214**, 305 (1993).

<sup>116</sup> D. W. Smith and L. Andrews, *J. Chem. Phys.* **55**, 5295 (1971).

<sup>117</sup> D. W. Smith and L. Andrews, *J. Chem. Phys.* **58**, 5222 (1973).

equal abundances ( $^{79}\text{Br}$ : 50.7%,  $^{81}\text{Br}$ : 49.3%). Although the detection of mono- and inter-halogen species arising from secondary reactions (such as  $\text{CH}_3\text{Cl}$ ,  $\text{CH}_2\text{Cl}$ ,  $\text{CH}_2\text{ICl}$  and  $\text{ICl}$ , see next paragraph) were clear evidence of the presence of the intermediate  $\text{CH}_2\text{I}$ , its production revealed to be more critical for some unknown reasons. In addition, the smaller dipole moment, 0.8 D (1.0 D for  $\text{CH}_2\text{Br}$ ) and a smaller lifetime let us legitimise that line intensities are significantly weaker than in the case of  $\text{CH}_2\text{Br}$ .

The Hamiltonian used in the analysis is that for a slightly asymmetric top radical in the doublet state:

$$H = H_{Rot} + H_{SR} + H_{\text{hf}}(X) + H_{\text{hf}}(\text{H}),$$

where  $H_{Rot}$  and  $H_{SR}$  denote the Watson's  $A$  reduction of the rotational Hamiltonian in the  $I'$  representation corrected for centrifugal distortion and of the spin-rotational term, respectively. The terms  $H_{\text{hf}}(X)$  and  $H_{\text{hf}}(\text{H})$  correspond respectively to the hyperfine interactions owing to the halogen and hydrogen nuclei.  $H_{\text{hf}}(X)$  includes the magnetic isotropic and anisotropic dipole-dipole interactions (Equations 1.7 and 1.8) of  $X$ , in addition to the electric quadrupole and nuclear spin-rotation interactions, whilst  $H_{\text{hf}}(\text{H})$  contains only the magnetic dipolar couplings.

The analysis of the fine- and hyperfine-structure constants led to a detailed understanding of the molecular and electronic properties (such as the spin density distribution within the radical). They are compared in the article on  $\text{CH}_2\text{I}$  (next page). The comparison indicated a monotonic trend in this series of radicals on going from fluoro- to iodo-substituents. A systematic increase of electron spin density with  $p$  character with increasing atomic number of the halogen was revealed.

# Hyperfine Resolved Fourier Transform Microwave and Millimeter-Wave Spectroscopy of the Iodomethyl Radical, $\text{CH}_2\text{I}$ ( $\tilde{X}^2B_1$ )<sup>†</sup>

Stéphane Bailleux,\* Patrik Kania,<sup>‡</sup> and Jan Skřínský

Laboratoire de Physique des Lasers, Atomes et Molécules, CERLA, UMR CNRS 8523, Université Lille 1, 59655 Villeneuve d'Ascq Cedex, France

Toshiaki Okabayashi, Mitsutoshi Tanimoto, and Satoshi Matsumoto

Graduate School of Science and Technology, Shizuoka University, Oya 836, Suruga-ku, Shizuoka 422-8529, Japan

Hiroyuki Ozeki

Department of Environmental Science, Faculty of Science, Toho University, 2-2-1 Miyama, Funabashi 274-8510, Japan

Received: September 28, 2009; Revised Manuscript Received: November 26, 2009

Fourier-transform microwave and millimeter-wave spectra of the iodomethyl radical,  $\text{CH}_2\text{I}$ , have been observed in the ground vibronic state in the frequency ranges 17–38 GHz and 200–610 GHz, respectively. The  $\pi$ -electron radical was produced either by iodine abstraction from diiodomethane ( $\text{CH}_2\text{I}_2$ ) or by hydrogen abstraction from iodomethane ( $\text{CH}_3\text{I}$ ). Seventy-three hyperfine resolved lines owing to the two hydrogen and to the iodine nuclei have been detected in the microwave region, including  $K_a = 0$  (*ortho* species) and  $K_a = 1$  (*para* species). No hyperfine splitting due to the hydrogen nuclei could be observed for the *para* species, directly confirming the planarity of the radical and that the ground electronic state is  $^2B_1$ . More than 400 *a*-type transitions that span the values  $N' \leq 35$ ,  $K_a \leq 6$ , were detected. A global least-squares analysis of the measured lines was conducted and led to the determination of an exhaustive list of molecular constants. In particular, the sign of the Fermi-contact constant of iodine was unambiguously determined to be negative, which is opposite to that of the other monosubstituted halomethyl radicals. This work allowed a systematic comparison of the structural and bonding properties among the  $\text{CH}_2\text{X}$  analogues (where  $X = \text{F}, \text{Cl}, \text{Br}, \text{and I}$ ) owing to the hyperfine coupling constants of both the hydrogen and halogen nuclei.

## Introduction

It has been well established that a progressive change occurs in the variety of some chemical properties of halogen-substituted compounds, such as chemical speciation or reactivity, on going from fluoro-, through chloro-, bromo-, and to iodo-containing molecules, with the difference between two successive halogens being most pronounced for fluorine and chlorine. A very interesting example of such seeming similarities is given by the methyl radical and its halogen-substituted derivatives, denoted  $\text{CH}_n\text{X}_{3-n}$  where  $n = 0-2$  and  $X = \text{F}, \text{Cl}, \text{Br}, \text{and I}$ . Indeed, early studies by electron spin resonance,<sup>1</sup> infrared<sup>2,3</sup> and microwave<sup>4</sup> spectroscopy, as well as photoionization measurements<sup>5</sup> and ab initio calculations<sup>6</sup> have provided numerous evidence that the interaction of the lone pairs of the halogen atom(s) with the unpaired electron affects the bonding considerably: the carbon–halogen stretching force constants exceed normal C–X values<sup>7–11</sup> (such as in  $\text{CH}_3\text{X}$  molecules), and large anharmonicity in the out-of-plane vibration modes<sup>8–11</sup> has been observed. Most notably, in the case of the fluorine-substituted analogues ( $\text{CH}_n\text{F}_{3-n}$ ), deviations from planarity with increasing fluorine substitution have been revealed:  $\text{CH}_3$  is well-known to

be planar,<sup>12</sup>  $\text{CH}_2\text{F}$  is quasiplanar,<sup>4</sup> while  $\text{CHF}_2$  and  $\text{CF}_3$  exhibit an increasing pyramidal structure.<sup>1–3,13–15</sup> In contrast, both  $\text{CH}_2\text{Cl}$  and  $\text{CH}_2\text{Br}$  radicals are clearly planar with significant electron delocalization on the corresponding halogen,<sup>16–18</sup> while the degree of electron delocalization in  $\text{CH}_2\text{F}$  is less pronounced.<sup>4</sup> These differences have been interpreted in terms of the much larger difference in the electronegativities of carbon and fluorine.<sup>19,20</sup> Accordingly, these “anomalies” lead to significant discrepancies with existing experimental data in the structural calculations of these halogen-substituted methyl radicals.<sup>21</sup>

Apart from these structural and spectroscopic aspects, the study of the halomethyl radicals (and of their cations) is of importance since their precursors are widely used in a variety of industrial and domestic applications such as chemical vapor deposition and plasma etching of semiconductors in integrated circuits manufacturing,<sup>22</sup> propellant systems,<sup>23,24</sup> halocarbon-based fire suppression,<sup>25,26</sup> halogenated solvents in syntheses,<sup>27</sup> refrigerants, insulators, etc. Their investigation also has essential social and economical impact since these transient intermediates play also key roles in atmospheric chemistry (ozone depletion), pollution (pesticides,<sup>27</sup> incinerators), and global warming.

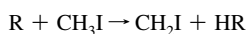
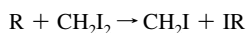
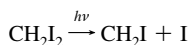
In particular, numerous studies in relation to the adverse impact of chlorine and bromine on ozone depletion have been published.<sup>28,29</sup> Attention has also been paid, but to a lower extent, to the potential role of iodine in the tropospheric chemistry of

<sup>†</sup> Part of the special section “30th Free Radical Symposium”.

\* Corresponding author. E-mail: stephane.bailleux@univ-lille1.fr.

<sup>‡</sup> Present address: Institute of Chemical Technology, Department of Analytical Chemistry, Technická 5, 166 28, Prague 6, Czech Republic.

ozone<sup>30,31</sup> and mercury<sup>32</sup> as well. For a decade or so, there has been increasing evidence that iodine plays a role<sup>33,34</sup> in atmospheric chemistry which could be enhanced by the presence of chlorine atoms. The high photolability of iodo-carbons containing two chromophores, such as CH<sub>2</sub>I<sub>2</sub>, CH<sub>2</sub>ICl, and CH<sub>2</sub>I<sub>2</sub>Br, makes them to be among the most efficient iodine atom precursors in the troposphere.<sup>35,36</sup> The photolysis together with the chemical reactions involving the two uppermost organic iodines found in ocean water, CH<sub>2</sub>I<sub>2</sub> and CH<sub>3</sub>I, lead to the formation of the iodomethyl radical according to the following reactions



where R stands for OH or Cl radicals. Since CH<sub>2</sub>I is known to absorb strongly in the UV–vis range,<sup>37</sup> this radical may therefore undergo subsequent photolysis to release another iodine atom. Carpenter has noted the importance of the fate of the iodomethyl radical in the photodissociation of diiodomethane and come to the conclusion of a fairly rapid release of both iodine atoms.<sup>33</sup> These iodine atoms in turn initiate catalytic cycles (that regenerate iodine atoms without concomitant oxygen atom formation) leading to the decomposition of ozone. Biogenic sources of mono- and di-iodomethane arise from emissions by phytoplankton and macroalgae in tidal zones, but the dominant production is now thought to arise from photochemical reactions in ocean water.<sup>38</sup> CH<sub>3</sub>I has several terrestrial sources<sup>33,38</sup> with emissions arising from natural wetlands,<sup>39</sup> rice paddies,<sup>40,41</sup> and biomass burning.<sup>42</sup>

Finally, it is interesting to point out that both iodomethane and diiodomethane could be significant anthropogenic sources of iodine as well, the former one owing to its large use as a methylation reagent in organic chemistry. The latter one is commonly used as a reagent for cyclopropanation of a wide variety of olefins where it is activated by UV photolysis.<sup>43</sup> These high yield cyclopropanation reactions are very important in organic and organometallic chemistry, but their reaction mechanisms are not yet well understood since the key reaction intermediates lack direct experimental observation.<sup>43</sup> In relation with these cyclopropanation reactions, the CH<sub>2</sub>I radical has been proposed to be partly responsible for the 385 and 570 nm transient absorption bands.<sup>44</sup>

High-resolution characterizations in the gas phase by microwave, laser magnetic resonance, and infrared spectroscopic techniques of the fluoro-,<sup>4,45,46</sup> chloro-,<sup>16,47,48</sup> and bromomethyl<sup>18,49</sup> radicals have been published starting from 1983. On the other hand, until now information on the iodine analogue has been rather scarce. Smith and Andrews first identified in 1973 the reactive molecule trapped in an argon matrix at 15 K by infrared spectroscopy.<sup>11</sup> Their vibrational analysis led to the assignments of the CH<sub>2</sub> scissor vibration ( $\nu_3 = 1331.5 \text{ cm}^{-1}$ ), the CI stretch mode ( $\nu_2 = 611.2 \text{ cm}^{-1}$ ), and the inversion mode ( $\nu_6 = 374.9 \text{ cm}^{-1}$ ). The sense of anharmonicity of this latter mode led these authors to suggest that CH<sub>2</sub>I is planar. They also rationalized the enhanced carbon–iodine bond strength by  $\pi$ -bonding, like in the CH<sub>2</sub>Cl and CH<sub>2</sub>Br radicals. Baughcum and Leone later detected infrared spectra in emission of vibrationally excited

CH<sub>2</sub>I in the gas phase produced by the photolysis of CH<sub>2</sub>I<sub>2</sub> at 248 nm.<sup>50</sup> They observed the same fundamental bands as Andrews et al.,<sup>11</sup> and in addition they reported a peak near 3050  $\text{cm}^{-1}$ , assignable to the C–H stretching frequencies (no distinction was made between the symmetric and the asymmetric modes, but this frequency should most probably be assigned to the symmetric one<sup>51</sup>). With these two studies, five vibrational modes in total have been assigned which have been compiled by Jacox.<sup>52</sup> Andrews et al. then reported unstructured vibrational bands by photoelectron spectroscopy and determined the adiabatic and first vertical ionization energies to be  $8.40 \pm 0.03 \text{ eV}$  and  $8.52 \pm 0.03 \text{ eV}$ , respectively.<sup>53</sup> In comparison to these limited spectroscopic investigations, some substantial attention has been paid to the kinetics of the reactions of chlorine atoms with the mono- and disubstituted halomethanes (CH<sub>3</sub>I, ref 54; CH<sub>2</sub>I<sub>2</sub>, ref 55; and CH<sub>2</sub>ICl, ref 56) and to the kinetics of the reactions, at atmospheric conditions, of the iodomethyl radical with species relevant to atmospheric chemistry: oxygen,<sup>57–59</sup> chlorine,<sup>60</sup> hydrogen bromide<sup>61</sup> and iodide,<sup>62</sup> iodine,<sup>63</sup> and nitrogen dioxide.<sup>64</sup> The oxidation mechanism of the CH<sub>2</sub>I radical was also investigated.<sup>55</sup> Ab initio structural calculations of this radical at various levels of theory have been reported by a number of authors, resulting in nearly as many as geometric parameters showing planar<sup>43,51,63,65</sup> and quasiplanar<sup>56,61,66</sup> equilibrium configurations with a dihedral angle comprised between 8.5° and 10.1°. Yet, the CH<sub>2</sub>I radical is expected to be planar in its equilibrium geometry by comparison with the chlorine and bromine analogues. Depending on the level used in the calculation, the C–I and C–H bond lengths span the ranges 2.044–2.103 Å and 1.070–1.083 Å, respectively. The values reported for the  $\angle\text{HCI}$  bond angle varied moderately and were generally close to 118.4°. A more recent calculation performed at a higher level (CASPT2 with inclusion of both scalar relativistic and spin–orbit effects) was reported by Liu et al. in their ab initio investigation of the photolysis of CH<sub>2</sub>BrI.<sup>67</sup> They obtained a planar equilibrium geometry with  $r(\text{C–I}) = 2.050 \text{ \AA}$ ,  $r(\text{C–H}) = 1.086 \text{ \AA}$ , and  $\angle\text{HCI} = 118.35^\circ$ .

The present paper describes the microwave and millimeter-wave spectra of the iodomethyl radical. Emphasis is given on the analysis of the hyperfine structure owing to the interactions of the iodine and hydrogen nuclear spins from which we obtained insights into the geometric structure and bonding properties of this unique species. Systematic comparison of the bonding and structural properties of the CH<sub>2</sub>X halomethyl radicals have been carried out, hence completing the high-resolution rotational spectroscopic investigations of these systems. Our results should also provide essential information applicable to thermodynamic and kinetic modeling of atmospheric and flame chemistry.

## Experimental Details

Two experimental setups have been used in the present study. One employed the Balle–Flygare-type pulsed discharged nozzle Fourier transform microwave spectrometer<sup>68,69</sup> located in Shizuoka University to record spectra between 17 and 38 GHz. The premixed gas composed of the diiodomethane (CH<sub>2</sub>I<sub>2</sub>) used as a precursor seeded in argon was released into the vacuum chamber from a nozzle (General Valve Co.) at a stagnation pressure of 1.5 atm. A 1.2 kV pulsed high voltage was applied to the electrodes attached to the nozzle for creating the discharge. To reduce the consumption of the precursor, most of the measurements were conducted without heating the sample, although heating the sample holder up to 50 °C increased slightly the intensity of the spectral lines. Earth's magnetic field was

canceled using three sets of Helmholtz coils placed perpendicularly to each other.

Measurements of the spectra in the 200–610 GHz frequency region were obtained using the 40 kHz source modulated millimeter-wave spectrometer with a 2 m free space cell located in Lille University. The CH<sub>2</sub>I radical was generated either by hydrogen abstraction from monoiodomethane or alternatively by iodine abstraction from diiodomethane by chlorine atoms in both abstraction reactions. Molecular chlorine diluted with helium (5%) was used as a source for atomic chlorine produced in a 2450 MHz microwave discharge using an Evenson-type microwave cavity.<sup>70</sup> Iodomethane and diiodomethane were stored in a glass container (both compounds are liquids at room temperature) and kept in darkness. Due to low vapor pressure of diiodomethane, the corresponding glass container was heated to 50 °C. The precursor gases were separately introduced into the double-jacketed free space cell via a horizontal Pyrex crosspiece (30 cm in length) and were mixed upstream of the free space cell. The absorption cell was equipped with a coil for creating an axial magnetic field (~200 G) to confirm that the detected lines were paramagnetic by on/off measurement. However, it was found afterward that the CH<sub>2</sub>I radical has a too short lifetime to reach the region of the absorption cell surrounded with the solenoid; consequently, we just found it appropriate to put a set of strong permanent magnets above the horizontal crosspiece where abstraction reactions occurred to check that the transitions were due to paramagnetic species. Interestingly, although obviously the radical did not reach part of the absorption cell cooled by liquid nitrogen, we found it essential to partially cool the gas mixture by limited flow of liquid nitrogen through the outer jacket. The more efficient cryogenic pumping and the trapping of unreacted precursor and of the otherwise observed stable byproduct (ICI in vibrationally excited states, CH<sub>2</sub>ICI and CH<sub>3</sub>CI) that often lead to strong absorption signals play certainly a major role. The cooling of the crosspiece with liquid nitrogen immediately condensed the iodine-containing sample on the walls, thus preventing the abstraction reactions to occur. The transient CH<sub>2</sub>Cl radical<sup>17</sup> was also detected in these experiments. Measurements of the spectra of the ICI and CH<sub>2</sub>ICI species (up to the THz region for ICI) are in progress, and their analysis will be published elsewhere. The optimized partial pressures (measured at room temperature) for CH<sub>3</sub>I and CH<sub>2</sub>I<sub>2</sub> were  $3 \times 10^{-3}$  and  $1.5 \times 10^{-3}$  mbar, respectively; the total pressure was in the range  $(7-8) \times 10^{-3}$  mbar. Even though the optimum partial pressure of diiodomethane was somewhat lower than that of iodomethane, the use of CH<sub>2</sub>I<sub>2</sub> resulted in about 25% larger line intensities.

**Prediction of the Spectrum.** Spectral line positions were predicted on the basis of the ab initio geometrical structure optimization<sup>43,51,63,65</sup> to provide the rotational constants that were needed to guide our search for the rotational spectrum of CH<sub>2</sub>I in the gas phase. Because of the disparity encountered in the structural calculations, we are grateful to Dufflot and Flament<sup>71</sup> who sent us privately their results performed at the U-CCSD(T) level. They obtained the following bond lengths and angle:  $r(\text{C}-\text{H}) = 1.078 \text{ \AA}$ ,  $r(\text{C}-\text{I}) = 2.050 \text{ \AA}$ , and  $\angle\text{HCI} = 118.46^\circ$ . The CH<sub>2</sub>I radical is a nearly prolate symmetric rotor ( $\kappa = -0.998$ ) of  $C_{2v}$  symmetry with its dipole moment<sup>71</sup> (0.8 D) along the *a* axis of symmetry. It possesses a single unpaired electron, and the nuclear spins of the iodine and the hydrogen atoms are 5/2 and 1/2, respectively. Lines falling in the microwave region were expected to be spread over wide frequency ranges (several hundreds of MHz) owing to the large nuclear spin of iodine. Therefore, we found it a necessary prerequisite to predict

accurately the hyperfine coupling constants. Those due to the nuclear spin of both protons were taken from the CH<sub>2</sub>Br radical<sup>18</sup> since they should vary marginally for  $\alpha$ -hydrogen in  $\pi$ -radicals with the unpaired electron mostly located on the neighboring carbon atom.

Values of the hyperfine constants arising from the nuclear spin of iodine, the Fermi-contact term, the magnetic dipole-dipole, and the quadrupole coupling constants, were empirically predicted as described below. The Fermi-contact term  $a_F$  can be interpreted in terms of electronic spin density with *s* character on the halogen using the atomic value of the halogen,  $A_F$ . More precisely, the observed electronic spin densities decrease monotonically with increasing atomic number of the halogen, going from 0.4% in CH<sub>2</sub>F,<sup>4</sup> through 0.2% in CH<sub>2</sub>Cl,<sup>16</sup> and to 0.08% in CH<sub>2</sub>Br,<sup>18</sup> the corresponding constants being all positive. Extrapolating this trend, a spin density with *s* character on the iodine atom in CH<sub>2</sub>I of 0.04% was presumed, and using the atomic value of iodine<sup>72</sup> (41 600 MHz) the Fermi-contact term was predicted to be +16.6 MHz.

The magnetic dipole-dipole interaction tensor *T* for CH<sub>2</sub>I was obtained adopting a similar approach. This tensor is determined in reference to the principal inertial axes system of the molecule. When one of the inertial axes coincides with the axis of the unpaired electron *p* orbital, the diagonal components of *T* approximately satisfy the ratios 4/5:−2/5:−2/5, where the values 4/5 and −2/5 apply to the axial and perpendicular components, respectively. Consequently, for species with an unpaired electron in an out-of-plane *p* orbital (*p<sub>π</sub>* radicals) the relationship  $T_{aa} \approx T_{bb} \approx -1/2T_{cc}$  is usually well satisfied. The unpaired electron spin density with *p* character can then be deduced from the ratio  $1/2T_{cc}/(2/5P)$  where *P* stands for the atomic magnetic dipole-dipole value of the halogen. The electronic spin densities with *p* character varied from 13.3% in CH<sub>2</sub>F,<sup>4</sup> to 15.7% in CH<sub>2</sub>Cl,<sup>16</sup> and 15.8% in CH<sub>2</sub>Br.<sup>18</sup> A spin density with *p* character of 16% was thus assumed in CH<sub>2</sub>I. The atomic magnetic dipole-dipole constant for iodine being  $P = 2031 \text{ MHz}$ ,<sup>72</sup> the  $T_{cc}$  constant of CH<sub>2</sub>I was evaluated to be +260 MHz.

An increase in delocalization of  $\pi$ -electrons on going from CH<sub>3</sub>X to CH<sub>2</sub>X systems (where X = Cl, Br) accounted for the value of  $\chi_{aa}(X)$  of CH<sub>2</sub>X radicals about 10% smaller in magnitude than that of CH<sub>3</sub>X (see refs 16 and 73 for the cases X = Cl and Br, respectively). A further inspection of the quadrupole coupling components  $\chi_{aa}(X)$  and  $\chi_{bb}(X)$  in these two CH<sub>2</sub>X species gave the nearly fixed negative ratio  $\chi_{bb}(X)/\chi_{aa}(X) \approx -0.62$ . Using  $\chi_{aa}(\text{I}) = -1934 \text{ MHz}$  for CH<sub>3</sub>I,<sup>74</sup> the  $\chi_{aa}(\text{I})$  and  $\chi_{bb}(\text{I})$  quadrupole coupling tensor components of CH<sub>2</sub>I were estimated to be −1741 and +1080 MHz, respectively.

**Identification of the Spectrum.** The search for the rotational spectrum of the CH<sub>2</sub>I radical in the gas phase was initiated in the microwave region, focusing on the detection of the  $N_{K_a, K_c} = 2_{0,2} \rightarrow 1_{0,1}$  and  $1_{0,1} \rightarrow 0_{0,0}$  lines. They were observed close to the predictions, and they account for 29 and 23 lines, respectively. Their assignment could only be made after reversing the sign of the Fermi-contact term of iodine. The large uncertainties of the ab initio *B*−*C* value (269 (±14) MHz) and of the fine structure constants prevented from detecting transitions corresponding to  $K_a = 1, N = 2 \rightarrow 1$  at this stage. We consequently focused on the detection of transitions with  $K_a = 0$  in the MMW region, between 420 and 470 GHz. After several attempts consisting in adjusting the experimental conditions, they were found close to the predictions. The observed hyperfine structures were in excellent agreement with those arising from the nuclear spin of iodine. We then searched for transitions with  $K_a = 1$ .

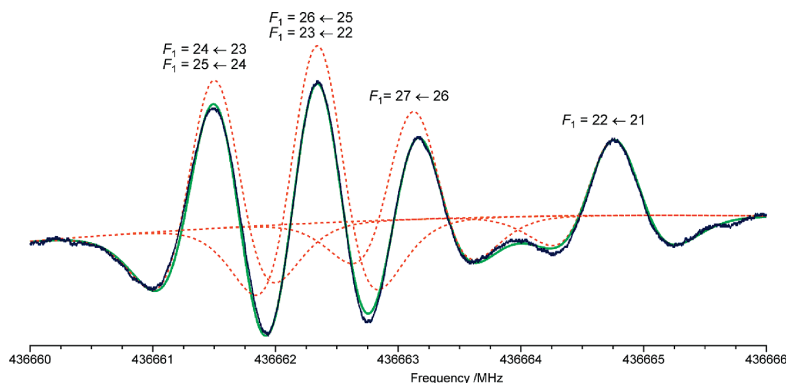


**Figure 1.** Hyperfine structure owing to the iodine nuclear spin in the  $N = 25 \leftarrow 24$ ,  $K_a = 4$ ,  $J = 24.5 \leftarrow 23.5$  mm-wave transition of CH<sub>2</sub>I obtained by iodine abstraction from CH<sub>2</sub>I<sub>2</sub>; recorded spectra (blue), individual line profiles (dotted, orange) as well as the convoluted four spectral lines (green) both calculated with IgorPro. The  $F_1 = J + I(I)$  quantum numbers are indicated above the lines. The spectrum was recorded by integrating 20 scans with a repetition rate of 1 Hz and with a lock-in amplifier time constant of 10 ms.

Since the hyperfine structure due to both protons is not resolved in the MMW region, the Pauli exclusion principle makes lines with odd values of  $K_a$  about three times less intense than those with  $K_a$  being even, as our observations confirmed. The expected frequency regions of the  $K_a = 1$  lines were carefully scanned, and their fine-structure components were ultimately observed. Transitions with higher  $K_a$  values (up to  $K_a = 6$ ) were routinely detected using the centrifugal distortion constants of CH<sub>2</sub>Br taken as an initial guess.<sup>18</sup> Subsequently, we were able to detect 21 transitions with  $K_a = 1$  corresponding to the  $2_{1,2} \rightarrow 1_{1,1}$  and  $2_{1,1} \rightarrow 1_{1,0}$  transitions in the microwave region. No additional splitting of these types of transitions could be observed, proving unambiguously the planarity of the radical in its equilibrium configuration since the planar structure results in the existence of the *ortho* and *para* molecules. In this case, the two protons are equivalent with respect to the *a* molecular axis, and the Pauli exclusion principle dictates that rotational levels with  $K_a$  being even and odd correspond to the *ortho* CH<sub>2</sub>I ( $I(H) = 1$ ) and *para* CH<sub>2</sub>I ( $I(H) = 0$ ), respectively, where  $I(H)$  stands for the total proton nuclear spin angular momentum. The former species gives rise to hyperfine splittings due to the hydrogen nuclei unlike the latter one.

Spectral measurements covered the 17–38 GHz and 200–610 GHz frequency regions resulting in total in the detection and assignment of 73 microwave (52 of these hyperfine components are assigned to *ortho* species or  $K_a = 0$  and 21 to *para* species or  $K_a = 1$ ) and 331 MMW transitions, respectively. Frequency errors ( $1\sigma$ ) are estimated to be 3 kHz and within 30–80 kHz in the microwave and millimeter-wave regions, respectively. The list of the observed and obsd – calcd transition frequencies are collected in the Supporting Information.

**Spectral Analysis.** Since we observed the fully resolved hyperfine spectra of the CH<sub>2</sub>I radical, the Hamiltonian used in the present analysis is that for an asymmetric top radical in the doublet state

$$H = H_{\text{rot}} + H_{\text{sr}} + H_{\text{hf}}(I) + H_{\text{hf}}(H)$$

where  $H_{\text{rot}}$  and  $H_{\text{sr}}$  denote the Watson's *A* reduction of the rotational Hamiltonian in the *V* representation and of the spin-rotational term, respectively, both including their centrifugal distortion effects. The terms  $H_{\text{hf}}(I)$  and  $H_{\text{hf}}(H)$  symbolize the hyperfine interactions owing to the iodine and hydrogen nuclei.

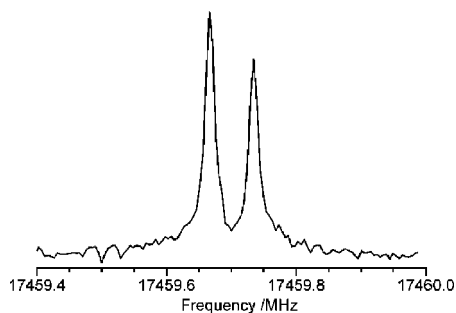


**Figure 2.** Example of the hyperfine  $N_{K_a, K_c} = 1_{0,1} \rightarrow 0_{0,0}$ ,  $J = 1.5 \rightarrow 0.5$  emission spectrum of CH<sub>2</sub>I near 17459.7 MHz. 800 free induction decay (FID) signals were averaged with a repetition rate of 5 Hz.

They include the magnetic dipole–dipole interactions (both isotropic and anisotropic) of the iodine and hydrogen nuclei together with the electric quadrupole and nuclear spin-rotation couplings only for the iodine nucleus. Because of the Pauli exclusion principle, in the ground vibronic state rotational levels with even and odd  $K_a$  are associated with  $I(H) = 1$  and  $I(H) = 0$ , respectively. As a consequence, the following coupling scheme of angular momenta was employed:  $\mathbf{J} = \mathbf{N} + \mathbf{S}$ ,  $\mathbf{F}_1 = \mathbf{J} + \mathbf{I}(I)$ ,  $I(H) = I(H_1) + I(H_2)$ , and  $\mathbf{F} = \mathbf{F}_1 + \mathbf{I}(H)$  for the *ortho* species, and  $\mathbf{J} = \mathbf{N} + \mathbf{S}$ ,  $\mathbf{F} = \mathbf{J} + \mathbf{I}(I)$  for the *para* species. The initial estimates of the hyperfine parameters of the iodine and hydrogen nuclei made it possible to readily assign the  $J$  and  $F$  values. All millimeter-wave line frequencies for individual hyperfine components owing to the iodine nucleus were determined by a nonlinear line profile analysis using IgorPro (wavemetrics). The line frequencies together with the peak intensities were adjusted assuming a second-derivative Voigt line shape with a common line width for each hyperfine component.

Figure 1 is a plot of the  $N = 25 \leftarrow 24$ ,  $K_a = 4$ ,  $J = 24.5 \leftarrow 23.5$  rotational transition illustrating the hyperfine structure owing to the iodine nuclear spin analyzed with IgorPro. Among the  $1_{0,1} \rightarrow 0_{0,0}$  transitions, the strongest line which was obtained by accumulating 800 FID (free induction decay) signals is depicted in Figure 2. In total, 404 distinct frequency lines were recorded in the present study, resulting in assignments of 1351 *a*-type rotational transitions. They were subjected to a least-squares analysis with Pickett's program SPFIT<sup>75</sup> using 33

adjustable parameters. Since CH<sub>2</sub>I is a near-prolate rotor, the asymmetry splitting for  $K_a \geq 1$  (i.e., the doubling of the  $K_a$  levels into  $K_c = N - K_a$  and  $K_c = N + 1 - K_a$  levels) decreases with increasing  $K_a$  and becomes negligible for  $K_a \geq 4$ . The weights of the data were taken as the inverse square of the accuracy of the frequency measurements. Completely blended lines (in the MMW region, unresolved hyperfine components due to the hydrogen nuclei and unresolved  $K$ -doublets) were fitted as the equally weighted average of their calculated components. Line frequencies with a difference between the observed and calculated values of more than 3.5 times the measurement accuracy were excluded from the present global fit; only 10 lines were rejected from the fit (6 and 4 in the microwave and MMW regions, respectively). The quantum numbers of assigned transitions encompass the values  $N' \leq 35$ ,  $K_a \leq 6$ . Separation of  $A$  and  $\Delta_K$  was not accomplished in the present analysis, and the latter was fixed to 24.25 MHz, a value obtained by scaling  $\Delta_K$  for CH<sub>2</sub>Cl and CH<sub>2</sub>Br.<sup>17,18</sup> The standard deviation of the fit is 29 kHz. The derived molecular constants with their one standard error as obtained after reformatting the output .fit file from SPFIT with the PIFORM program of Kisiel<sup>16</sup> are listed in Table 1 together with the predicted hyperfine constants of the iodine nucleus. The constants obtained in the  $S$  reduction are also given in Table 1. The standard deviation, 29.4 kHz, is slightly larger than that obtained in the  $A$  reduction of the Hamiltonian.

Figure 3 shows the observed and calculated stick spectra of the  $1_{0,1} \rightarrow 0_{0,0}$  transition near 17.600 GHz. As can be seen, assigned lines are in excellent agreement with their calculated frequencies and relative intensities.

## Results and Discussion

The present gas phase investigation has completed the series of studies by high-resolution rotational spectroscopy of the monohalogen-substituted methyl radicals CH<sub>2</sub>X, with X = F, Cl, Br, and I. The rotational constants of CH<sub>2</sub>I in the ground vibronic state have been accurately determined, and they compare well with the ab initio calculations giving a planar equilibrium structure<sup>43,51,65,71</sup> except the ones by Dymov et al.<sup>63</sup>

The effective rotational constants have been transformed into the Watson's determinable parameters, as follows (constants in MHz, one standard deviation between parentheses):  $A_0 = 276675.97(252)$ ,  $B_0 = 8896.5037(15)$ , and  $C_0 = 8613.9648(15)$ . The small positive value of the inertial defect obtained from the determinable rotational constants,  $\Delta_0 = 0.03665(3)$  amu Å<sup>2</sup>, strongly suggests the planarity of the molecule. Planarity is firmly confirmed, as mentioned previously in the "Identification of the Spectrum" section, by the observed proton hyperfine structure (no additional splitting due to the hydrogen nuclei of *para* transitions). Therefore the ground electronic state belongs to <sup>2</sup>B<sub>1</sub>. Our result for  $\Delta_0$  may be compared with those obtained for the various CH<sub>2</sub>X halo-species. The value for CH<sub>2</sub>I is somewhat larger than those of CH<sub>2</sub>Cl (0.0328 amu Å<sup>2</sup>)<sup>16,17</sup> and CH<sub>2</sub>Br (0.0322 amu Å<sup>2</sup>)<sup>18,73</sup> which are planar radicals, whereas CH<sub>2</sub>F has a quasiplanar geometry (−0.0090 amu Å<sup>2</sup>).<sup>4</sup> With only three rotational constants, the three structural parameters of CH<sub>2</sub>I cannot be uniquely determined. Since bond angles are in principle well determined by ab initio calculations, the  $\angle$ HCI angle was fixed to 118.4° (ref 71). Under the planarity constraint (the dihedral angle between the two HCl planes holds at 180°), the two remaining geometric parameters were then derived from Watson's determinable constants using the STRFIT program developed by Kisiel.<sup>76</sup> We obtained  $r(C-I) = 2.0388(7)$  Å and  $r(C-H) = 1.086(5)$  Å. These bond lengths compare well with

**TABLE 1: Spectroscopic Parameters (in MHz, I<sup>a</sup> Representation) of CH<sub>2</sub>I**

A reduction	determined	S reduction	determined	predicted
$A$	276675.9(25) <sup>a</sup>	$A$	276679.2(25)	279413 <sup>b</sup>
$B$	8896.5213(11)	$B$	8896.24093(18)	8806 <sup>b</sup>
$C$	8613.4204(11)	$C$	8613.70036(20)	8537 <sup>b</sup>
$10^3 \times \Delta_N$	7.62790(22)	$10^3 \times D_N$	7.59072(18)	
$\Delta_{NK}$	0.248075(37)	$D_{NK}$	0.248299(38)	
$\Delta_K$	24.25 <sup>c</sup>	$D_K$	24.25 <sup>c</sup>	
$10^3 \times \delta_N$	0.23601(11)	$10^3 \times d_1$	−0.23613(11)	
$\delta_K$	0.14027(53)	$10^3 \times d_2$	−0.018343(72)	
$10^9 \times \phi_N$	−3.39(13)	$10^9 \times H_N$	−3.63(13)	
$10^6 \times \phi_{NK}$	0.228(26)	$10^6 \times H_{NK}$	0.142(27)	
$10^6 \times \phi_{KN}$	8.75(40)	$10^6 \times H_{KN}$	8.99(41)	
$\epsilon_{aa}$	−29409.781(10)	$\epsilon_{aa}$	−29409.763(10)	
$\epsilon_{bb}$	−926.527(21)	$\epsilon_{bb}$	−926.2842(16)	
$\epsilon_{cc}$	208.809(21)	$\epsilon_{cc}$	208.5652(15)	
$^s\Delta_{KN}$	1.0109(15)	$^sD_{KN}$	1.0135(15)	
$10^3 \times ^s\Delta_N$	0.9003(87)	$10^3 \times ^sD_N$	0.6687(37)	
$^s\Delta_K$	1.634(15)	$^sD_K$	1.632(16)	
$10^3 \times ^s\delta_N$	0.2204(54)	$10^3 \times ^s d_1$	0.2180(56)	
$10^3 \times ^s\delta_K$	119(11)	$10^3 \times ^s d_2$	0.1179(42)	
$a_F(I)$	−15.83740(47)	$a_F(I)$	−15.83810(47)	+16.6 <sup>d</sup>
$10^3 \times a_F^N(I)$	0.132(41)	$10^3 \times a_F^N(I)$		
$10^3 \times a_F^P(I)$	−7.7(15)	$10^3 \times a_F^P(I)$		
$T_{aa}(I)$	−152.96434(65)	$T_{aa}(I)$	−152.96436(68)	−130 <sup>e</sup>
$T_{bb}(I)$	−138.9880(18)	$T_{bb}(I)$	−139.0008(20)	−130 <sup>e</sup>
$T_{cc}(I)^f$	291.9524(18)	$T_{cc}(I)^f$	291.9652(20)	260 <sup>e</sup>
$\chi_{aa}(I)$	−1745.0218(25)	$\chi_{aa}(I)$	−1745.0219(26)	−1741 <sup>g</sup>
$\chi_{bb}(I)$	1089.5756(57)	$\chi_{bb}(I)$	1089.6087(100)	1080 <sup>g</sup>
$\chi_{cc}(I)^f$	655.4462(57)	$\chi_{cc}(I)^f$	655.4131(100)	661 <sup>g</sup>
$\chi_{aa}^N(I)$	−0.00257(38)	$\chi_{aa}^N(I)$	−0.00238(39)	
$\chi_{aa}^K(I)$	0.0894(36)	$\chi_{aa}^K(I)$	0.0885(46)	
$C_{aa}(I)$	0.38874(90)	$C_{aa}(I)$	0.38042(101)	
$C_{bb}(I)$	0.03359(33)	$C_{bb}(I)$	0.03224(33)	
$C_{cc}(I)$	0.02318(38)	$C_{cc}(I)$	0.02405(38)	
$a_F(H)$	−57.60362(72)	$a_F(H)$	−57.60464(72)	
$T_{aa}(H)$	−20.7056(21)	$T_{aa}(H)$	−20.7086(21)	
$T_{bb}(H)$	18.9(10)	$T_{bb}(H)$	20.01(10)	
$T_{cc}(H)^f$	1.8(10)	$T_{cc}(H)^f$	0.69(10)	
$10^3 \times \sigma$ (fit)	29.0	$10^3 \times \sigma$ (fit)	29.4	

<sup>a</sup> Values in parentheses denote the standard deviation (1 $\sigma$ ) and apply in units of the last digits of the constants. <sup>b</sup> Equilibrium rotational constants obtained from ref 71. <sup>c</sup> Fixed to the value scaled from those of CH<sub>2</sub>Cl (refs 16 and 17) and CH<sub>2</sub>Br (ref 18). <sup>d</sup> Predicted using the same electronic spin density with  $s$  character as those of CH<sub>2</sub>Br; see text for details. <sup>e</sup> Predicted using the same electronic spin density with  $p$  character as those of CH<sub>2</sub>Br; see text for details. <sup>f</sup> Derived using the  $T_{cc} = -(T_{aa} + T_{bb})$  and  $\chi_{cc} = -(\chi_{aa} + \chi_{bb})$  relationships. <sup>g</sup> Predicted using  $\chi_{aa}(I) = -1934$  MHz of CH<sub>3</sub>I (ref 74) together with the ratio  $\chi_{bb}(I)/\chi_{aa}(I) = -0.62$  in CH<sub>2</sub>X radicals, where X = Cl, Br; see text for details.

our initial prediction<sup>71</sup> or with the theoretical calculations made by Marshall et al. (2.049 and 1.081 Å),<sup>51</sup> by Odelius et al. (2.066 and 1.083 Å),<sup>65</sup> and by Liu et al. (2.050 and 1.086 Å)<sup>67</sup> but not with the values by Dymov et al. (2.103 and 1.070 Å).<sup>63</sup> Our result for the  $r(C-H)$  bond length is also very close to that obtained for CH<sub>2</sub>Br ( $r_0(C-H) = 1.084$  Å)<sup>73</sup> and CH<sub>3</sub>I ( $r_e(C-H) = 1.085$  Å, ref 19, p. 219). Our value for  $r(C-I)$  in CH<sub>2</sub>I is smaller than that in CH<sub>3</sub>I ( $r_e(C-I) = 2.133$  Å, ref 19, p. 219). A difference of this magnitude (0.090 Å) for the C–Br bond lengths also exists between the CH<sub>2</sub>Br and CH<sub>3</sub>Br species.<sup>73,19</sup> Measurements of the rotational spectrum of the deuterated isotopologue, CD<sub>2</sub>I, are planned to be conducted in the near future; as a result, these structural parameters will likely evolve to become more accurate.

Because rotational transitions with relatively high  $N$  and  $K_a$  values have been measured, centrifugal distortion terms up to the sextic order have been accurately determined. They are consistent with the corresponding values of CH<sub>2</sub>Cl and CH<sub>2</sub>Br when available.<sup>17,18</sup> A systematic decrease of their magnitudes with increased size of the halogen atom is observed. Thus, the

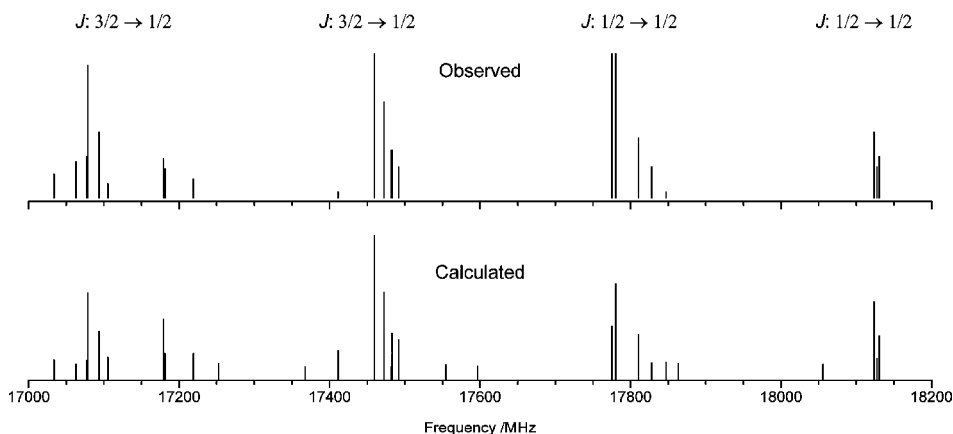


**Figure 3.** Stick diagrams of the observed (upper panel) and calculated (lower panel, assuming a temperature of 100 K) emission spectra of the  $1_{0,1} \rightarrow 0_{0,0}$  transition near 17 600 MHz. See the Supporting Information for the assignment of the lines.

**TABLE 2: Comparison of Hyperfine Coupling Constants (A Reduction, I' Representation) of CH<sub>2</sub>X Radicals (X = F, Cl, Br, and I)**

	CH <sub>2</sub> F <sup>a</sup>	CH <sub>2</sub> <sup>35</sup> Cl <sup>b</sup>	CH <sub>2</sub> <sup>79</sup> Br <sup>c</sup>	CH <sub>2</sub> I <sup>d</sup>
		hyperfine coupling constant (in MHz)		
$a_F(X)$	184.103(42) <sup>e</sup>	8.532(90)	22.79041(86)	-15.83740(47)
$T_{aa}(X)$	-255.205(40)	-32.297(29)	-149.7182(19)	-152.96434(65)
$T_{bb}(X)$	-212.310(52)	-23.00(83)	-107.98(18)	-138.9880(18)
$T_{cc}(X)^f$	467.515(66)	55.30(83)	257.70(18)	291.9524(18)
$\chi_{aa}(X)$		-66.070(77)	518.3387(39)	-1745.0218(26)
$\chi_{bb}(X)$		42.8(164)	-325.556(56)	1089.5756(57)
$\chi_{cc}(X)^f$		23.3(164)	-192.780(56)	655.4462(57)
$C_{aa}(X)$	0.376(30)		0.3192(42)	0.38874(90)
$C_{bb}(X)$			0.04385(57)	0.03359(33)
$C_{cc}(X)$				0.02318(38)
$a_F(H)$	-60.734(23)	-61.756(176)	-60.208(13)	-57.60362(72)
$T_{aa}(H)$	-25.676(26)	-21.832(50)	-21.8941(33)	-20.7056(21)
$T_{bb}(H)$	24.2(9)	17.6(17)	25.0(13)	18.9(10)
$T_{cc}(H)^f$	1.4(9)	4.2(17)	-3.1(13)	1.8(10)
		unpaired electron density on the halogen X (in %)		
<i>s</i> -character	0.35	0.15	0.071	-0.038
<i>p</i> -character	13.3	15.7	15.8	18.0

<sup>a</sup> Ref 4. <sup>b</sup> Refs 16 and 17. <sup>c</sup> Ref 18. <sup>d</sup> Present work. <sup>e</sup> 1 $\sigma$  error in units of the last digits. <sup>f</sup> Derived using the  $T_{cc} = -(T_{aa} + T_{bb})$  or  $\chi_{cc} = -(\chi_{aa} + \chi_{bb})$  relationships.

quartic centrifugal distortion constants of CH<sub>2</sub>I are typically 1 order of magnitude lower than those of CH<sub>2</sub>F.<sup>4,45</sup>

All hyperfine constants for both iodine and hydrogen atoms are determined in this investigation for the first time, and the values obtained for CH<sub>2</sub>I may be compared with those of the CH<sub>2</sub>X analogues (X = F, Cl, and Br), as outlined in Table 2. In particular, the absolute values of the Fermi-contact term, the magnetic dipolar coupling constants, and the diagonal components of the nuclear quadrupole coupling tensor are very close to their invaluable estimate, the differences being about 5–15% for the isotropic and anisotropic magnetic coupling constants and less than 1% for the quadrupole coupling parameters (Table 1). Going into detail, since the signs of the Fermi-contact terms,  $a_F(X)$  for X = F, Cl, and Br, are all positive,  $a_F(I)$  was supposed to be positive as well at the initial stage of the FT-MW spectral assignments. However, the observed FT-MW spectra could be understood only when the sign of  $a_F(I)$  was set to be negative. This apparent contradiction can be rationalized partly by a spin polarization effect through  $\sigma$  bonding orbital as discussed by Mishra et al.;<sup>77</sup> indeed the amount of the Fermi-contact term can be interpreted as a consequence of the balance between

$\alpha$ -spin (spin on the halogen atom, giving a positive contribution) and  $\beta$ -spin (spin on carbon, with a negative contribution) acting on the  $\sigma$  bonding electrons. The latter contribution is a function of the halogen *s*-character for the  $\sigma$  bonding electrons. If the former one is dominant, then the sign of the Fermi constant is positive, while it is negative if the latter is larger. Surprisingly, despite the increased delocalization of the unpaired electron onto the halogen atom on going from fluorine to iodine substituents (see the discussion below on the magnetic dipolar tensor components in relation with the unpaired electron spin density on the halogen atom), the contribution of  $\alpha$ -spin on the *s* orbital induced by a spin polarization effect decreases systematically from 0.35% in CH<sub>2</sub>F to 0.071% in CH<sub>2</sub>Br, and to -0.038% in CH<sub>2</sub>I when the corresponding atomic values are used for this estimation.<sup>72</sup> Another mechanism that takes into account the relativistic effects<sup>72,78</sup> in heavy atoms like iodine may be responsible for the negative sign of the Fermi-contact term. These effects, most likely the dominant ones, have been invoked by Miller and Cohen in their studies on the iodine mono- and dioxides.<sup>79</sup> The Fermi-contact term in these radicals is interestingly negative, contrary to the scalar hyperfine coupling constant

in their chlorine and bromine analogues. The fact that we also obtained a negative value shows the consistency of the least-squares analysis and demonstrates the importance of the relativistic effects in species that contain heavy elements.

As can be seen from Table 2, the relationship for  $\pi$  radicals,  $T_{aa} \approx T_{bb} \approx -1/2 T_{cc}$ , is well satisfied for all halogen-substituted derivatives of the methyl radical. This result also supports the view that the ground electronic state of  $\text{CH}_2\text{I}$  is of  ${}^2B_1$  symmetry like all the  $\text{CH}_2\text{X}$  halogen analogues. From the determined  $T_{cc}(\text{I})$  value, the unpaired electron density on the  $p_\pi$  orbital of the halogen atom is found to be 18.0% showing a monotonic increase from fluorine to iodine (13.3% in  $\text{CH}_2\text{F}$ , 15.7% in  $\text{CH}_2\text{Cl}$ , and 15.8% in  $\text{CH}_2\text{Br}$ ), as summarized in Table 2. A closer inspection of the magnetic dipolar constants reveals that the two in-plane components,  $T_{aa}$  and  $T_{bb}$ , though very close, are not equal to each other, thus indicating that the spatial distribution of the unpaired electron is not cylindrically symmetrical about the out-of-plane  $c$  inertial axis. Rather, the electron spin density is slightly more prominent in the  $a$ -axis than in the  $b$ -axis direction. The same feature is shown by the various  $\text{CH}_2\text{X}$  analogues (Table 2), although less pronounced in the case of  $\text{CH}_2\text{I}$ .

The nuclear quadrupole coupling constants have been accurately determined in the present investigation together with the  $N$  and  $K$  dependences of  $\chi_{aa}(\text{I})$  (see Table 1). As was guessed in our predictions, the axial component of the iodine nuclear quadrupole coupling constant,  $\chi_{aa}(\text{I})$ , is about 10% smaller in magnitude in  $\text{CH}_2\text{I}$  ( $-1745.02$  MHz) than in  $\text{CH}_3\text{I}$  ( $-1934.13$  MHz).<sup>74</sup> Therefore, an increase in delocalization of  $\pi$  electrons of similar magnitude from  $\text{CH}_3\text{X}$  to  $\text{CH}_2\text{X}$  molecules can be inferred for the  $\text{X} = \text{Cl, Br, and I}$  series. More precisely, the difference in electron population in the  $\pi_b$  and  $\pi_c$  orbitals,  $n_b - n_c$ , is related to the asymmetry parameter  $\eta$  ( $\eta = (\chi_{bb} - \chi_{cc})/\chi_{aa}$ ) in the nuclear quadrupole coupling tensor  $\chi$  by the relation<sup>19</sup>

$$n_b - n_c = \frac{2}{3} \left( \frac{\chi_{bb} - \chi_{cc}}{eQq_{510}} \right) = \frac{2}{3} \left( \frac{\chi_{aa}}{eQq_{510}} \right) \eta$$

where  $eQq_{510}$  represents the nuclear quadrupole coupling of the iodine atom by an electron in the  $3p_z$  orbital.<sup>19,80</sup> When the value of  $\eta$ ,  $-0.249$ , is used with  $eQq_{510}$  of  $2292.71$  MHz (ref 19, p 752), the quantity  $n_b - n_c$  is estimated to be  $0.126$ , indicating that about  $0.126$  electrons are delocalized from the  $\pi_c$  orbital of iodine. It is then possible to evaluate the ionic character  $i_\sigma$  of the  $\text{C-I}$   $\sigma$  bond through the relation (ref 19, p 759)

$$\chi_{aa} = - \left( \frac{n_b + n_c}{2} - 1 - i_\sigma \right) eQq_{510}$$

Using the spin density with  $p$  character on the iodine atom (18.0%), the quantities  $n_c = 2 - 0.180 = 1.820$  and  $n_b = n_c + 0.126 = 1.946$  are obtained, giving  $i_\sigma = 0.122$ . This value is very close to that of  $\text{CH}_3\text{I}$  (0.13, ref 19, p 760). Comparable results were derived between the analogous  $\text{CH}_3\text{X}/\text{CH}_2\text{X}$  systems with  $\text{X} = \{\text{Cl; Br}\}$  as is summarized in Table 3. This can be understood by the difference in effective electronegativity of the carbon to which the halogen atom under investigation is bonded.<sup>19,20</sup>

The values of the hydrogen hyperfine coupling constants are discussed. They are typical of the  $\alpha$ -hydrogen of  $\pi$ -radicals; i.e., (i) the Fermi-contact term is of the order of  $-60$  MHz, implying that the unpaired electron is mostly located on the

**TABLE 3: Comparison of Ionic Character of  $\sigma$  C–X Bonds ( $i_\sigma$ ) Estimated from the Halogen Nuclear Quadrupole Coupling Constants for  $\text{CH}_3\text{X}$  and  $\text{CH}_2\text{X}$  ( $\text{X} = \text{Cl, Br, and I}$ )**

	ionic character $i_\sigma$	
	$\text{CH}_3\text{X}$	$\text{CH}_2\text{X}$
$\text{X} = {}^{35}\text{Cl}$	0.35 <sup>a</sup>	0.34 <sup>b</sup>
$\text{X} = {}^{79}\text{Br}$	0.25 <sup>a</sup>	0.23 <sup>c</sup>
$\text{X} = {}^{127}\text{I}$	0.13 <sup>a</sup>	0.12 <sup>d</sup>

<sup>a</sup> Ref 19, p 760. <sup>b</sup> Ref 16. <sup>c</sup> Recalculated using the data taken from ref 18. <sup>d</sup> This work.

neighboring carbon atom<sup>81</sup> as seen in the above discussion, and (ii) the anisotropic hyperfine coupling constants verify  $T_{aa} \approx -T_{bb}$ ,  $T_{cc} \approx 0$ .<sup>82</sup> It is to be noted that the hydrogen dipolar coupling constants are in principle difficult to interpret because the unpaired electron is mainly localized about the carbon–halogen bond. No simple trend in their values going from the fluorine species to the iodine species can be readily seen from Table 2. On one hand, this may be related to the fact that the geometric structure of the  $\text{CH}_2$  moiety does not change upon substitution by any halogen atom, as is supported by theoretical calculations.<sup>83</sup> On the other hand, the constants  $T_{bb}(\text{H})$  and  $T_{cc}(\text{H})$  are in principle mainly determined from transitions of the *para*-species (namely,  $K_a = 1$  transitions), and since the total proton nuclear spin  $I(\text{H})$  vanishes for these transitions (thus eliminating the hyperfine structure due to the hydrogen nuclei), a large uncertainty results on the  $T_{bb}(\text{H})$  and  $T_{cc}(\text{H})$  constants. Altogether, the comparison of the hydrogen hyperfine constants (Table 2) clearly demonstrates that the unpaired electron distribution around the two protons is relatively invariable in the  $\text{CH}_2\text{X}$  halogen-substituted methyl radicals.

The spin-rotation constants are finally considered. The observed electron spin-rotation constants behave similarly to those of the  $\text{CH}_2\text{X}$  halogen analogues, but in fact it is difficult to assess their significance because no information is available on the excited electronic states of the  $\text{CH}_2\text{I}$  radical. The electron spin-rotation constant  $\varepsilon_{cc}$  has been found to be relatively small as it should be for an unpaired electron mainly located in the out-of-plane  $p_\pi$  orbital.<sup>84</sup> The values of the electron spin-rotation coupling constants for the  $\text{CH}_2\text{X}$  systems are given in Table 4 for the sake of comparison. It is interesting to point out that the  $\text{CH}_2\text{X}$  halo-species all have negative  $\varepsilon_{aa}$  and  $\varepsilon_{bb}$  constants.<sup>4,16,18</sup> Since in second-order perturbation theory the electron spin-rotation constants are proportional to the rotational constants  $B_i$ , it is more appropriate to compare values of  $\varepsilon_{ii}/B_i$  (Table 4), where  $i$  designates the  $a$ ,  $b$ , and  $c$  principal axes. The values obtained for the reduced  $\varepsilon_{aa}/A$  and  $\varepsilon_{bb}/B$  constants of  $\text{CH}_2\text{I}$  are nearly equal. This is consistent with planar radicals with  ${}^2B_1$  symmetry in the ground electronic state<sup>85</sup> and demonstrates the reliability of our results. Table 4 shows also that the ratios  $\varepsilon_{ii}/B_i$  obtained for the  $\text{CH}_2\text{X}$  radicals increase in magnitude monotonically with increasing atomic number of the halogen atom. This result may be mainly ascribed to an increase of the spin–orbit coupling constant with increasing atomic number of the halogen. Indeed, as already discussed by Endo et al. in their paper on  $\text{CH}_2\text{Cl}$  (ref 16), two main contributions affect the electron spin-rotation tensor components: the spin–orbit coupling constant of the molecule under consideration and the energy difference between an excited electronic state and the ground state. The method to calculate an effective value for the spin–orbit coupling constant in  $\text{CH}_2\text{I}$  was the same as that for  $\text{CH}_2\text{Cl}$  (ref 16) or for  $\text{CH}_2\text{Br}$  (ref 18); we obtained  $1392.3$   $\text{cm}^{-1}$  for  $A_{SO}$  in  $\text{CH}_2\text{I}$  with the value of  $7603$   $\text{cm}^{-1}$  taken for the spin–orbit coupling constant for atomic iodine.<sup>86</sup> This value

**TABLE 4: Comparison of the Axial Components of the Electron Spin–Rotation Coupling Tensor (A Reduction,  $\Gamma$  Representation) for the CH<sub>2</sub>X Radicals (X = F, Cl, Br, and I)**

	CH <sub>2</sub> F <sup>a</sup>	CH <sub>2</sub> <sup>35</sup> Cl <sup>b</sup>	CH <sub>2</sub> <sup>37</sup> Cl <sup>b</sup>	CH <sub>2</sub> <sup>79</sup> Br <sup>c</sup>	CH <sub>2</sub> <sup>81</sup> Br <sup>c</sup>	CH <sub>2</sub> <sup>127</sup> I <sup>d</sup>
$\epsilon_{aa}$	−1075.96	−3149.708	−3149.811	−12569.803	−12569.893	−29409.781
$\epsilon_{bb}$	−185.77	−237.626	−234.000	−699.229	−696.356	−926.527
$\epsilon_{cc}$	−1.41	11.794	11.622	68.388	67.843	208.809
$\epsilon_{aa}/A$	−0.00406	−0.01148	−0.01148	−0.04591	−0.04591	−0.10630
$\epsilon_{bb}/B$	−0.00600	−0.01490	−0.01490	−0.06136	−0.06134	−0.10414

<sup>a</sup> Ref 4. <sup>b</sup> Refs 16 and 17. <sup>c</sup> Ref 18. <sup>d</sup> This work.

is 2.3-fold that found for CH<sub>2</sub>Br (606.7 cm<sup>−1</sup>, recalculated using the correct value for the spin–orbit constant for atomic bromine: 3685 cm<sup>−1</sup>).<sup>16,86</sup> Assuming a contribution from a single excited state (of *B*<sub>2</sub> symmetry), the first excited electronic state is found to lie 52 400 cm<sup>−1</sup> (6.5 eV) above the ground state. No values have been reported thus far on the excited electronic states of the CH<sub>2</sub>I radical, but this energy difference may be compared with the adiabatic ionization energy of 8.40 eV determined by Andrews et al.<sup>53</sup>

The three nuclear spin-rotation interaction constants were determined to be 0.38874(90), 0.03359(33), and 0.02318(38) for the *a*, *b*, and *c* axis components, respectively. Endo et al. derived an approximate relation between the electron and the nuclear spin-rotation interaction constants<sup>4</sup> which is given by:  $|C_{ii}(I)/\epsilon_{ii}| = |a/A_{SO}|$ ; the constant *a* denotes the off-diagonal orbital hyperfine coupling constant which can be taken as  $a = 5/4T_{cc}(I) \approx 365$  MHz. With the *A*<sub>SO</sub> value obtained above (41 740 104 MHz), the nuclear spin-rotation constants are calculated to be 0.257, 0.008, and 0.002 MHz, respectively. Keeping in mind the approximations made (i.e., the main contribution to the nuclear-spin rotation parameters is expected to arise from spin–orbit coupling in second order), the orders of magnitude of these values agree with the observed ones.

## Conclusion

The CH<sub>2</sub>I radical has been characterized in the gas phase by Fourier transform microwave and millimeter-wave spectroscopy for the first time. The analysis of the observed fine and hyperfine structures owing to the iodine and hydrogen nuclear spins yielded information on the electronic structure of this species. This investigation has completed the series of studies of the high-resolution rotational spectrum of the monohalogen-substituted methyl radicals. An extensive set of molecular constants has been obtained, allowing a systematic comparison of the structural and electronic properties to be made among the entire series. While CH<sub>2</sub>F can be considered as almost planar, the other members of this series are clearly planar radicals with a <sup>2</sup>B<sub>1</sub> ground electronic state. Both the Fermi-contact and the magnetic dipolar coupling constants of the halogen indicate a monotonic trend on going from the fluoro- to the iodo-substituents. In particular, a systematic increase of electron spin density with *p* character with increasing atomic number of the halogen has been revealed. Although no trend was found for the magnetic dipole constants of the protons, their values are consistent with each other and are typical of the  $\alpha$ -hydrogen of  $\pi$ -radicals.

**Acknowledgment.** S.B. gratefully acknowledges financial support for this research from the ARCUS (Actions en Régions de Coopération Universitaire et Scientifique) program. P.K. acknowledges support through the European Union Marie-Curie human resources and mobility programme for his postdoctoral fellowship under Contract MCRTN-CT-2004-512302 (Molec-

ular Universe). D. Duflot is thanked for providing the ab initio calculations and for helpful discussions. The unknown Reviewer 2 is acknowledged for pointing out the relativistic effects that mainly contribute to the negative sign of the Fermi-contact term.

**Supporting Information Available:** Listing of observed and obsd – calcd transition frequencies, molecular constants, and correlation matrix (output file with extension .fit from Pickett’s SPFIT<sup>75</sup> reformatted with the PIFORM program<sup>76</sup> from Kisiel). Corresponding ascii file available on request to the corresponding author. This material is available free of charge via the Internet at <http://pubs.acs.org>.

## References and Notes

- (1) Fessenden, R. W.; Schuler, R. H. *J. Chem. Phys.* **1965**, *43*, 2704.
- (2) Carlson, G. A.; Pimentel, G. E. *J. Chem. Phys.* **1966**, *44*, 4053.
- (3) Milligan, D. E.; Jacox, M. E.; Comeford, J. J. *J. Chem. Phys.* **1966**, *44*, 4058.
- (4) Endo, Y.; Yamada, C.; Saito, S.; Hirota, E. *J. Chem. Phys.* **1983**, *79*, 1605.
- (5) Koenig, T.; Balle, T.; Snell, W. *J. Am. Chem. Soc.* **1975**, *97*, 662.
- (6) Dyke, J.; Jonathan, N.; Lee, E.; Morris, A. *J. Chem. Soc., Faraday Trans. 2* **1976**, *72*, 1385. Golob, L.; Jonathan, N.; Morris, A.; Okuda, M.; Ross, K. J. *J. Electron. Spectrosc.* **1972/1973**, *1*, 506.
- (7) Morokuma, K.; Pedersen, L.; Karplus, M. *J. Chem. Phys.* **1968**, *48*, 4801.
- (8) Jacox, M. E.; Milligan, D. E. *J. Chem. Phys.* **1969**, *50*, 3252. Jacox, M. E. *J. Chem. Phys.* **1981**, *59*, 199.
- (9) Jacox, M. E.; Milligan, D. E. *J. Chem. Phys.* **1970**, *53*, 2688.
- (10) Andrews, L.; Smith, D. W. *J. Chem. Phys.* **1970**, *53*, 2956.
- (11) Smith, D. W.; Andrews, L. *J. Chem. Phys.* **1971**, *55*, 5295.
- (12) Smith, D. W.; Andrews, L. *J. Chem. Phys.* **1973**, *58*, 5222.
- (13) Yamada, C.; Hirota, E.; Kawaguchi, K. *J. Chem. Phys.* **1981**, *75*, 5256.
- (14) Karplus, M.; Fraenkel, G. K. *J. Chem. Phys.* **1961**, *35*, 13. Schrader, D. M.; Karplus, M. *J. Chem. Phys.* **1964**, *40*, 1593.
- (15) Inada, N.; Saito, K.; Hayashi, M.; Ozeki, H.; Saito, S. *Chem. Phys. Lett.* **1998**, *284*, 142.
- (16) Yamada, C.; Hirota, E. *J. Chem. Phys.* **1983**, *78*, 1703.
- (17) Endo, Y.; Saito, S.; Hirota, E. *Can. J. Phys.* **1984**, *62*, 1347.
- (18) Baillieux, S.; Dréan, P.; Zelinger, Z.; Godon, M. *J. Mol. Spectrosc.* **2005**, *229*, 140.
- (19) Ozeki, H.; Okabayashi, T.; Tanimoto, M.; Saito, S.; Baillieux, S. *J. Chem. Phys.* **2007**, *127*, 224301.
- (20) Gordy, W.; Cook, R. L. *Microwave Molecular Spectra*. In *Techniques of Chemistry*, 3rd ed.; Weissberger, A., Ed.; Wiley-Interscience: New York, 1984; Vol. XVIII.
- (21) Levchenko, S. V.; Krylov, A. I. *J. Phys. Chem. A* **2002**, *106*, 5169, and reference 13 therein.
- (22) Byrd, E. F. C.; Sherrill, C. D.; Head-Gordon, M. *J. Phys. Chem. A* **2001**, *105*, 9736.
- (23) Shul, R. J.; Pearton, S. J., Eds. *Handbook of Advanced Plasma Processing Techniques*; Springer: Berlin, 2000.
- (24) Barbieri, U.; Polacco, G.; Massimi, R. *Macromol. Symp.* **2006**, *234*, 51.
- (25) Procaccini, C.; Bozzelli, J. W.; Longwell, J. P.; Smith, K. A.; Sarofim, A. F. *Environ. Sci. Technol.* **2000**, *34*, 4565.
- (26) Su, J. Z.; Kim, A. K. *Fire Technol.* **2002**, *38*, 7.
- (27) Tapscott, R. E.; Sheinson, R. S.; Babushok, V.; Nyden, M. R.; Gann, R. G. *NIST Technical Note 1443: Alternative Fire Suppressant Chemicals: A Research Review with Recommendations*, **2001**.
- (28) Taylor, P. H.; Dellinger, B. *J. Anal. Appl. Pyrolysis* **1999**, *49*, 9.

- (28) Finlayson-Pitts, B. J.; Pitts, J. N., Jr. *Chemistry of the Upper and Lower Atmosphere: theory, experiments, and applications*; Academic Press: San Diego, CA, 2000.
- (29) Lary, D. J. *J. Geophys. Res.* **1997**, *102*, 21515. Lary, D. J. *J. Geophys. Res.* **1996**, *101*, 1505.
- (30) Calvert, J. G.; Lindberg, S. E. *Atmos. Environ.* **2004**, *38*, 5087.
- (31) Adams, J. W.; Cox, R. A. *J. Phys. IV France (Proc.)* **2002**, *12*, 105.
- (32) Calvert, J. G.; Lindberg, S. E. *Atmos. Environ.* **2004**, *38*, 5105.
- (33) Carpenter, L. *Chem. Rev.* **2003**, *103*, 4953.
- (34) Vogt, R. *Iodine Compounds in the Atmosphere; The Handbook of Environmental Chemistry (Book Series), Part E; Reactive Halogen Compounds in the Atmosphere (Book)*; Fabian, P., Singh, O. N., Eds.; Springer-Verlag: Berlin Heidelberg, 1999; Vol. 4, pp 113–126.
- (35) O'Dowd, C. D.; Jimenez, J. L.; Bahreini, R.; Flagan, R. C.; Seinfeld, J. H.; Hämeri, K.; Pirjola, L.; Kulmala, M.; Jennings, S. G.; Hoffmann, T. *Nature* **2002**, *417*, 632.
- (36) Kolb, C. E. *Nature* **2002**, *417*, 597.
- (37) Kroger, P. M.; Demou, P. C.; Riley, S. J. *J. Chem. Phys.* **1976**, *65*, 1823.
- (38) Orlando, J. J. *Atmospheric Chemistry of Organic Bromine and Iodine Compounds; The Handbook of Environmental Chemistry (Book Series), Part R; Series Anthropogenic Compounds (Book)*; Neilson, A. H., Ed.; Springer-Verlag: Berlin Heidelberg, 2003; Vol. 3, pp 253–299.
- (39) Dimmer, C. H.; Simmonds, P. G.; Nickless, G.; Bassford, M. R. *Atmos. Environ.* **2001**, *35*, 321.
- (40) Muramatsu, Y.; Yoshida, S. *Atmos. Environ.* **1995**, *29*, 21.
- (41) Redeker, K. R.; Wang, N. Y.; Low, J. C.; McMillan, A.; Tyler, S. C.; Cicerone, R. J. *Science* **2000**, *290*, 966.
- (42) Bell, N.; Hsu, L.; Jacob, D. J.; Schultz, M. G.; Blake, D. R.; Lobert, J. M.; Maier-Reimer, E. *J. Geophys. Res.* **2002**, *107*, 4340.
- (43) Phillips, D. L.; Fang, W. H.; Zheng, X. *J. Am. Chem. Soc.* **2001**, *123*, 4197. Phillips, D. L.; Fang, W. H. *J. Org. Chem.* **2001**, *66*, 5890.
- (44) Tarnovsky, A. N.; Sundström, V.; Åkesson, E.; Pascher, T. *J. Phys. Chem. A* **2004**, *108*, 237.
- (45) Nolte, J.; Wagner, H. G.; Sear, T. J.; Temps, F. *J. Mol. Spectrosc.* **1999**, *195*, 43.
- (46) Whitney, E. S.; Dong, F.; Nesbitt, D. J. *J. Chem. Phys.* **2006**, *125*, 054304.
- (47) Sears, T. J.; Temps, F.; Wagner, H. G. G.; Wolf, M. *J. Mol. Spectrosc.* **1994**, *168*, 136.
- (48) Whitney, E. S.; Haerber, T.; Schuder, M. D.; Blair, A. C.; Nesbitt, D. J. *J. Chem. Phys.* **2006**, *125*, 054303.
- (49) Davies, P. B.; Liu, Y.; Liu, Z. *Chem. Phys. Lett.* **1993**, *214*, 305.
- (50) Baughcum, S. L.; Leone, S. R. *J. Chem. Phys.* **1980**, *72*, 6531.
- (51) Marshall, P.; Srinivas, G. N.; Schwartz, M. *J. Phys. Chem. A* **2005**, *109*, 6371.
- (52) Jacox, M. E. *Vibrational and electronic energy levels of polyatomic transient molecules*; *J. Phys. Chem. Ref. Data*, Monograph 3; American Chemical Society and American Institute of Physics: Washington DC, 1994.
- (53) Andrews, L.; Dyke, J. M.; Jonathan, N.; Keddar, N.; Morris, A. *J. Phys. Chem.* **1984**, *88*, 1950.
- (54) Kambanis, K. G.; Lazarou, Y. G.; Papagiannakopoulos, P. *Chem. Phys. Lett.* **1997**, *268*, 498. Lazarou, Y. G.; Kambanis, K. G.; Papagiannakopoulos, P. *Chem. Phys. Lett.* **1997**, *271*, 280.
- (55) Stefanopoulos, V. G.; Papadimitriou, V. C.; Lazarou, Y. G.; Papagiannakopoulos, P. *J. Phys. Chem. A* **2008**, *112*, 1526.
- (56) Kambanis, K. G.; Argyris, D. Y.; Lazarou, Y. G.; Papagiannakopoulos, P. *J. Phys. Chem. A* **1999**, *103*, 3210.
- (57) Masaki, A.; Tsunashima, S.; Washida, N. *J. Phys. Chem.* **1995**, *99*, 13126.
- (58) Eskola, A. J.; Pastuszka, D. W.; Ratajczak, E.; Timonen, R. S. *Phys. Chem. Chem. Phys.* **2006**, *8*, 1416.
- (59) Enami, S.; Ueda, J.; Goto, M.; Nakano, Y.; Aloisio, S.; Hashimoto, S.; Kawasaki, M. *J. Phys. Chem. A* **2004**, *108*, 6347.
- (60) Seetula, J. A.; Gutman, D. *J. Phys. Chem.* **1991**, *95*, 10688.
- (61) Seetula, J. A. *Phys. Chem. Chem. Phys.* **2002**, *4*, 455.
- (62) Seetula, J. A.; Gutman, D. *J. Phys. Chem.* **1991**, *95*, 3626.
- (63) Dymov, B. P.; Skorobogatov, G. A.; Tschuikow-Roux, E. P. *Russ. J. Gen. Chem.* **2004**, *74*, 1686.
- (64) Eskola, A. J.; Pastuszka, D. W.; Ratajczak, E.; Timonen, R. S. *J. Phys. Chem. A* **2006**, *110*, 12177.
- (65) Odelius, M.; Kadi, M.; Davidsson, J.; Tarnovsky, A. N. *J. Chem. Phys.* **2004**, *121*, 2208.
- (66) Lazarou, Y. G.; Prosimis, A. V.; Papadimitriou, V. C.; Papagiannakopoulos, P. *J. Phys. Chem. A* **2001**, *105*, 6729.
- (67) Liu, Y. J.; Ajitha, D.; Krogh, J. W.; Tarnovsky, A. N.; Lindh, R. *Chem. Phys. Chem.* **2006**, *7*, 955.
- (68) Balle, T. J.; Flygare, W. H. *Rev. Sci. Instrum.* **1981**, *52*, 33.
- (69) Yamamoto, S.; Habara, H.; Kim, E.; Nagasaka, H. *J. Chem. Phys.* **2001**, *115*, 6007.
- (70) Fehsenfeld, F. C.; Evenson, K. M.; Broida, H. P. *Rev. Sci. Instrum.* **1965**, *36*, 294.
- (71) Dufloy, D.; Flament, J. P. private communication, 2008.
- (72) Morton, J. R.; Preston, K. F. *J. Magn. Reson.* **1978**, *30*, 577.
- (73) Bailleux, S.; Dréan, P.; Zelinger, Z.; Svatoopluk, C.; Ozeki, H.; Saito, S. *J. Chem. Phys.* **2005**, *122*, 134302.
- (74) Carocci, S.; Di Lieto, A.; De Fanis, A.; Minguzzi, P.; Alanko, S.; Pietilä, J. *J. Mol. Spectrosc.* **1998**, *191*, 368.
- (75) Pickett, H. M. *J. Mol. Spectrosc.* **1991**, *148*, 371.
- (76) Kisiel, Z. *J. Mol. Spectrosc.* **2003**, *218*, 58. PROSPE - Programs for ROtational SPEctroscopy, <http://info.ifpan.edu.pl/~kisiel/prospe.htm>.
- (77) Mishra, S. P.; Neilson, G. W.; Symons, M. C. R. *J. Chem. Soc., Faraday Trans. 2* **1974**, *70*, 1165.
- (78) Pyykkö, P.; Wiesefeld, L. *Mol. Phys.* **1981**, *43*, 557.
- (79) Miller, C. E.; Cohen, E. A. *J. Chem. Phys.* **2003**, *118*, 6309, and references therein. Miller, C. E.; Cohen, E. A. *J. Chem. Phys.* **2001**, *115*, 6459.
- (80) Harris, K. R.; Becker, E. D.; Cabral de Menezes, S. M.; Goodfellow, R.; Granger, P. *Pure Appl. Chem.* **2001**, *73*, 1795.
- (81) McConnell, H. M.; Chesnut, D. B. *J. Chem. Phys.* **1958**, *28*, 107.
- (82) Morton, J. R. *Chem. Rev.* **1964**, *64*, 453.
- (83) Li, Q. S.; Zhao, J. F.; Xie, Y.; Schaefer, H. F., III. *Mol. Phys.* **2002**, *100*, 3615.
- (84) Curl, R. F. *J. Chem. Phys.* **1962**, *37*, 779.
- (85) Hirota, E. *High-resolution spectroscopy of transient molecules*; Springer-Verlag: Berlin, 1985.
- (86) Davies, S. J.; McDermott, W. E.; Heaven, M. C. *Gas Lasers. Chapter 9: Atomic Iodine Lasers*; Endo, M., Walter, R. F., Eds.; CRC Press: New York, 2006; pp 413–448. See also the webpage of the National Institute of Standards and Technology on the Handbook of Basic Atomic Spectroscopic Data at: [http://physics.nist.gov/PhysRefData/Handbook/element\\_name.htm](http://physics.nist.gov/PhysRefData/Handbook/element_name.htm).



## 2.4 Stable iodine-bearing species: ICl and CH<sub>2</sub>ICl

Difficulties in the production of the CH<sub>2</sub>I radical with the Lille millimetre-wave spectrometer led us to use two precursors, the mono- and diiodomethane in order to verify the presence of several by-products as due to abstraction reactions with atomic chlorine. We paid particular attention to two species: ICl, generated with any of the above mentioned compounds, and CH<sub>2</sub>ICl, arising from the iodine abstraction from CH<sub>2</sub>I<sub>2</sub> (primary reaction) followed by CH<sub>2</sub>I recombination with Cl. Observation of their millimetre-wave spectra gave indirect but clear evidence of the production of CH<sub>2</sub>I.

### 2.4.a ICl

Starting from 1931, ICl ( $X^1\Sigma^+$ ) has been the subject of numerous studies aimed at rationalizing the unusual properties that this mixed halide diatomic species exhibits. In particular, ICl has long been observed by high-resolution molecular spectroscopy in the microwave,<sup>118</sup> millimetre-wave<sup>119</sup> and infrared regions.<sup>120</sup> The millimetre-wave study covered the rotational states from  $J=12$  to  $J=44$  and vibrational states  $v=0$  to  $v=3$ , corresponding to a frequency range from 85 to 300 GHz. The latter infrared work yielded mass-reduced Dunham constants in addition to the standard Dunham coefficients. It is remarkable that although Dunham first published his model for the energy levels of diatomic molecules nearly 80 years ago, it continues to provide the basis for the analysis of their high-resolution spectra. However, this model was modified to incorporate effects of Born-Oppenheimer breakdown because of growing accuracy of

---

<sup>118</sup> R. T. Weidner, *Phys. Rev.* **72**, 1268 (1947); C. H. Townes, B. D. Wright and F. R. Merritt, *Phys. Rev.* **73**, 1249 (1948).

<sup>119</sup> R. E. Willis and W. W. Clark, *J. Chem. Phys.* **72**, 4946 (1980).

<sup>120</sup> H. G. Hedderich, P. F. Bernath and G. A. McRae, *J. Mol. Spectrosc.* **155**, 384 (1992).

spectroscopic measurements. The procedure for doing this for  $^1\Sigma^+$  species was published by Watson<sup>121</sup> and Bunker.<sup>122</sup>

We extended the measurement of the millimetre-wave spectrum of ICl below 470 GHz by including 45 new lines covering  $J=61$  to  $J=71$ , for  $\nu=0$  to  $\nu=4$  vibrational states. The available millimetre-wave data were combined to carry out the mass-invariant analysis using the expression:

$$E_{\nu,J} = \sum_{i,j} U_{ij} \mu^{-(i/2+j)} \left(1 + \frac{m_e}{M_{\text{Cl}}} \Delta_{ij}^{\text{Cl}}\right) \left(\nu + \frac{1}{2}\right)^i J^j (J+1)^j$$

where the  $U_{ij}$  are the mass-invariant Dunham parameters,  $\mu$  the reduced-mass of the molecule,  $m_e$  and  $M_{\text{Cl}}$  are the electron and Cl masses, respectively. The terms  $\Delta_{ij}^{\text{Cl}}$  allow for the inclusion of the Watson's first-order correction due to breakdown of the Born-Oppenheimer approximation for Cl, of which only the  $\Delta_{01}^{\text{Cl}}$  terms are significant. This work resulted in the determination of  $\Delta_{01}^{\text{Cl}}$  in addition to seven mass-independent Dunham parameters (Table 2.1). Given in MHz, our value of  $\Delta_{01}^{\text{Cl}}$  compares very well with that found in AlCl (-1.443(29))<sup>123</sup> and in TlCl (-1.243(49)).<sup>124</sup> Enough data have been obtained to evaluate the isotopically independent Born-Oppenheimer internuclear distance  $r_e$  of ICl. This is an equilibrium distance in which volume effects are included, and was determined

with:<sup>122</sup>  $r_e = \sqrt{\frac{\hbar}{4\pi U_{01} m_u}}$  ( $m_u = 1.66053892(8) \cdot 10^{-27}$  kg, NIST value). The value derived is:  $r_e = 2.32011152(49)$  Å.

---

<sup>121</sup> J. K. G. Watson, *J. Mol. Spectrosc.* **45**, 99 (1973); J. K. G. Watson, *J. Mol. Spectrosc.* **80**, 411 (1973).

<sup>122</sup> P. R. Bunker *J. Mol. Spectrosc.* **35**, 307 (1970); P. R. Bunker *J. Mol. Spectrosc.* **68**, 367 (1977).

<sup>123</sup> H. Hedderich, M. Dulick and P. F. Bernath, *J. Chem. Phys.* **99**, 8363 (1993).

<sup>124</sup> E. Tiemann, H. Arnst, W. U. Steida, T. Törring and J. Hoeft, *Chem. Phys.* **67**, 133 (1982).

**Table 2.1** Mass-independent Dunham parameters  $U_{ij}$  and Born-Oppenheimer breakdown coefficient  $\Delta_{01}^{Cl}$  for ICl.

	ICl ( $X^1\Sigma^+$ )
$U_{01}$ (MHz amu)	93820.9758(40)
$U_{11}$ (MHz amu <sup>3/2</sup> )	-2292.289(54)
$U_{21}$ (MHz amu <sup>2</sup> )	-27.232(100)
$U_{31}$ (MHz amu <sup>5/2</sup> )	-2.503(77)
$U_{02}$ (MHz amu <sup>2</sup> )	-0.907480(75)
$U_{12}$ (MHz amu <sup>5/2</sup> )	-0.025940(67)
$U_{03} \times 10^{-6}$ (MHz amu <sup>3</sup> )	-5.98(27)
$\Delta_{01}^{Cl}$	-1.293(26)

#### 2.4.b CH<sub>2</sub>ICl

The surface ocean is an important source of reactive organic iodine compounds such as CH<sub>3</sub>I, CH<sub>2</sub>I<sub>2</sub>, CH<sub>2</sub>ICl and CH<sub>2</sub>BrI to the marine boundary layer.<sup>125</sup> The high photolability of these species, and particularly those containing two chromophores, makes them efficient active iodine atom precursors in the troposphere. The subsequent reaction of I with O<sub>3</sub> to form IO radical initiates various tropospheric ozone depleting cycles.<sup>102,126</sup>

From the spectroscopic point of view, very little is known on CH<sub>2</sub>ICl, on both experimental and theoretical aspects. The microwave spectrum of this dihalomethane containing two quadrupolar nuclei was first investigated in the frequency region 9-35 GHz in 1987,<sup>127</sup> and a number of *b*-

<sup>125</sup> L. J. Carpenter, P. S. Liss and S. A. Penkett, *J. Geophys. Res.* **108**, 4256 (2003).

<sup>126</sup> G. McFiggans, J. M. C. Plane, B. J. Allan, L. J. Carpenter, H. Coe and C. O'Dowd, *J. Geophys. Res.* **105**, 14371 (2000).

<sup>127</sup> I. Ohkoshi, Y. Niide and M. Takano, *J. Mol. Spectrosc.* **124**, 118 (1987).

type  $R$ - and  $Q$ -branch transitions were assigned. Discrepancies between observed and calculated frequencies as large as 700 KHz were attributed to the absence of the off-diagonal element of the  $\chi$  tensor in the least-squares analysis of the  $^{35}\text{Cl}$  and  $^{37}\text{Cl}$  isotopologues. A subsequent study in which this term was incorporated led to reduced discrepancies.<sup>128</sup> However, incoherent values of the centrifugal distortion constants between the two chlorine isotopologues remained in the second paper. Likewise, the  $^{35/37}\text{Cl}$  isotopic ratio reported for  $\chi_{zz}$  (where  $z$  is the principal axis of the  $\chi$  tensor, coinciding with the C-I bond), 1.4969, was anomalously too large in comparison with the ratio of the nuclear values of the quadrupole moment of the Cl atoms, 1.2688.<sup>129</sup>

We accordingly decided to investigate the microwave and millimetre-wave spectra of  $\text{CH}_2\text{ICl}$ , making use of both higher precision and accuracy of current microwave spectrometers. The presence of two different quadrupolar nuclei, Cl and I, having nuclear spin of  $3/2$  and  $5/2$ , respectively, complicates substantially the spectra. This is true not only in the microwave region, but in the millimetre-wave region as well because of the large quadrupole moment of the iodine nucleus which is similar in size as the  $B$  rotational constant.

$\text{CH}_2\text{ICl}$  ( $X^1A'$ ) is an asymmetric top close to the prolate limit ( $\kappa = -0.994$ ) with its dipole moment aligned to a large extent along the  $b$ -inertial axis. Its geometry is illustrated in Figure 2.6. The Hamiltonian used in the analysis is the summation of the rotational part, the nuclear quadrupole interaction term of the two halogen nuclei and the nuclear spin-rotation coupling part of the iodine nucleus:

---

<sup>128</sup> I. Ohkoshi and Y. Niide, *J. Mol. Spectrosc.* **126**, 282 (1987).

<sup>129</sup> R. K. Harris *et al.*, *Magn. Reson. Chem.* **40**, 489 (2002).

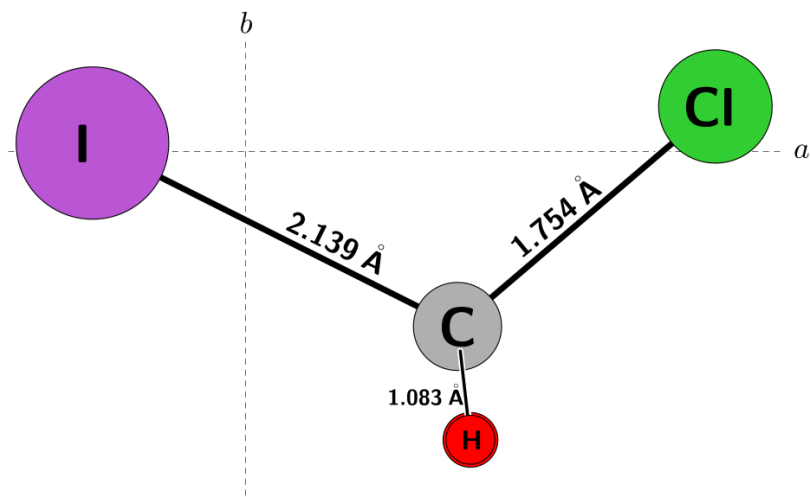


**Figure 2.6** Geometry of  $\text{CH}_2\text{ICl}$  ( $X^1A'$ ).

$$\mathbf{H} = \mathbf{H}_R + \mathbf{H}_Q + \mathbf{H}_{NSR}$$

$\mathbf{H}_R$  is the Watson-type Hamiltonian and includes the centrifugal distortion terms up to octic order using the  $I^r$  representation in the  $S$  reduction.  $\mathbf{H}_Q$  is the sum of two terms,  $\mathbf{H}_{Q,i}$  with  $i = \{\text{I, Cl}\}$ , which are the Hamiltonians describing the quadrupole coupling interactions of iodine and chlorine, respectively.  $\mathbf{H}_{Q,i}$  is given by Bragg<sup>130</sup> and Casimir<sup>131</sup> as:

$$\mathbf{H}_{Q,i} = -\frac{1}{6} \mathbf{Q}_i : \nabla E_i$$

which is the inner product ( $:$ ) between the nuclear quadrupole tensor  $\mathbf{Q}_i$  and the electric field gradient tensor due to the electrons at nucleus  $i$ ,  $\nabla E_i$  (including the off-diagonal elements), respectively. The quadrupole coupling constants of nucleus  $i$  used in the least-squares analysis,  $\chi_{\alpha\beta}\{i\}$ , are related to the electric field gradients tensor components  $V_{\alpha\beta,i}$  with the expression:

<sup>130</sup> J. K. Bragg, *Phys. Rev.* **74**, 533 (1948).

<sup>131</sup> H. B. G. Casimir in: *On the Interaction between Atomic Nuclei and Electrons* (Teyler's Tweede Genootschap, Haarlem, 1936; reprinted by Freeman, San Francisco, 1963).

$$\chi_{\alpha\beta}\{i\} = eQ_i V_{\alpha\beta,i} ,$$

with  $\alpha, \beta$  referring to the inertial axes and  $eQ_i$  being the quadrupole moment of the  $i^{\text{th}}$  nucleus.  $\mathbf{H}_{NSR}$  is given by:

$$\mathbf{H}_{NSR} = \mathbf{I} \cdot \mathbf{C} \cdot \mathbf{J} ,$$

where  $\mathbf{C}$  denotes the nuclear spin-rotation coupling tensor relevant for the iodine nuclear spin. We employed the coupling scheme of angular momenta as follows:  $\mathbf{F}_1 = \mathbf{J} + \mathbf{I}$  and  $\mathbf{F} = \mathbf{F}_1 + \mathbf{I}_{\text{Cl}}$ . The molecular constants for both isotopologues were obtained from the least-squares analysis of 1476 distinct transition frequencies (of which 907 -61 percent- belong to the  $\text{CH}_2^{35}\text{Cl}$  isotopologue) observed from 15 to 646 GHz. The measured transitions involve  $J \leq 108$ ,  $K_a \leq 12$ , and the rms error of the fit is 68 kHz. This value may seem a bit large but is in fact dominated by the large *obs. – calc.* values of the early microwave studies. The rotational and centrifugal distortion parameters are listed in Table 2.2., whilst the hyperfine structure coefficients are given in Table 2.3. Values derived from previous microwave study<sup>128</sup> are included for comparison. The set of parameters determined for the two isotopologues, including the hyperfine coupling constants, is now consistent. For best interpretation, the values in the principal axes of the quadrupole coupling tensors for both halogen atoms were obtained by diagonalizing the quadrupole coupling tensors in the principal inertial axes system and are shown in Table 2.4. In both cases, the  $z$  axis was assumed to lie along the C- $X$  bond ( $X = \text{Cl}, \text{I}$ ). The angle  $\theta_{za}$  between the principal  $a$  axis and the C-I bond was found to be  $26^\circ 12'$  and  $26^\circ 36'$  for the  $^{35}\text{Cl}$  and  $^{37}\text{Cl}$  isotopologues, respectively. In the case of the C-Cl bond, that angle was found to be  $39^\circ 27'$  and  $39^\circ 14'$ , respectively.

**Table 2.2** Rotational and centrifugal distortion constants of CH<sub>2</sub>ICl isotopologues in Watson's  $S$  reduction,  $I'$  representation.

Parameter	CH <sub>2</sub> I <sup>35</sup> Cl		CH <sub>2</sub> I <sup>37</sup> Cl	
	This work	Ref. 128	This work	Ref. 128
<b><i>A</i></b> (MHz)	27418.70476(36)	27418.61(55)	27261.22123(56)	27261.07(67)
<b><i>B</i></b> (MHz)	1621.931046(48)	1621.944(13)	1562.221124(84)	1562.347(25)
<b><i>C</i></b> (MHz)	1545.836186(45)	1545.863(24)	1491.033341(73)	1491.273(50)
<b><i>D<sub>J</sub></i></b> (kHz)	0.3966995(74)	0.529(67)	0.370611(17)	0.09(13)
<b><i>D<sub>JK</sub></i></b> (kHz)	-14.74436(21)	-10.1(37)	-14.29169( 46)	-39.0(77)
<b><i>D<sub>K</sub></i></b> (kHz)	429.7198(53)		426.048(17)	
<b><i>d<sub>1</sub></i></b> (Hz)	-31.8246(57)		-28.904(12)	
<b><i>d<sub>2</sub></i></b> (Hz)	-0.7263(26)		-0.6500(43)	
<b><i>H<sub>J</sub></i></b> (mHz)	0.13891(58)		0.1293(19)	
<b><i>H<sub>JK</sub></i></b> (mHz)	2.369(27)		2.240(46)	
<b><i>H<sub>KJ</sub></i></b> (Hz)	-0.97569(70)		-0.9413(29)	
<b><i>H<sub>K</sub></i></b> (Hz)	23.283(26)		23.19(16)	
<b><i>h<sub>1</sub></i></b> (μHz)	37.26(45)		36.1(12)	
<b><i>h<sub>2</sub></i></b> (μHz)	6.14(30)		9.12(63)	
<b><i>h<sub>3</sub></i></b> (μHz)	1.013(59)			

**Table 2.3** Hyperfine coupling constants of CH<sub>2</sub>ICl isotopologues.

Parameter	CH <sub>2</sub> I <sup>35</sup> Cl		CH <sub>2</sub> I <sup>37</sup> Cl	
	This work	Ref. 128	This work	Ref. 128
<b><math>\chi_{aa}\{I\}</math></b> (MHz)	-1421.6753(26)	-1421.9(19)	-1412.7269(29)	-1418.4(25)
<b><math>\chi_{aa}^J\{I\}</math></b> (kHz)	-0.67(12)			
<b><math>\chi_{aa}^K\{I\}</math></b> (kHz)	38.1(15)		48.9(20)	
<b><math>\chi_{bb}\{I\}</math></b> (MHz)	392.3602(27)	392.6(10)	383.4384(33)	386.5(27)
<b><math> \chi_{ab} \{I\}</math></b> (MHz)	1177.102(27)	1174.9(17)	1183.901(30)	1181.8(17)
<b><i>C<sub>aa</sub></i></b> $\{I\}$ (kHz)	15.55(31)		15.56(39)	
<b><i>C<sub>bb</sub></i></b> $\{I\}$ (kHz)	3.91(17)		3.67(21)	
<b><i>C<sub>cc</sub></i></b> $\{I\}$ (kHz)	6.58(17)		6.36(23)	
<b><math>\chi_{aa}\{Cl\}</math></b> (MHz)	-30.9448(32)	-31.1(11)	-24.7129(40)	-21.1(17)
<b><math>\chi_{bb}\{Cl\}</math></b> (MHz)	-9.1429(39)	-9.0(6)	-6.8720(49)	-8.5(9)
<b><math> \chi_{ab} \{Cl\}</math></b> (MHz)	55.601(53)	53.6(42)	43.684(73)	34.6(14)

**Table 2.4** Nuclear quadrupole coupling constants (in MHz) of CH<sub>2</sub>ICI isotopologues in the inertial system and in the principal system.<sup>a</sup>

Parameter	CH <sub>2</sub> I <sup>35</sup> Cl		CH <sub>2</sub> I <sup>37</sup> Cl	
	This work	Ref. 128	This work	Ref. 128
<b>Iodine coupling</b>				
$\chi_{aa}$	-1421.6753(26)	-1421.9(19)	-1412.7269(29)	-1418.4(25)
$\chi_{bb}$	392.3602(27)	392.6(10)	383.4384(33)	386.5(27)
$\chi_{cc}$	1029.3151(38)	1029.3(21)	1029.2429(44)	1031.9(36)
$ \chi_{ab} $	1177.102(27)	1174.9(17)	1183.901(30)	1181.8(17)
$\chi_{xx}$	971.361(22)	969.7(35)	971.348(24)	971.0(47)
$\chi_{yy}$	1029.3151(38)	1029.3(21)	1029.2429(44)	1031.9(36)
$\chi_{zz}$	-2000.676(22)	-1999.0(29)	-2000.637(24)	-2002.9(31)
$\eta^b$	0.0290	0.0298	0.0289	0.0304
<b>Chlorine coupling</b>				
$\chi_{aa}$	-30.9448(32)	-31.1(11)	-24.7129(40)	-21.1(17)
$\chi_{bb}$	-9.1429(39)	-9.0(6)	-6.8720(49)	-8.5(9)
$\chi_{cc}$	40.0877(51)	40.1(12)	31.5849(64)	29.6(19)
$ \chi_{ab} $	55.601(53)	53.6(42)	43.684(73)	34.6(14)
$\chi_{xx}$	36.616(52)	34.6(22)	28.793(72)	20.4(26)
$\chi_{yy}$	40.0877(51)	40.1(12)	31.5849(64)	34.6(14)
$\chi_{zz}$	-76.703(52)	-74.7(19)	-60.378(72)	-50.0(19)
$\eta^b$	0.0453	0.0736	0.0462	0.1840

<sup>a</sup> The molecular inertial system (*a*, *b*, *c*) correlates with the principal axis system (*z*, *x*, *y*) of both  $\chi$  tensors.

<sup>b</sup>  $\eta = (\chi_{xx} - \chi_{yy}) / \chi_{zz}$ .

The small values of the asymmetry parameter  $\eta$  given for both isotopologues in Table 2.4 by:  $\eta = (\chi_{xx} - \chi_{yy}) / \chi_{zz}$  shows that the  $\chi$  tensors have nearly axial symmetry around the C-*X* bond (the *z* axis), with *X*=I, Cl. In addition, the <sup>35/37</sup>Cl isotopic ratio obtained for  $\chi_{zz}$ , 1.2704, is in excellent agreement with that of the nuclear values of the quadrupole moment of the Cl atoms (1.2688). Finally, the rotational constants of both isotopologues have been used in a least-squares analysis<sup>132</sup> to determine the  $r_0$  structure of the molecule. The floating variables were the  $r_{Cl}$  and  $r_{Cl}$  ef-

<sup>132</sup> Z. Kisiel: <http://www.ifpan.edu.pl/~kisiel/prospe.htm>; StrFit program; Z. Kisiel, in: *Spectroscopy from Space* (J. Demaison *et al.* (Eds.), Kluwer Academic Publishers, Dordrecht, 2001).

fective bond lengths for the ground vibrational state, and the  $\alpha(\text{ICCl})$  and  $\alpha(\text{ClCH})$  bond angles, while  $r_{\text{CH}}$  and  $\alpha(\text{HCH})$  were kept fixed at their *ab initio* values (CCSD(T)). The results are cast in Table 2.5. The derived CI and CCl bond lengths agree well with those found in other halocarbon species such as methyl iodide, methyl chloride and dichloromethane. A paper is currently in preparation to report the results of this study.

**Table 2.5**  $r_0$  structure of  $\text{CH}_2\text{ICl}$ ; Bond lengths in Å and bond angle in degree.

$r_{\text{CI}}$	$r_{\text{CCl}}$	$r_{\text{CH}}$	$\alpha(\text{HCH})$	$\alpha(\text{ICCl})$	$\alpha(\text{ClCH})$
2.1485	1.7541	1.0832	107.93	113.03	112.16

## 2.5 Future prospects

There are quite a lot of halogen-containing species, either radicals, ionic or neutrals, which are interesting to be investigated by high-resolution millimetre-wave spectroscopy. In the near future, the microwave and millimetre-wave spectra of  $\text{CH}_2\text{IBr}$  will be measured in collaboration with H. Ozeki. No experimental high-resolution spectroscopic data for this species has yet been reported, and its *ab initio* structure has recently been published.<sup>133</sup> The study of reactive iodine species should also be completed with the detection of the HCl carbene ( $X^1\text{A}'$ ) and of the iodo-methylidyne radical, CI ( $X^2\Pi$ ). The rotational spectra of their bromine analogues produced by 193 nm photolysis of bromoform were recently observed in Lille.<sup>134</sup> The ionic counterparts of the halocarbons,  $\text{CH}_2\text{X}^+$ , present some interests as well. These ionic species have been studied with

<sup>133</sup> Y.-J. Liu, D. Ajitha, J. W. Krogh, A. N. Tarnovsky and R. Lindh, *Chem. Phys. Chem.* **7**, 955 (2006).

<sup>134</sup> C. Duan, M. Hassouna, A. Walters, M. Godon, P. Dréan and M. Bogey, *J. Mol. Spectrosc.* **220**, 113 (2000); M. Hassouna, A. Walters, C. Demuyneck and M. Bogey, *J. Mol. Spectrosc.* **220**, 113 (2000).

mass spectroscopic techniques and many theoretical researches have been undertaken to predict their structure and spectroscopic properties; yet experimental detection is lacking. In 2006, a communication reported the first gas-phase detection of the electronic spectrum of a halocarocation:  $\text{CH}_2\text{I}^+$ .<sup>135</sup> Likewise, directly related to the studies given in this chapter, are the  $\text{CHX}_2$  radicals, with  $X = \text{F}, \text{Cl}, \text{Br}$  and  $\text{I}$ . Their rotational spectra are expected to be more complicated than the parent  $\text{CH}_2\text{X}$  molecules, as exemplified by the first observation of inversion doubling,<sup>136</sup> giving rise to fluorine hyperfine structure alternation in the rotational spectrum of  $\text{CHF}_2$ . Although the authors were not able to determine the energy separation between the inversion levels, this preliminary analysis *suggested* a high barrier to inversion. The silicon analogues  $\text{SiH}_2\text{X}$  are also of importance in silicon etching processes in halogen based plasmas.<sup>137</sup>

In addition to these halospecies, the investigation of the hydroxymethyl radical,  $\text{CH}_2\text{OH}$ , is very exciting. Although Evenson characterized this molecule more than three decades ago by far-infrared LMR spectroscopy,<sup>138</sup> its rotational spectrum has long resisted detection. Recently, Feng *et al.* reported the rotationally resolved IR spectrum of this intermediate<sup>139</sup> which presumably plays a fundamental role in hydrocarbon combustion and atmospheric processes. They observed hybrid *a/b*-type of the OH and CH symmetric stretch bands whilst a pure *b*-type transition for the CH asymmetric stretch was recorded. In these studies (among others), this radical was generated by hydrogen-abstraction from methanol with atomic chlorine.

---

<sup>135</sup> C. Tao, C. Mukarakate and S. A. Reid, *J. Am. Chem. Soc.* **128**, 9320 (2006).

<sup>136</sup> N. Inada, K. Saito, M. Hayashi, H. Ozeki and S. Saito, *Chem. Phys. Lett.* **284**, 142 (1998).

<sup>137</sup> M. Kogelschatz, G. Cunge and N. Sadeghi, *J. Phys. D.: Appl. Phys.* **37**, 1954 (2004).

<sup>138</sup> H. E. Radford, K. M. Evenson and D. A. Jennings, *Chem. Phys. Lett.* **78**, 589 (1980).

<sup>139</sup> L. Feng, J. Wei and H. Reisler, *J. Phys. Chem. A.* **108**, 7903 (2004).

# SMALL TRANSIENTS OF ASTROPHYSICAL SIGNIFICANCE

---

### 3.1 Introduction

As already mentioned in the first chapter, interstellar chemistry began about seven decades ago with the *spectroscopic* detections of the diatomic species CH, CH<sup>+</sup> and CN (the neutrals are radicals) which were observed in many diffuse clouds. The next molecule to be identified in interstellar space came much later with the radio observation of the OH radical.<sup>140</sup> The radio discoveries of interstellar polyatomic species with the microwave emission from the inversion transition of ammonia in 1968<sup>141</sup> broke the diatomic barrier. Since then many more species have been observed in a variety of astronomical sources,<sup>26,142</sup> and the list of molecules detected so far grows at an increasing rate (no less than ten species were identified in 2010). Judging from Table 1.1, the molecules range in size from 2 to 13

---

<sup>140</sup> S. Weinreb, A. H. Barrett, M. L. Meeks and J. C. Henry, *Nature* **200**, 829 (1963).

<sup>141</sup> A. C. Cheung, D. M. Rank, C. H. Townes, D. D. Thornton and J. W. Welch, *Phys. Rev. Lett.* **21**, 1701 (1968).

<sup>142</sup> [http://www.astrochymist.org/astrochymist\\_ism.html](http://www.astrochymist.org/astrochymist_ism.html), website maintained by D. E. Woon.

atoms and thus can be quite complex. A closer look at Table 1.1 reveals that all molecules with at least five atoms are organic, with the exception of SiH<sub>4</sub>. In addition, the C<sub>60</sub> and C<sub>70</sub> have even been ultimately detected in the young planetary nebula Tc 1,<sup>143</sup> and according to the authors the abundance of these two fullerenes, which most likely reside on dust grains surface, amount to a few percent of the available cosmic carbon in this region. Most of the species are seen in emission in dense interstellar clouds or circumstellar shells through their rotational transitions occurring in the millimetre- or submillimetre-wave regions.

Thus radio astronomy unveiled relatively recently how exceptionally rich the chemistry in space can be. Radio telescopes can operate from the ground benefiting from the radio atmospheric window in the millimetre-wave region. At shorter wavelengths, although ground-based observatories using windows of transparency through the atmosphere exist, a number of airborne and satellite observatories supplement the formers. For interstellar molecules considered as blackbody emitters residing in cold, dense clouds with typical temperature of 20 K, the peak thermal spectral line emission given by:  $\nu \approx 3 \cdot 10^{-9} kT/h$  occurs near 1.2 THz, *i.e.* 40 cm<sup>-1</sup> (where  $\nu$ ,  $T$ ,  $k$  and  $h$  stand for the frequency in THz, the temperature in Kelvin, and the Boltzmann and Planck constants, respectively).<sup>144</sup> As a result, new facilities like the Herschel<sup>145</sup> space-based, the SOFIA<sup>146</sup> airborne and the ALMA<sup>147</sup> ground-based observatories have been designed to operate in the terahertz frequency domain. This part of the electromagnetic spectrum, rich in astrophysical information, only starts to

---

<sup>143</sup> J. Cami, J. Bernard-Salas, E. Peeters and S. E. Malek, *Science* **329**, 1180 (2010).

<sup>144</sup> W. Klemperer, *Annu. Rev. Phys. Chem.* **62**, 173 (2011).

<sup>145</sup> <http://sci.esa.int/science-e/www/area/index.cfm?fareaid=16>

<sup>146</sup> [http://www.nasa.gov/mission\\_pages/SOFIA/index.html](http://www.nasa.gov/mission_pages/SOFIA/index.html)

<sup>147</sup> <http://www.almaobservatory.org/>

be explored. Many lines with unidentified carriers (U-lines) have been recorded and their number increases somewhat in parallel with the sensitivity and the frequency range of new observational systems, to a typical amount of tens of percent of all of the observed lines. Therefore there is considerable interest in identifying these carriers; some should be associated with known interstellar molecules, but there are surely a large number of species not yet detected in space considering the rich chemistry mentioned above.

As a result, there is urgent need for laboratory characterization by rotational spectroscopy, up to and above the THz frequency region, of molecules. Small, transient species (ions, radicals and neutrals) are thought to be the building blocks of larger molecules and consequently deserve a particular emphasis. These studies are important for modeling the formation and the destruction of molecules in various astrophysical environments. For example, ion-molecule reactions have been shown to drive astronomical chemistry. This is due to the fact that much of gas-phase interstellar chemistry occurs at temperatures as low as 10 K at which relevant reactions require no or little activation energy. Ion-molecule reaction scheme has long been used to account for much of the complex molecules in dark and diffuse clouds. While in dense, dark clouds, interstellar ion chemistry is initiated by cosmic ray ionization of the most abundant species, molecular hydrogen and helium,<sup>148</sup> in diffuse clouds ionization rather starts from photoionization.<sup>149</sup> A number of ions have been observed ( $\sim 25$ , see Table 1.1), and while some are surprisingly missing such as  $\text{NO}^+$  and  $\text{H}_2\text{CO}^+$  (they are expected to be present in space

---

<sup>148</sup> E. Herbst and W. Klemperer, *Astrophys. J.* **185**, 505 (1973); A. Dalgarno and G. Black, *Rep. Prog. Phys.* **39**, 573 (1976).

<sup>149</sup> J. H. Black and A. Dalgarno, *Astrophys. J. Suppl.* **34**, 405 (1977).

and their neutrals have been detected),<sup>144</sup> some negatively-charged molecular ions (close-shells) have unexpectedly been observed with large abundance, bringing considerable excitement in radio astronomy. This latter fact is illustrated with the recent laboratory and astronomical detection in very different environments by the Harvard-Smithsonian group of the negative carbo-ions  $C_{2n}H^-$  (Ref. 150) and  $C_{2n-3}N^-$  (Ref. 151), with  $n=2-4$ , through their millimetre-wave spectra; so far  $C_6H^-$  and  $C_8H^-$  are the largest charged molecules found in space. These results will force a drastic revision of theoretical models of interstellar chemistry,<sup>152</sup> since they have largely neglected the presence of anions (although their presence was discussed as early as 1973).<sup>153</sup> It is interesting to note that no laboratory data are at present available for the  $C_5N^-$  anion. The submillimetre-wave spectroscopy of negative ions was pioneered in the PhLAM laboratory with the identification of  $SH^-$  (and  $SD^-$ , both not yet detected in space) which resulted from the study of their Doppler shift.<sup>154</sup> Other negative ions studied by microwave techniques include  $OD^-$  (Ref. 155) and more recently  $NCO^-$ ,<sup>156</sup> making their number in fact pretty small.

Heterogeneous chemistry, such as that taking place on the surface of interstellar dust, plays an important role in the molecular growth.<sup>157</sup> A close relation between gas-phase ion-molecule reactions and grain surface pro-

---

<sup>150</sup> H. Gupta, C.A. Gottlieb, M.C. McCarthy and P. Thaddeus, *Astrophys. J.* **691**, 1494 (2009).

<sup>151</sup> J. Cernicharo, M. Guélin, M. Agúndez, M. C. McCarthy and P. Thaddeus, *Astrophys. J.* **688**, L83 (2009), and references therein.

<sup>152</sup> C. Walsh, N. Harada, E. Herbst and T. J. Millar, *Astrophys. J.* **700**, 752 (2009).

<sup>153</sup> A. Dalgarno and R. A. Mc Cray, *Astrophys. J.* **181**, 95 (1973).

<sup>154</sup> S. Civiš, A. Walters, M. Yu. Tretyakov, S. Bailleux and M. Bogey, *J. Chem. Phys.* **108**, 8369 (1998).

<sup>155</sup> G. Cazzoli and C. Puzzarini, *J. Chem. Phys.* **123**, 041101 (2005); *ibid* *Astrophys. J.* **648**, L79 (2006).

<sup>156</sup> V. Lattanzi, C. A. Gottlieb, P. Thaddeus, S. Thorwirth and M. C. McCarthy, *Astrophys. J.* **720**, 1717 (2010).

<sup>157</sup> E. Herbst and E. M. Cuppen, *Proc. Natl. Acad. Sci. USA* **103**, 12257 (2006).

cesses was recently suggested in trying to solve the low H<sub>2</sub>O and O<sub>2</sub> abundances observed towards dense molecular clouds, a long standing puzzling problem.<sup>158</sup> Non-uniform chemistry has also been brought out in the study of protostellar regions within dense molecular clouds.<sup>159</sup> Physical conditions in such environments (abundances, densities and temperatures) produce highly non-statistical isotopic distributions, *i.e.* molecular isotopic enrichment with respect to the atomic cosmic abundance.<sup>160</sup> In particular, nearly thirty deuterated species of simple interstellar molecules have been detected in interstellar clouds, with abundance ratios relative to their hydrogenated analogues much larger than the cosmic D:H ratio ( $1.5 \cdot 10^{-5}$ ). This is ascribed to chemical reactions extracting deuterium from its reservoir, HD, in molecular cloud. This process is intrinsically a low temperature phenomenon since at low temperature, small zero-point energy differences in H<sub>2</sub> and HD species favors incorporation of a D atom rather than an H atom. Singly and doubly deuterated species have been identified in a number of molecular clouds. Even the triply deuterated ammonia (ND<sub>3</sub>, for which the abundance ratio relative to NH<sub>3</sub> is about two orders of magnitude larger than that of the cosmic D:H) and methanol (CD<sub>3</sub>OH) have recently been observed in cold molecular clouds; this high deuterium fractionation has been an important issue in recent astrochemistry.

Thus, molecules are excellent probes of the physical conditions and processes in the astronomical regions where they reside, in particular *via* the estimation of their abundance which is sensitive to temperature and density. As part of the collaborative effort (between astronomers, astrochem-

---

<sup>158</sup> H. Robert and E. Herbst, *Astron. Astrophys.* **395**, 233 (2002).

<sup>159</sup> E. F. van Dishoeck, *Proc. Natl. Acad. Sci. USA* **103**, 12249 (2006).

<sup>160</sup> T. J. Millar, *Space Sci. Rev.* **106**, 73 (2003).

ists and experimentalists) to better understand our *molecular universe*, two successful studies are presented: the *first* detection by submillimetre-wave spectroscopy of the molecular ion  $\text{CS}^+$  (an open-shell) and of the mixed isotopologue of the methylene biradical, CHD. Only a brief summary is provided below before drawing some future prospects.

### 3.2 The $\text{CS}^+$ radical cation

A relatively large number of sulphur-containing molecules have been detected in the interstellar medium (Table 1.1). Among them are simple ions like  $\text{SH}^+$  and  $\text{HCS}^+$  and the neutrals  $\text{C}_n\text{S}$  with  $n = 1 - 3$ ; the largest one is  $\text{CH}_3\text{SH}$  with six atoms. In cosmic abundance, sulfur ranks tenth among the elements. In view of this high cosmic abundance, it is not surprising that CS is one of the main sulfur-bearing molecules in space (it has been found in a variety of astrophysical environments, including extragalactic sources) identified for the first time four decades ago. CS is sufficiently abundant to be used as a tracer of dense cloud structure and temperature. Carbon monosulfide should also be related to the most carbon-bearing astromolecule, carbon monoxide. Surprisingly, although CS has a low ionization potential of 11.335 eV, until now the  $\text{CS}^+$  ion ( $X^2\Sigma^+$ ) has not been detected in space. This ion is supposed to be an important intermediate in interstellar sulfur chemistry where it could be the precursor of gas-phase reactions leading to the formation of CS. In contrast, the isovalent cation  $\text{CO}^+$  has been detected in several sources by its rotational spectrum.

From the spectroscopic point of view, before our studies carried out in collaboration with A. Walters (Centre d'Etude Spatiale des Rayonnements, Université Toulouse 3), only two electronic band systems of  $\text{CS}^+$  were

measured in the near infrared and UV regions. Their rotational analysis yielded accurate ground-state rotational and fine-structure parameters from which accurate equilibrium internuclear distance in the ground state could be derived ( $r_e = 1.492\,156(78)$  Å). Despite this, experimental difficulties prevented the characterization of this fundamental ion by millimetre-wave spectroscopy until this research was conducted. The least-squares analysis of the rotational transitions measured for the first time did not give any difficulties. Except for  $N=0$ , each rotational level is split into two sub-levels  $E_1$  and  $E_2$  which correspond to the spin-components  $F_1$  ( $N = J + 1/2$ ) and  $F_2$  ( $N = J - 1/2$ ) respectively. If  $H_{\text{ROT}}$  stands for the rotational part of the Hamiltonian, with  $H_{\text{ROT}} = B N(N + 1) - D N^2(N + 1)^2$ ,  $E_1$  and  $E_2$  can then be expressed with the following equations:

$$E_1 = H_{\text{ROT}} + 1/2 \gamma N$$

$$E_2 = H_{\text{ROT}} - 1/2 \gamma (N + 1).$$

Our identification of the  $\text{CS}^+$  cation led to a more accurate determination of the  $B$ ,  $D$ , and  $\gamma$  molecular constants (errors are from one to two orders of magnitude smaller than those obtained in previous studies), which in turn were used to provide rotational frequencies up to about 1 THz to facilitate its radioastronomical detection. Unfortunately, no report has so far been published on the radioastronomical observation of this ion. The results were published in the *Astrophysical Journal* (next page).

## THE SUBMILLIMETER-WAVE SPECTRUM OF THE CS<sup>+</sup> RADICAL ION

STÉPHANE BAILLEUX,<sup>1</sup> ADAM WALTERS,<sup>2</sup> EVA GRIGOROVA,<sup>1</sup> AND LAURENT MARGULÈS<sup>1</sup>

Received 2007 September 26; accepted 2007 December 1

### ABSTRACT

The submillimeter-wave spectrum of the CS<sup>+</sup> radical cation in its ground electronic state ( $X^2\Sigma^+$ ) has been observed for the first time, in a flowing positive column discharge in a CS<sub>2</sub>-Ar mixture partially cooled with a limited flow of liquid nitrogen. Nine rotational transition frequencies were recorded between 414 and 622 GHz, leading to the determination of accurate molecular constants  $B_0 = 25908.8560(41)$  MHz,  $D_0 = 41.344(18)$  kHz, and  $\gamma_0 = 597.629(41)$  MHz, which we use to predict transition frequencies up to the terahertz region in order to stimulate new attempts at astronomical detection.

*Subject headings:* methods: laboratory — molecular data — techniques: spectroscopic

### 1. INTRODUCTION

Many sulfur compounds such as HCS<sup>+</sup> (Thaddeus et al. 1981), C<sub>2</sub>S (Saito et al. 1987), C<sub>3</sub>S (Yamamoto et al. 1987; Bell et al. 1993), and C<sub>5</sub>S (Bell et al. 1993) have been observed in the interstellar medium. The first molecule containing sulfur that was detected in interstellar space was carbon monosulfide (Penzias et al. 1971). CS is present in a variety of astrophysical environments, such as dense clouds and star-forming regions (Hasegawa et al. 1984; Hayashi et al. 1985; Walker et al. 1986; Hauschildt et al. 1993), diffuse clouds (Drdla et al. 1989), circumstellar envelopes (Lindqvist et al. 1988), the shocked molecular gas associated with the supernova remnant IC 443 (van Dishoeck et al. 1993), carbon-rich stars (Bregman et al. 1978), and comets (Smith et al. 1980; Jackson et al. 1982). Although CS has a low ionization potential (11.335 eV; Huber & Herzberg 1979), the CS<sup>+</sup> radical cation has proved elusive and has not been identified in the interstellar medium. No direct experimental measurement of its rotational spectrum has yet been published.

In the laboratory, two electronic band systems of CS<sup>+</sup> are known and have been measured between the near-infrared and UV regions. Coxon et al. (1976) first measured the CS<sup>+</sup>  $A^2\Pi_i - X^2\Sigma^+$  system excited by the reaction of metastable He with CS<sub>2</sub>. The rotational analysis of observed electronic spectra of CS<sup>+</sup> has revealed that some vibrational levels of the  $A^2\Pi_i$  state, especially the  $v' = 1$ ,  $v' = 5$ , and  $v' = 6$  levels, are strongly perturbed by high vibrational levels of the  $X^2\Sigma^+$  state. Gauyacq & Horani (1978) recorded the rotationally resolved emission spectrum and carried out a deperturbation analysis of the (2, 0), (3, 0), (4, 0), and (5, 0) bands. They used a low-pressure hot-cathode discharge through carbon disulfide to create the ion. Later, Horani & Vervloet (1992) re-examined this system using Fourier transform emission spectroscopy between 5800 and 14,000 cm<sup>-1</sup>. Production was again with metastable He and CS<sub>2</sub>. Subsequently, Liu et al. (2000) measured the near-infrared absorption spectrum of the (1, 0) band of the ion using velocity modulation laser spectroscopy. For production they used an AC discharge in a flowing mixture of CS<sub>2</sub> and helium. This was followed by another measure of the (5, 0) band, a new measure of the (6, 0) band, a new deperturbation analysis, and a new set of equilibrium constants for both the  $X$ - and  $A$ -states (Liu

et al. 2002). Finally, the (7, 1) band was measured (Duan et al. 2003). Cossart (1994) has also recorded the  $B^2\Sigma^+ - X^2\Sigma^+$  system in the UV region from 230 to 330 nm. Attempts to identify the electronic spectrum of CS<sup>+</sup> in interstellar space by absorption in the line of sight to stars have proved unsuccessful (Ferlet et al. 1986).

Measurement of the submillimeter spectrum provides more precise rotational frequencies but is less sensitive than electronic spectroscopy. The laboratory study of ions is complicated by the difficulty in producing them with a sufficient number density in an absorption cell and because of their short lifetime. Optimal production conditions are often different from those used in electronic and vibrational spectroscopy, since, for example, total cell pressure should be lower in the submillimeter region in order to avoid excessive line broadening. The use of helium as a buffer gas is often reported in electronic and vibrational spectroscopy in discharges used to create ions, whereas it is our experience that argon produces the best results (see, e.g., Civiš et al. 1998). For all these reasons, a certain number of fundamental ions such as CS<sup>+</sup> have not yet been observed in the submillimeter region despite the publication of their electronic and vibrational spectra. For CS<sup>+</sup>, two additional experimental difficulties may explain the lack of identification of the laboratory rotational spectrum up to the present. First, the precursor CS<sub>2</sub> is a liquid (melting point  $-111^\circ\text{C}$  at atmospheric pressure), so that, a priori, the cell cannot be cooled to liquid-nitrogen temperature (Dixon & Woods 1975) as is often done to increase the signal of ions produced from gaseous precursors. Second, magnetically enlarged negative glow discharges, used to enhance positive ion concentration (De Lucia et al. 1983), cannot be used for CS<sup>+</sup>, since it is an open shell. In addition, the low ab initio calculated dipole moment of CS<sup>+</sup> in its ground vibronic state (0.509 D; Blöcker et al. 1990) is not favorable for its detection by conventional absorption-spectroscopy techniques.

We report here first measurements of the millimeter-wave spectrum of CS<sup>+</sup>, produced in a flowing positive column discharge in a CS<sub>2</sub>-Ar mixture. The objective is mainly to provide precise frequencies for astrophysical work, which should aid detection of the ion or help to confirm upper limits on its number density.

Quarta & Singh (1981) suggested that CS<sup>+</sup> could be a potential interstellar molecule and suggested some reactions in which it could be produced. Horani & Vervloet (1992) also discussed this. An involvement of the cation in the formation of CS in diffuse clouds has also been proposed (Drdla et al. 1989). An extensive compilation of reactions involving CS<sup>+</sup> (for both its formation and destruction) is given in the UMIST database (Woodall et al.

<sup>1</sup> Laboratoire de Physique des Lasers, Atomes et Molécules, UMR CNRS 8523, CERLA, Université des Sciences et Technologies de Lille, F-59655 Villeneuve d'Ascq Cedex, France; stephane.bailleux@univ-lille1.fr.

<sup>2</sup> Centre d'Etude Spatiale des Rayonnements, CNRS, Université Paul Sabatier, F-31028 Toulouse Cedex 4, France.

2007),<sup>3</sup> where its chemistry can be compared with CO<sup>+</sup>, a similar reactive ion that has already been detected in space. There are a number of formation routes for CS<sup>+</sup> that have rate constants similar overall to those quoted for CO<sup>+</sup>. For example, the ion can be formed by a reaction between H<sup>+</sup> and CS. Analogously to CO<sup>+</sup>, CS<sup>+</sup> reacts with H<sub>2</sub>, the dominant collision partner in space, to form HCS<sup>+</sup> (McAllister 1978; Decker et al. 2001) and could be an important intermediate in the formation of the latter. As is the case for CO<sup>+</sup>, CS<sup>+</sup> could have a detectable abundance in sources where the formation is rapid and hydrogen is mostly in the H<sup>+</sup> ionized atomic form. CO<sup>+</sup> has been detected in various photodissociation regions (NGC 7027 and M17 SW [Latter et al. 1993; Störzer et al. 1995; Fuente et al. 2003], the Orion bar [Störzer et al. 1995; Fuente et al. 2003], NGC 7023 [Fuente & Martín-Pintado 1997; Fuente et al. 2003], Mon R2 and G29.960–02 [Rizzo et al. 2003], and S140 and NGC 2023 [Savage & Ziurys 2004]), including toward the prototypical starburst galaxy M82 (Fuente et al. 2006). Observations indicate that its total column density remains roughly constant for a wide range of densities and UV radiation fields (Rizzo et al. 2003). CO<sup>+</sup> has also been tentatively detected in the X-ray-dominated region toward the nucleus of the galaxy Cygnus A (Fuente et al. 2000), and the formation of CO<sup>+</sup> in M82 has also been attributed principally as being due to X-ray radiation (Spaans & Meijerink 2007). In general, chemical models fail to account for the observed reactive ions' column densities (Black 1998; Fuente et al. 2000), which are generally much higher than predicted. Modeling of gas-phase chemistry in translucent, dark and dense, and diffuse clouds also fails to predict correct abundances of sulfur-bearing molecules (Lucas & Liszt 2002). Hence, a search for the elementary sulfur-containing reactive ion CS<sup>+</sup> is particularly interesting, to verify and refine chemical models and to provide additional information, for example, on possible missing mechanisms.

As expected, we failed to find lines of CS<sup>+</sup> in the spectral survey of the solar-type protostar IRAS 16293–2422 (Castets et al. 2005) to which we had immediate access. Frequencies were also sent to J. Cernicharo in Madrid, who checked in both his 2 mm and 3 mm spectral surveys. Lines of CS<sup>+</sup> were not seen in the spectra of IRC +10216, and no firm identification could be made in the spectrum of Orion. The possibility has also been evoked that the spectra of CS<sup>+</sup> could be observed in comets (Smith et al. 1980; Leach 1987).

Accurate predictions may now be made over the whole range of Earth-based millimeter and submillimeter telescopes, as well as within the range of the high spectral resolution HIFI instrument (Heterodyne Instrument for the Far-Infrared) of the *Herschel Space Observatory*, due for launch in 2008. The relatively small dipole moment of CS<sup>+</sup> may also complicate its astrophysical detection. The ALMA (Atacama Large Millimeter Array) international interferometer will come into service in the next decade, providing unprecedented sensitivity and allowing new searches to be made for previously unidentified potential astrophysical species.

## 2. EXPERIMENTAL OBSERVATIONS

The spectrometer used in this experiment has been described extensively elsewhere (Bailleux et al. 2002). Measurements were taken between 414 and 622 GHz. The submillimeter-wave radiation was provided by two phase-locked backward-wave oscillators (a Thomson-CSF carcinotron below 470 GHz and a tube from the Istok company [Russia] above 518 GHz). A liquid-helium-cooled InSb bolometer (QMC Instruments) was used as detector. For improved sensitivity, we used frequency modulation at 42 kHz

and lock-in detection at twice the modulation frequency, resulting in a second-derivative line shape.

In order to search for the CS<sup>+</sup> ion, we set up a positive column discharge in CS<sub>2</sub>. The absorption cell was a 2 m long, 5 cm internal diameter, double-jacketed Pyrex tube, allowing liquid-nitrogen flow through the outer jacket to cool the plasma. The precursor CS<sub>2</sub> was introduced together with argon, allowing in situ production of reactive species. Liquid CS<sub>2</sub> was provided by Sigma-Aldrich (spectrophotometric grade, with purity of 99%) and used without further purification. It was degassed by using freeze-pump-thaw cycles and stored in darkness. The precursor gas (vapor pressure 296 torr at 20°C) was mixed with the carrier gas flow before it entered the absorption cell's inlet.

For the measurement of the near-infrared spectrum of CS<sup>+</sup>, discharge currents in the range 140–200 mA were used by Liu et al. (2000, 2002), and the absorption cell was kept at room temperature. Liu et al. also reported that CS<sub>2</sub> should be present in a trace amount and that its partial pressure was rather critical for the detection of the cation.

In order to observe the millimeter-wave spectrum of CS<sup>+</sup>, we found it necessary to cool the cell using a limited flow of liquid nitrogen, that is to say, with the outer jacket of the cell partially filled. The optimum discharge current was 200 mA, and the partial pressures (measured at room temperature) giving the best signal-to-noise ratio were respectively 6 and 2 mtorr for Ar and CS<sub>2</sub>. We first searched for the two strongest fine-structure components ( $J = 9\frac{1}{2} \leftarrow 8\frac{1}{2}$  and  $J = 8\frac{1}{2} \leftarrow 7\frac{1}{2}$ ) of the  $N = 9 \leftarrow 8$  transition using predictions based on the work of Liu et al. (2002). We identified both transitions (around 466 GHz) close to the predictions. The frequency interval of 597.7 MHz between the transitions matched accurately the value of  $\gamma_0$ , the fine-splitting constant ( $597.696 \pm 0.420$ ) MHz given in the aforementioned work. An example of the  $(N, J) = (9, 9\frac{1}{2}) \leftarrow (8, 8\frac{1}{2})$  line is depicted in Figure 1. Following a further measurement of the two strongest  $N = 8 \leftarrow 7$  lines around 414 GHz, we were able to make a new preliminary fit leading to accurate predictions ( $\pm 400$  kHz) for the transitions falling in the 518–622 GHz frequency range. Five new lines were accordingly identified within  $\pm 200$  kHz of the predictions, securing the identification of the CS<sup>+</sup> ion. In total, nine transitions have been measured in the range 414–622 GHz, corresponding to  $7 \leq N'' \leq 11$ ; Table 1 lists the observed frequencies. Because of the weak signal-to-noise ratio, each line was measured three times, and the experimental uncertainty indicated in Table 1 was deduced from the reproducibility of the measurements. The uncertainty also corresponds to that typically determined in similar measurements with comparable signal-to-noise ratio.

Even under optimum conditions, lines of the cation were near the detection limit of our spectrometer, and the conditions used were critical for their observation. For comparison, the major isotopologue of CS saturated our detection system under the same conditions, and the intensity of the  $J = 9 \leftarrow 8$  C<sup>34</sup>S line (433750.984 MHz; Gottlieb et al. 2003) is around 2 orders of magnitude higher than the lines of the CS<sup>+</sup> ion. At room temperature, lines of CS<sup>+</sup> were not observed. If the cell was cooled beyond the optimum value, lines diminished and disappeared. This is due to a rapid reduction of partial pressure of CS<sub>2</sub>, as evidenced by a similar extinction of the line of C<sup>34</sup>S. Our present experimental setup does not allow precise control of the temperature inside the cell, which would be an extensive technical challenge. Hence, the temperature was adjusted dynamically by increasing and reducing liquid-nitrogen flow to optimize line intensity.

Ions produced in a discharge have an axial drift velocity that may Doppler-shift line frequencies in single-pass setups such as used here. This shift, used for velocity modulation detection in

<sup>3</sup> See <http://www.udfa.net>.

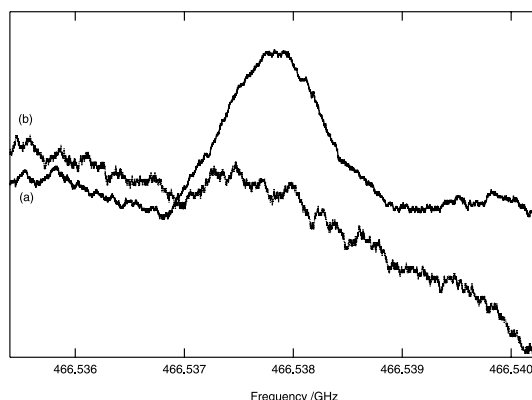


Fig. 1.—Recording of the  $(N, J) = (9, 9\frac{1}{2}) - (8, 8\frac{1}{2})$  rotational transition of  $\text{CS}^+$  in the ground electronic state  $X^2\Sigma^+$  (averaged over 48 acquisitions with 10 ms of lock-in time constant) (a) without and (b) with a magnetic field applied.

the infrared, is much smaller in millimeter-wave measurements but may in certain cases be large enough to be detected (Civiš et al. 1998). The shift was not measurable for lines attributed to  $\text{CS}^+$ ; however, there are several explanations. First, the shift is small (typically tens to hundreds of kilohertz) and difficult to identify in cases of low signal-to-noise ratio as here. Second, ion mobility is related to molecular weight and is expected to be most significant for light ions; it is relevant to compare the value of the shift of 12 kHz at 560 GHz obtained by Cazzoli & Puzzarini (2005) for the lighter ion  $\text{N}_2\text{H}^+$  with our experimental uncertainties of over 50 kHz. Third, it has been our experience in previous measurements of other ions that the size of the Doppler shift is strongly dependent on discharge conditions (as the electric field “seen” by the ions changes); in this case it was not possible to change the conditions without the lines disappearing. Fourth, the method available to us to show this shift was to reverse the polarity of the discharge; however, this led to noisy discharge conditions and even worse signal-to-noise ratio. Finally, for the ions that are produced in the negative glow region, which is a nearly field-free region, no frequency shift due to drift velocity would be expected to be observed (De Lucia et al. 1983; Hirao & Amano 2003 and references therein). Since no magnetic field can be used, this region is small but is that in which a far higher concentration of cations is expected; hence, it is difficult to determine the relative contribution of the negative glow and positive column regions to the observed signal.

We are nevertheless confident that the identification of  $\text{CS}^+$  is secure for several reasons, listed below. For the first two lines observed no others were seen in a 20 MHz range, and subsequent lines were seen where predicted. All pairs of lines of the same  $J$  have the correct fine splitting and, as expected, similar intensities. All nine new measured lines fit correctly and with the infrared results, giving similar constants to those already published for the cation. With a single precursor molecule ( $\text{CS}_2$ ), the number of species that can be formed is limited, even allowing for oxygen-containing species resulting from small air leaks. The observed transitions do not correspond to known frequencies for species such as  $\text{CS}$ ,  $\text{C}_2\text{S}$ ,  $\text{C}_3\text{S}$ ,  $\text{SO}$ , and  $\text{SO}_2$ . The cell was equipped with a solenoid coil to generate an axial magnetic field (100 G, typically) in the discharge plasma in order to distinguish between paramagnetic and nonparamagnetic absorption signals. All lines attributed to the ion were, as expected, paramagnetic, which rules out all non-radical species.

TABLE 1  
OBSERVED TRANSITION FREQUENCIES OF  $\text{CS}^+$  IN THE GROUND  $X^2\Sigma^+$  STATE

$N''$	$J''$	Observed <sup>a</sup> (MHz)	Obs. - Calc. (MHz)
7.....	$6\frac{1}{2}$	414158.125(80)	-0.092
	$7\frac{1}{2}$	414755.898(80)	0.058
8.....	$7\frac{1}{2}$	465940.013(50)	-0.028
	$8\frac{1}{2}$	466537.696(50)	0.033
9.....	$8\frac{1}{2}$	517712.932 <sup>b</sup>	...
	$9\frac{1}{2}$	518310.565(80)	0.008
10.....	$9\frac{1}{2}$	569475.989(60)	0.086
	$10\frac{1}{2}$	570073.514(60)	-0.012
11.....	$10\frac{1}{2}$	621227.961(60)	0.004
	$11\frac{1}{2}$	621825.509(60)	-0.070

<sup>a</sup> Values in parentheses are 1  $\sigma$  experimental error on the last digits.

<sup>b</sup> Calculated line.

### 3. RESULTS AND DISCUSSION

Each rotational level (except  $N = 0$ ) of  $\text{CS}^+$  is split into two sublevels ( $N + \frac{1}{2}$  and  $N - \frac{1}{2}$ ) by coupling with the spin of the unpaired electron. For each rotational transition, a triplet of lines is possible: two corresponding to  $\Delta J = \Delta N = 1$  and one to  $\Delta J = 0$  (2 orders of magnitude weaker in our frequency range). The observed absorption lines were all found approximately 4 MHz higher in frequency than predictions made using the molecular constants obtained by Liu et al. (2002). The accurate predictions were very valuable for us, owing to the low signal-to-noise ratio of the rotational spectrum combined with the critical experimental conditions to produce the  $\text{CS}^+$  cation. All lines were found within 1  $\sigma$  uncertainty of the predictions, permitting an obvious identification in laboratory measurements with a limited number of possible species in the cell. However, this offset could cause confusion in astrophysical spectra resulting from many different species, especially for weaker lines making up the spectrally dense “grass” of close-lying lines observed in objects showing chemical complexity.

Our new measured frequencies were then included in a global analysis including the 852 ground-state combination differences deposited as an EPAPS document by Liu et al. (2002). The program SPFIT (Pickett 1991) was used for the weighted linear least-squares fitting procedure, which gave a standard deviation of 50 kHz. The measured lines fit well with the ground-state combination differences, and the determination of the molecular parameters has, as expected, improved. Parameters are given in Table 2, together with the constants derived previously by Horani & Vervloet (1992) and Liu et al. (2002) for comparison. It is interesting to note that our results for the rotational and centrifugal parameters  $B_0$  and  $D_0$  are closer to the former (earlier) published work, although taking into

TABLE 2  
MOLECULAR CONSTANTS FOR THE GROUND  $X^2\Sigma^+$  STATE OF  $\text{CS}^+$

Constant (MHz)	Horani & Vervloet <sup>a</sup>	Liu et al. <sup>b</sup>	This Work <sup>c</sup>
$B_0$ .....	25908.99(34)	25908.57(22)	25908.8560(41)
$10^3 D_0$ .....	41.07(30)	40.94(17)	41.344(18)
$\gamma_0$ .....	596.89(90)	597.70(42)	597.629(41)

NOTE.—Values in parentheses are 1  $\sigma$  errors in units of the last digits.

<sup>a</sup> Horani & Vervloet 1992.

<sup>b</sup> Liu et al. 2002.

<sup>c</sup> Values obtained from a global fit including 852 ground-state combination differences.

TABLE 3  
SELECTION OF PREDICTED ROTATIONAL LINES OF CS<sup>+</sup> ( $X^2\Sigma^+$ )

$N' \leftarrow N''$	$J' \leftarrow J''$	Frequency <sup>a</sup> (MHz)	$\log A_{21}(\text{s}^{-1})^b$	Energy Level ( $\text{cm}^{-1}$ )
1 $\leftarrow$ 0	1/2 $\leftarrow$ 1/2	51219.917(42)	-6.869	0.0000
	3/2 $\leftarrow$ 1/2	52116.361(22)	-6.847	0.0000
2 $\leftarrow$ 1	3/2 $\leftarrow$ 1/2	103335.287(27)	-5.955	1.7085
	5/2 $\leftarrow$ 3/2	103932.916(25)	-5.868	1.7384
3 $\leftarrow$ 2	5/2 $\leftarrow$ 3/2	155149.857(31)	-5.346	5.1554
	7/2 $\leftarrow$ 5/2	155747.486(30)	-5.311	5.2052
4 $\leftarrow$ 3	7/2 $\leftarrow$ 5/2	206961.450(36)	-4.941	10.3306
	9/2 $\leftarrow$ 7/2	207559.079(34)	-4.921	10.4004
5 $\leftarrow$ 4	9/2 $\leftarrow$ 7/2	258769.074(39)	-4.634	17.2341
	11/2 $\leftarrow$ 9/2	259366.703(37)	-4.621	17.3238
6 $\leftarrow$ 5	11/2 $\leftarrow$ 9/2	310571.737(41)	-4.386	25.8657
	13/2 $\leftarrow$ 11/2	311169.366(39)	-4.377	25.9754
7 $\leftarrow$ 6	13/2 $\leftarrow$ 11/2	362368.447(41)	-4.179	36.2253
	15/2 $\leftarrow$ 13/2	362966.076(39)	-4.172	36.3549
8 $\leftarrow$ 7	15/2 $\leftarrow$ 13/2	414158.125(80) <sup>c</sup>	-4.000	48.3126
	17/2 $\leftarrow$ 15/2	414755.898(80) <sup>c</sup>	-3.995	48.4621
9 $\leftarrow$ 8	17/2 $\leftarrow$ 15/2	465940.013(50) <sup>c</sup>	-3.843	62.1274
	19/2 $\leftarrow$ 17/2	466537.696(50) <sup>c</sup>	-3.838	62.2969
10 $\leftarrow$ 9	19/2 $\leftarrow$ 17/2	517712.932(31)	-3.703	77.6695
	21/2 $\leftarrow$ 19/2	518310.565(80) <sup>c</sup>	-3.699	77.8589
11 $\leftarrow$ 10	21/2 $\leftarrow$ 19/2	569475.989(60) <sup>c</sup>	-3.576	94.9386
	23/2 $\leftarrow$ 21/2	570073.514(60) <sup>c</sup>	-3.573	95.1479
12 $\leftarrow$ 11	23/2 $\leftarrow$ 21/2	621227.961(60) <sup>c</sup>	-3.461	113.9342
	25/2 $\leftarrow$ 23/2	621825.538(60) <sup>c</sup>	-3.458	114.1635
13 $\leftarrow$ 12	25/2 $\leftarrow$ 23/2	672968.115(62)	-3.355	134.6562
	27/2 $\leftarrow$ 25/2	673565.745(62)	-3.353	134.9054
14 $\leftarrow$ 13	27/2 $\leftarrow$ 25/2	724695.368(90)	-3.258	157.1040
	29/2 $\leftarrow$ 27/2	725292.997(90)	-3.255	157.3731
15 $\leftarrow$ 14	29/2 $\leftarrow$ 27/2	776408.729(125)	-3.167	181.2772
	31/2 $\leftarrow$ 29/2	777006.358(125)	-3.165	181.5663
16 $\leftarrow$ 15	31/2 $\leftarrow$ 29/2	828107.206(166)	-3.082	207.1754
	33/2 $\leftarrow$ 31/2	828704.835(167)	-3.080	207.4844
17 $\leftarrow$ 16	33/2 $\leftarrow$ 31/2	879789.807(215)	-3.002	234.7981
	35/2 $\leftarrow$ 33/2	880387.436(216)	-3.000	235.1270
18 $\leftarrow$ 17	35/2 $\leftarrow$ 33/2	931455.540(271)	-2.927	264.1447
	37/2 $\leftarrow$ 35/2	932053.170(272)	-2.925	264.4936
19 $\leftarrow$ 18	37/2 $\leftarrow$ 35/2	983103.413(336)	-2.856	295.2148
	39/2 $\leftarrow$ 37/2	983701.042(336)	-2.854	295.5835
20 $\leftarrow$ 19	39/2 $\leftarrow$ 37/2	1034732.433(408)	-2.788	328.0076
	41/2 $\leftarrow$ 39/2	1035330.063(409)	-2.787	329.3963

<sup>a</sup> Values in parentheses are 1  $\sigma$  errors in units of the last digits

<sup>b</sup> Base-10 logarithm of the Einstein coefficient for spontaneous emission with  $\mu = 0.509$  D.

<sup>c</sup> Measured frequency.

account the uncertainties, this may be coincidental. However, the value we determined for the spin-rotation constant  $\gamma_0$  was closer to that of Liu et al. (2002). We also performed a fit including solely our submillimeter-wave transitions, and the molecular constants obtained are nearly identical.

The parameters can be used to predict accurate transition frequencies of astrophysical interest up to the terahertz region. Selected calculations are reported in Table 3 up to just over 1 THz. The significantly weaker  $\Delta J = 0$  transitions are not given except for  $N = 1 \leftarrow 0$ , where only two transitions are possible. Also, the difference in intensity between  $\Delta J = 0$  and the other transitions increases rapidly with  $N$  and is not significant for the first rotational transition. We have also included 1  $\sigma$  uncertainties, as well as energy levels and Einstein  $A$ -coefficients, which can be used to predict astrophysical spectra in various conditions. To situate in the commonly used astrophysical unit, the 1  $\sigma$  estimated uncertainty of around 35 kHz at 207 GHz corresponds to around  $0.05 \text{ km s}^{-1}$ .

Additional rotational transition frequencies or predictions of astrophysical intensities are available upon request to the authors.<sup>4</sup> During this work, we also observed transitions of CCS and CCCS. These molecules are also of astrophysical interest, and presently spectra are only reported to 300 GHz (Lovas et al. 1992). We hence plan to publish measurements up to 650 GHz in the near future.

#### 4. SUMMARY

We have measured nine lines of the rotational spectrum of the CS<sup>+</sup> radical cation in its ground electronic and vibrational state, allowing accurate determination of the molecular parameters, which have been used to calculate precise transition frequencies up to the terahertz region. Other information needed for simulating astrophysical spectra is provided. It is hence hoped to stimulate searches

<sup>4</sup> At adam.walters@cesr.fr.

for the rotational spectrum of this species, in particular in photo-dissociation regions and X-irradiated molecular gas.

CERLA is partly supported by the French Research Ministry, the Nord-Pas-de-Calais Region, and the European Funds for Re-

gional Economic Development. S. B. and E. G. thank the ARCUS (Actions en Régions de Coopération Universitaire et Scientifique) program and the QUASAAR network for financial support of this project. A. W. thanks the Observatoire Midi-Pyrénées for financing his travel to Lille for the measurements. An undergraduate project student, Audrey Coutens, also participated in the experimental work.

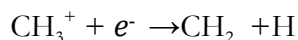
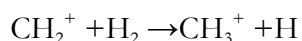
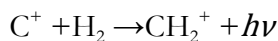
## REFERENCES

- Bailleux, S., Bogey, M., Demuyne, C., Liu, Y., & Walters, A. 2002, *J. Mol. Spectrosc.*, 216, 465
- Bell, M. B., Avery, L. W., & Feldman, P. A. 1993, *ApJ*, 417, L37
- Black, J. H. 1998, *Faraday Discuss.*, 109, 257
- Blöcker, J. H., Reinsch, E.-A., Rosmus, P., Werner, H.-J., & Knowles, P. J. 1990, *Chem. Phys.*, 147, 99
- Bregman, J. D., Goebel, J. H., & Strecker, D. W. 1978, *ApJ*, 223, L45
- Castets, A., et al. 2005, in *ASP Conf. Ser.* 344, *The Cool Universe: Observing Cosmic Dawn*, ed. C. Lidman & D. Alloin (San Francisco: ASP), 212
- Cazzoli, G., & Pizzarini, C. 2005, *J. Chem. Phys.*, 123, No. 041101
- Civiš, S., Walters, A., Tretyakov, M. Yu., Bailleux, S., & Bogey, M. 1998, *J. Chem. Phys.*, 108, 8369
- Cossart, D. 1994, *J. Mol. Spectrosc.*, 167, 11
- Coxon, J. A., Marcoux, P. J., & Setser, D. W. 1976, *Chem. Phys.*, 17, 403
- Decker, B. K., Adams, N. G., & Babcock, L. M. 2001, *Int. J. Mass Spectrom.*, 208, 99
- De Lucia, F. C., Herbst, E., Plummer, G. M., & Blake, G. A. 1983, *J. Chem. Phys.*, 78, 2312
- Dixon, T. A., & Woods, R. C. 1975, *Phys. Rev. Lett.*, 34, 61
- Drda, K., Knapp, G. R., & van Dishoeck, E. F. 1989, *ApJ*, 345, 815
- Duan, C., Wu, L., Chen, Y., & Liu, Y. 2003, *J. Mol. Spectrosc.*, 217, 146
- Ferlet, R., Roueff, E., Czamy, J., & Felenbok, P. 1986, *A&A*, 168, 259
- Fuente, A., Black, J. H., Martín-Pintado, J., Rodríguez-Franco, A., García-Burillo, S., Planesas, P., & Lindholm, J. 2000, *ApJ*, 545, L113
- Fuente, A., García-Burillo, S., Gerin, M., Rizzo, J. R., Usero, A., Teyssier, D., Roueff, E., & Le Bourlot, J. 2006, *ApJ*, 641, L105
- Fuente, A., & Martín-Pintado, J. 1997, *ApJ*, 477, L107
- Fuente, A., Rodríguez-Franco, A., García-Burillo, S., Martín-Pintado, J., & Black, J. H. 2003, *A&A*, 406, 899
- Gauyacq, D., & Horani, M. 1978, *Canadian J. Phys.*, 56, 587
- Gottlieb, C. A., Myers, P. C., & Thaddeus, P. 2003, *ApJ*, 588, 655
- Hasegawa, T., et al. 1984, *ApJ*, 283, 117
- Hauschildt, H., Güsten, R., Phillips, T. G., Schilke, P., Serabyn, E., & Walker, C. K. 1993, *A&A*, 273, L23
- Hayashi, M., Omodaka, T., Hasegawa, T., & Suzuki, S. 1985, *ApJ*, 288, 170
- Hirao, T., & Amano, T. 2003, *ApJ*, 597, L85
- Horani, M., & Vervloet, M. 1992, *A&A*, 256, 683
- Huber, K.-P., & Herzberg, G. 1979, *Molecular Spectra and Molecular Structure IV: Constants of Diatomic Molecules* (New York: Van Nostrand Reinhold)
- Jackson, W. M., Halpern, J. B., Feldman, P. D., & Rahe, J. 1982, *A&A*, 107, 385
- Latter, W. B., Walker, C. K., & Maloney, P. R. 1993, *ApJ*, 419, L97
- Leach, S. 1987, *A&A*, 187, 195
- Lindqvist, M., Nyman, L.-Å., Olofsson, H., & Winnberg, A. 1988, *A&A*, 205, L15
- Liu, Y., Duan, C., Liu, J., Wu, L., Xu, C., Chen, Y., Hamilton, P. A., & Davies, P. B. 2002, *J. Chem. Phys.*, 116, 9768
- Liu, Y., Liu, H., Gao, H., Duan, C., Hamilton, P. A., & Davies, P. B. 2000, *Chem. Phys. Lett.*, 317, 181
- Lovas, F. J., Suenram, R. D., Ogata, T., & Yamamoto, S. 1992, *ApJ*, 399, 325
- Lucas, R., & Liszt, H. S. 2002, *A&A*, 384, 1054
- McAllister, T. 1978, *ApJ*, 225, 857
- Penzias, A. A., Solomon, P. M., Wilson, R. W., & Jefferts, K. B. 1971, *ApJ*, 168, L53
- Pickett, H. M. 1991, *J. Mol. Spectrosc.*, 148, 371
- Quarta, M. L., & Singh, P. D. 1981, *A&A*, 98, 384
- Rizzo, J. R., Fuente, A., Rodríguez-Franco, A., & García-Burillo, S. 2003, *ApJ*, 597, L153
- Saito, S., Kawaguchi, K., Yamamoto, S., Ohishi, M., Suzuki, H., & Kaifu, N. 1987, *ApJ*, 317, L115
- Savage, C., & Ziurys, L. M. 2004, *ApJ*, 616, 966
- Smith, A. M., Stecher, T. P., & Casswell, L. 1980, *ApJ*, 242, 402
- Spaans, M., & Meijerink, R. 2007, *ApJ*, 664, L23
- Störzner, H., Stutzki, J., & Sternberg, A. 1995, *A&A*, 296, L9
- Thaddeus, P., Guélin, M., & Linke, R. A. 1981, *ApJ*, 246, L41
- van Dishoeck, E. F., Jansen, D. J., & Phillips, T. G. 1993, *A&A*, 279, 541
- Walker, C. K., Lada, C. J., Young, E. T., Maloney, P. R., & Wilking, B. A. 1986, *ApJ*, 309, L47
- Woodall, J., Agúndez, M., Markwick-Kemper, A. J., & Millar, T. J. 2007, *A&A*, 466, 1197
- Yamamoto, S., Saito, S., Kawaguchi, K., Kaifu, N., Suzuki, H., & Ohishi, M. 1987, *ApJ*, 317, L119

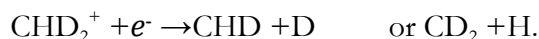
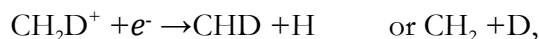


### 3.3 The CHD bi-radical

There are several reasons why it is worthwhile studying CHD ( $X^3A''$ ). On the one hand, the methylene radical,  $\text{CH}_2$ , is the parent carbene and is the simplest triatomic molecule having a triplet electronic ground state ( $X^3B_1$ ). Hence this molecule is chemically very reactive, particularly towards hydrocarbons, and thus plays a fundamental role in many chemical environments.<sup>161</sup> It is a known interstellar molecule which, according to gas-phase chemical models of dense and diffuse molecular clouds, is a key intermediate produced early in the sequence of ion-molecule reactions:



The methyl ion,  $\text{CH}_3^+$ , is also a basic ion in interstellar carbon chemistry, and in warm interstellar clouds where deuterium fractionation process is important its monodeuterated isotopologue,  $\text{CH}_2\text{D}^+$ , is likely present as well. A tentative detection of  $\text{CH}_2\text{D}^+$  in the vicinity of Orion has recently been reported. Therefore deuterated methylene radicals can be produced from this ion or from  $\text{CHD}_2^+$  by dissociative recombination with an electron:



Laboratory measurements of the rest frequencies for any isotopologue of the methylene radical are an essential prerequisite to their radioastronomical detections.

---

<sup>161</sup> R. A. Moss and M. Jones, Jr. in: *Carbens* (Wiley-Interscience, New York, 1975).

On the other hand, although high-resolution spectroscopy of both CH<sub>2</sub> and CD<sub>2</sub> has been reported, no field-free high-resolution spectrum of CHD was known before our investigation of this species in the terahertz region. In 1994, six rotational transitions detected by far infrared laser magnetic resonance spectroscopy (FIT-LMR) have been reported. This limited number of observed lines is the reason why energy levels of this isotopologue especially are determined with a rather poor accuracy. This is supported by the fact that the two field-free, pure rotational transitions of CHD that we observed were shifted by as much as 2 GHz from the predictions made using their set of molecular constants. Probably, part of the reason should be ascribed to the unique physical properties of the methylene radical: it possesses a bent ( $r_e = 1.090 \text{ \AA}$ ,  $\theta_e = 133.93^\circ$ ) and exceedingly floppy molecular structure, which results in the breakdown of the Watson model for this species. As a result the Euler approach, introduced by Pickett *et al.* for the analysis of the related water molecule fairly recently,<sup>162</sup> has been employed in a global analysis in order to account for the high-resolution terahertz data recently published on CH<sub>2</sub>. In addition, since methylene is a very light molecule with its permanent dipole moment ( $\sim 0.6 \text{ D}$ ) aligned along the  $C_{2v}$  molecular  $b$ -axis, most of the rotational transitions occur in the terahertz region and only a few lines of CH<sub>2</sub> (6), CD<sub>2</sub> (4) and CHD (2) have been measured with microwave accuracy until now. Thus observation of additional transitions is highly desirable to better understand the potential energy surface of this fundamental molecule.

In our analysis of the observed lines (six in total), equations 1.2 (electron spin-rotation interaction) and 1.4 (spin-spin coupling constants) were used to describe to fine-structure Hamiltonian (as expected for the high

---

<sup>162</sup> H. M. Pickett, J. C. Pearson and C. E. Miller, *J. Mol. Spectrosc.* **233**, 174 (2005).

values of the  $N$  quantum number, no hyperfine-structure splitting could readily be observed). The  $B$  and  $C$  rotational constants and the  $\epsilon_{bb}$ ,  $\epsilon_{cc}$ , and  $\beta$  fine-structure coupling parameters could be determined and should be viewed as *preliminary* molecular constants. Further measurement is obviously needed for CHD and should be done above 1 THz, which will be a difficult, challenging task.

The paper related to the first submillimetre /terahertz spectroscopic detection of CHD recently published in *Astronomy & Astrophysics* is presented in the next pages before a discussion on the future prospects.

# Terahertz spectroscopy of the CHD radical ( $\tilde{X}^3 A''$ )

H. Ozeki<sup>1</sup>, S. Bailleux<sup>2</sup>, and G. Wlodarczak<sup>2</sup>

<sup>1</sup> Department of Environmental Science, Faculty of Science, Toho University, 2-2-1 Miyama, Funabashi 274-8510, Japan  
e-mail: ozeki@env.sci.toho-u.ac.jp

<sup>2</sup> Laboratoire de Physique des Lasers, Atomes et Molécules, UMR CNRS 8523, CERLA, Université Lille 1,  
59655 Villeneuve d'Ascq Cedex, France  
e-mail: stephane.bailleux@univ-lille1.fr

Received 2 November 2010 / Accepted 26 November 2010

## ABSTRACT

**Context.** Pure rotational spectra in the field-free condition of the CH<sub>2</sub> and CD<sub>2</sub> isotopologues of the methylene radical have already been reported, whereas only six rotational transitions of the mono-deuterated species, CHD, detected by FIR-LMR spectroscopy have been.

**Aims.** Spectra of the mono-deuterated methylene radical in its ground electronic state ( $\tilde{X}^3 A''$ ) were observed in the field-free condition for the first time in the frequency region below 1 THz.

**Methods.** CHD was generated in a positive column discharge in a CH<sub>2</sub>D<sub>2</sub> – Ar mixture cooled with liquid nitrogen.

**Results.** Two rotational transitions, each split into three fine-structure components, were measured. The *B* and *C* rotational constants, the  $\epsilon_{fb}$  and  $\epsilon_{cc}$  spin-rotation constants, and the  $\beta$  spin-spin constant were revised.

**Conclusions.** The reported frequencies are suitable for astronomical searches.

**Key words.** line: identification – molecular data – ISM: molecules – submillimetre: ISM

## 1. Introduction

The methylene radical, CH<sub>2</sub>, is known as an interstellar molecule that has been detected towards hot cores in dense interstellar clouds (Hollis et al. 1995; Polehampton et al. 2005). In the gas phase chemical models of both dense and diffuse molecular clouds, the methylene radical is thought to be one of the fundamental molecules of the carbon chemistry, and it is produced primarily by dissociative recombination of the methyl ion, CH<sub>3</sub><sup>+</sup> (Herbst 2001; Vejby-Christensen et al. 1997). Recently tentative detection of the mono-deuterated methyl ion, CH<sub>2</sub>D<sup>+</sup> have been reported toward an infrared source in the vicinity of Orion (Lis et al. 2009), along with its supporting laboratory spectroscopic measurements (Amano 2010; Gärtner et al. 2010). Mono-deuterated methylene CHD can be produced from this ion or its counterpart ion, CHD<sub>2</sub><sup>+</sup>, by dissociative recombination with an electron as shown in the chemical reactions:



Thus, both CHD and CD<sub>2</sub> can be observed in warm interstellar clouds, where the deuterium fractionation process is important (see Turner 2001; Roueff 2007; Parise 2009). Precise laboratory reference data are therefore desirable for such a radio-astronomical observation of these molecules.

More than half a century has passed since the pioneering spectroscopic work on the methylene radicals, CH<sub>2</sub> and its deuterated isotopomers by Herzberg et al. (1959, 1971). However, it is still an ongoing project to characterize or understand the nature of this species by spectroscopy in various wavelength regions. This difficulty arises from the unique chemical and physical properties of the molecule. The methylene radical is the prototype of the “carbene” and is known to be kinetically

a very unstable species (Moss & Jones, Jr. 1975). Therefore this short-lived molecule is very hard to generate in concentrations that are high enough for carrying out spectroscopic studies in laboratory conditions. In the ground electronic state, the CH<sub>2</sub> molecule possesses <sup>3</sup>B<sub>1</sub> symmetry with a bent and exceedingly floppy molecular structure. The latter characteristic leads to the breakdown of the Watson model for this species. Such a complicated situation has stimulated many theoretical studies on CH<sub>2</sub>, and various models have been proposed in order to represent its bending potential (see Bunker & Landsberg 1977; Bunker & Jensen 1983; Jensen et al. 1982; Bunker et al. 1986; Jensen 1988). The fidelity of these theoretical models can be validated by comparative studies of the energy levels of methylene and its deuterated analogues obtained by high-resolution molecular spectroscopy.

High-resolution spectroscopy of the methylene radical has been conducted mainly by infrared/far-infrared laser magnetic resonance spectroscopy (IR/FIR-LMR) or infrared diode laser spectroscopy (Bunker 1985). Thanks to these extensive works in mid 70's to early 80's, pure rotational transitions frequencies for CH<sub>2</sub> and CD<sub>2</sub> can be predicted with the accuracy of less than several tens of MHz, and laboratory microwave spectra of CH<sub>2</sub> and CD<sub>2</sub> were successfully observed (Lovas 1983; Ozeki & Saito 1995, 1996). In the best-studied case of CH<sub>2</sub>, six rotational transitions having *K<sub>a</sub>* = 0, 1 have been observed up to almost 2 THz with microwave spectroscopic precision (Michael et al. 2003; Brünken et al. 2004, 2005). Since *b*-type transitions are allowed, those measured near 1 and 2 THz involve *N* = 1, 2 and include the 1<sub>10</sub> ← 1<sub>01</sub> ground-state transition of *para*-CH<sub>2</sub> (see the definition of *ortho*- and *para*-CH<sub>2</sub> in the results and discussion section), while the ones measured in the lower frequency region correspond to higher rotational quantum numbers with

energy levels of several hundred Kelvin. The inadequacy of a Watson-type Hamiltonian for fitting spectra of methylene radical also led Brünken et al. (2005) to employ a Hamiltonian based on Euler functions to successfully carry out the global analysis of the experimental spectrum of  $\text{CH}_2$ . The number of observed lines is, however, still limited due to its lightness and the fact that  $b$ -type asymmetric rotor selection rules apply. As for  $\text{CD}_2$ , only four rotational transitions below 600 GHz have been reported so far by laboratory microwave spectroscopy (Ozeki & Saito 1996). To our knowledge, no field-free high-resolution spectrum has been reported for the CHD radical. Nolte et al. (1994) published FIR-LMR spectroscopy of the CHD radical in the ground electronic state. An insufficient number of observed spectral lines (six rotational transitions) meant that their proposed set of molecular constants was a composite of the ones derived both experimentally and theoretically (Bunker et al. 1983). As a consequence the energy levels of CHD are not as reliable as those of  $\text{CH}_2$  and  $\text{CD}_2$ , which presumably makes it hard to achieve spectral measurement of this species. We report in the present paper field-free, pure rotational spectra of the CHD radical up to the terahertz frequency region with an accuracy the same order as conventional microwave spectroscopy.

## 2. Experiment

The spectrometer used in this experiment has been described extensively elsewhere (Baillieux et al. 2002). Submillimetre-wave and terahertz radiations in the frequency range 0.55–0.97 THz were provided by two phase-locked backward-wave oscillators (Istok company, Russia). Emitted power at observed transition frequencies was in the mW range. A liquid-helium-cooled InSb bolometer (QMC Instruments) was used as detector. Source modulation at 5 kHz and lock-in detection at twice the modulation frequency was employed for improved sensitivity, resulting in a second-derivative line shape. A positive column discharge in various isotopologues of methane used as precursors,  $\text{CH}_2\text{D}_2$  and  $\text{CD}_4$  (Cambridge Isotope Laboratories Inc., USA), was setup. The absorption cell was a 2 m long, 5 cm inner diameter, double-jacketed Pyrex tube, allowing liquid-nitrogen flow through the outer jacket to cool the plasma. The cell was equipped with a solenoid coil for creating an axial magnetic field to ensure that the lines are paramagnetic by on/off measurements. The precursor was pre-mixed with argon used as buffer gas before it entered the absorption cell's inlet for in situ production of reactive species. In addition to the above-mentioned precursors,  $\text{CH}_4$  was also available in order to check for the chemistry of the reactions that occur in the absorption cell.

## 3. Spectroscopic measurements

We first optimized the experimental conditions to produce  $\text{CH}_2$  as trial species using  $\text{CH}_4$  as precursor. For this purpose, reported rotational lines below 600 GHz were observed. The conditions were further confirmed by the observation of the di-deuterated analogue,  $\text{CD}_2$ , using  $\text{CD}_4$  as precursor. We found that the optimum discharge current was in the range 20–30 mA and that the partial pressures (measured downstream at room temperature) giving the best signal-to-noise ratio were 13 and 2.5 mTorr for Ar and  $\text{CH}_4$  or  $\text{CD}_4$ , respectively. The outer jacket of the cell partially filled with liquid nitrogen (~30% of the maximum liquid nitrogen load) resulted in an increase in the intensity of the signals. Using these conditions, we have successfully observed the as yet unreported three fine-structure components of the

$N_{K_a, K_c} = 7_{07} \leftarrow 6_{16}$  rotational transition of  $\text{CD}_2$  near 799 GHz, which will be published elsewhere with additional lines measured, if possible. Optimization of the conditions also allowed us to gauge both the production efficiency and the line intensity we could expect for the mono-deuterated methylene radical. Indeed, our method of production differs markedly from the one reported in previous studies, continuous glow discharge in ketene. As a result, our production efficiency, although lower than the one obtained with the discharge in ketene, was satisfactory to expect the detection of rotational transitions of CHD.

We afterwards guided our search for the  $N_{K_a, K_c} = 7_{07} \leftarrow 6_{16}$  rotational transition of CHD,  $\text{CH}_2\text{D}_2$  serving as precursor. The three fine-structure components were expected to occur near 944.5 GHz, based on the predictions made using the molecular constants provided by the FIR-LMR work (Nolte et al. 1994). A careful search of 2 GHz around the predicted frequencies using the same experimental conditions as for  $\text{CH}_2$  and  $\text{CD}_2$  showed very clean spectra. A limited number of unidentified lines were detected, but all were found to belong to diamagnetic species. We thus decided to extend the search region further, proceeding toward the high frequencies. We detected one set of three paramagnetic lines within 512 MHz. We checked the chemistry to produce these lines and found that they were not observable when  $\text{CD}_4$  or  $\text{CH}_4$  were used as precursors instead of  $\text{CH}_2\text{D}_2$ . However, they could be detected when  $\text{CD}_4$  and  $\text{CH}_4$  were introduced simultaneously, with a signal-to-noise ratio about five times weaker than with  $\text{CH}_2\text{D}_2$ . These chemical tests showed that the newly observed species contains both H and D atoms. Convinced that this species was the monodeuterated methylene radical, we decided to detect the  $N_{K_a, K_c} = 6_{06} \leftarrow 5_{15}$  rotational transition predicted around 580.3 GHz and started to scan upwards. We subsequently discovered another set of three paramagnetic transitions above 581 GHz that showed identical behaviour with the chemical tests. The detection of two additional rotational transitions, the  $N_{K_a, K_c} = 5_{05} \leftarrow 4_{14}$  and the  $N_{K_a, K_c} = 1_{11} \leftarrow 2_{02}$ , predicted near 221 and 821 GHz, respectively, was attempted. It is likely that the lack of accurate predictions (within 100 MHz) and their weaker intensity, especially for the  $N_{K_a, K_c} = 1_{11} \leftarrow 2_{02}$ ,  $J = 2 \leftarrow 3$  fine-structure component that is expected to be split into several hyperfine-structure components, prevented us from detecting them.

## 4. Results and discussion

Although the number of observed lines is limited, we are confident that identification of the CHD radical in its ground electronic state ( $\tilde{X}^3A''$ ) is secure. Three fine-structure components for each rotational transition were detected, as expected for a species in a triplet ground electronic state. Wide regions were scanned (several GHz) around the predictions, and only the transition frequencies reported in Table 1 showed paramagnetic behaviour. The chemistry for all six lines was carefully checked, proving that they belong to a species that contains both H and D atoms. As for  $\text{CH}_2$  and  $\text{CD}_2$ , all fine-structure components were found to be very sensitive to the magnetic field applied: a magnetic field in the range 2–50 Gauss was sufficient to observe the disappearance of the lines, the  $F_3$  and  $F_2$  components being the most and least sensitive, respectively. Similar to the spectrum of  $\text{CD}_2$  at 799 GHz, the  $F_2$  component was detected with stronger signal-to-noise ratio than the  $F_1$  and  $F_3$  components. These observations are in accordance with the prediction that includes the hyperfine-structure due to H and D nuclei since all hyperfine-structure components are overlapped on a single line only for the  $F_2$  component. An example of the

**Table 1.** Observed rotational transitions frequencies of CHD ( $\bar{X}^3A''$ ), in MHz.

Transition	Component <sup>a</sup>	$\nu_{\text{obs}}^b$	$\nu_{\text{obs}} - \nu_{\text{calc}}$
$6_{06} \leftarrow 5_{15}$	$F_1$	581 021.489(60) <sup>c</sup>	0.046
	$F_2$	581 506.679(20)	-0.012
	$F_3$	581 580.606(50)	0.040
$7_{07} \leftarrow 6_{16}$	$F_1$	946 609.805(40)	-0.022
	$F_2$	946 800.636(25)	0.019
	$F_3$	947 121.971(60)	-0.060

**Notes.** The standard deviation of the fit is 38 kHz. Calculated frequencies were obtained from molecular constants given in Table 2. <sup>(a)</sup>  $\Delta J = \Delta N = 1$  fine-structure components. For the upper and lower energy levels,  $F_1: J = N + 1$ ,  $F_2: J = N$ ,  $F_3: J = N - 1$ . <sup>(b)</sup> Values in parentheses are  $1\sigma$  experimental error on the last digits. <sup>(c)</sup> Hyperfine-structure for this line was partly resolved as a doublet, and the average of the two observed transition frequencies was used in the least-squares analysis.

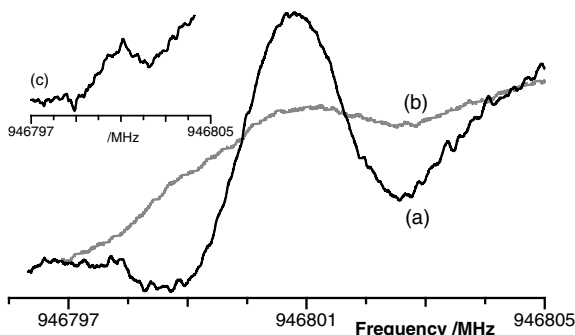


**Fig. 1.** Observed spectra of the  $N_{K_a, K_c} = 7_{07} \leftarrow 6_{16}$ ,  $J = 7 \leftarrow 6$  ( $F_2$  component) rotational transition of the CHD radical produced in dc glow discharge ( $\sim 20$  mA) using  $\text{CH}_2\text{D}_2$  as precursor recorded **a)** without magnetic field applied and **b)** with a magnetic field of only 15 Gauss applied. Inset **c)**: same transition detected using  $\text{CH}_4$  and  $\text{CD}_4$  as precursors, about five times less intense. These spectra were recorded by integrating 36 scans with 0.5 Hz repetition rate and 10 ms time constant of the lock-in amplifier.

$N_{K_a, K_c} = 7_{07} \leftarrow 6_{16}$ ,  $J = 7 \leftarrow 6$  ( $F_2$  component) recorded near 946 801 MHz is depicted in Fig. 1.

In the present study, no hyperfine-structure due to H and D nuclei could be observed for these high  $N$  rotational transitions, except for the  $F_1$  component of the  $6_{06} \leftarrow 5_{15}$  rotational transition, which appeared as a weak, partly resolved doublet with a frequency gap of 1.34(12) MHz. This value was obtained from a nonlinear line profile analysis for individual components using IGOR Pro (wavemetrics). The line frequencies and the peak intensities for this doublet were adjusted by assuming a second derivative Voigt line shape with the same linewidth for both hyperfine-structure components. This result is consistent with our preliminary prediction of the hyperfine-structures by assuming that the hyperfine interaction constants for H and D nuclei are the same as those of  $\text{CH}_2$  and  $\text{CD}_2$ , respectively. The calculated hyperfine pattern for these high  $N$  rotational quantum numbers shows that the  $F_2$  components should be observed as a singlet, while the  $F_1$  and  $F_3$  components should each appear as a doublet with a frequency gap of less than 3.0 and 2.5 MHz,

**Table 2.** Molecular constants for CHD ( $\bar{X}^3A''$ ), in MHz.

Constant	Present study	FIR LMR work <sup>a</sup>
$B$	170 344.0470(28)	170 233.7(21)
$C$	148 139.235(32)	149 100.6(21)
$\epsilon_{bb}$	-112.66(18)	-105.527
$\epsilon_{cc}$	-110.93(50)	-83.342
$\beta$	1339.584(75)	1382.0(75)

**Notes.** Only constants determined in this preliminary study are reported. All other molecular constants have been fixed to their values reported in Table IV from Reference 1. <sup>(a)</sup> Reference 1. Values originally reported in  $\text{cm}^{-1}$  were converted to MHz.

**References.** (1) Nolte et al. (1994).

respectively. It should also be noted that, at these high frequencies, the Doppler broadening of the lines prevents the observation of the hyperfine-structure. The observed transition frequencies (Table 1) were subjected to least-squares analysis (which does not include hyperfine constants) using Pickett's program SPFIT (Pickett 1991). The rotational constants  $B$  and  $C$ , the electron spin-rotation constants  $\epsilon_{bb}$  and  $\epsilon_{cc}$ , and the electron spin-electron spin constant  $\beta$  were the adjustable parameters. A least-squares analysis using the combinations of constants  $A - \frac{1}{2}(B + C)$ ,  $\frac{1}{2}(B + C)$ ,  $\epsilon_{aa} - \frac{1}{2}(\epsilon_{bb} + \epsilon_{cc})$ , and  $\frac{1}{2}(\epsilon_{bb} + \epsilon_{cc})$ , in addition to  $\beta$ , resulted in a fit with a standard deviation of  $\sim 0.7$  MHz. The determined constants are provided in Table 2, together with their values obtained from the previous FIR-LMR study for comparison. We checked that no significant correlation occurred between the floated parameters.

Obviously, the rotational constants determined in the present study do not fit the quoted error range of the ones obtained by the previous FIR-LMR work. This is true in particular for the  $C$  constant. In contrast, the fine-structure parameters of the two studies compare much better. Indeed, the frequency differences between two successive fine-structure components of the  $N = 6 \leftarrow 5$  and  $7 \leftarrow 6$  rotational transitions predicted from the LMR work can be compared with those obtained from our measurements. The frequency differences from the LMR work, given in MHz as  $(F_2 - F_1, F_3 - F_2)$  are (460, 112) and (168, 363) for the  $N = 6 \leftarrow 5$  and  $7 \leftarrow 6$  transitions, respectively. The corresponding differences calculated from Table 1 are (485, 74) and (191, 321).

The set of molecular constants reported by Nolte et al. (1994) consisted of eight adjusted and nine fixed parameters for both the rotational and spin-rotational parts. The fitted parameters were determined by a limited number of measured lines and theoretically calculated energy levels, while eight out of the nine fixed parameters were constrained to the average of their values for  $\text{CH}_2$  and  $\text{CD}_2$ . The estimated errors (10 to 15 MHz) for their measured lines are almost certainly underestimated, as they stated. Considering these facts, it is not surprising that the transition frequencies observed in the present study are found shifted by as much as 1 to 2 GHz from the FIR-LMR predicted values. This shows a striking contrast to the cases of spectroscopy of  $\text{CH}_2$  and  $\text{CD}_2$ , as FIR-LMR data for those species were quite reliable. Our constants will undoubtedly evolve as further rotational transitions of this species will be measured in the future. Since the errors on our constants are model-dependent, they are underestimated as well. Our reported frequencies can be useful as the precise laboratory reference data for astronomical observation, though the upper levels of the observed transitions are

relatively high (220–300 cm<sup>-1</sup>, corresponding to temperatures of 300–400 K).

Finally, the ground-state rotational transition deserves a few comments. There are no two equivalent nuclei in CHD. Thus no spin statistics have to be obeyed, and only one ground-state transition for this species exists, the  $I_{11} \leftarrow 0_{00}$ . The rest frequencies of this transition, not taking the fine and hyperfine interactions into account, is predicted to occur near 1773 GHz and 1774 GHz, based on our results and on the LMR work, respectively. In contrast, CH<sub>2</sub> and CD<sub>2</sub> have  $^3B_1$  as a ground state and should follow the Fermi-Dirac and Bose-Einstein spin statistics, respectively. Therefore *ortho*- and *para*-states, which are represented by even and odd values of  $K_a + K_c$ , respectively, co-exist. The ground-state transitions of the two *ortho*-species lie near 2.35 and 1.23 THz, and in addition, two fundamental transitions of the *para*-species occur, namely the  $I_{10} \leftarrow I_{01}$  and the  $2_{12} \leftarrow 1_{01}$ . Their lower energy level is 15.1 cm<sup>-1</sup> and 7.4 cm<sup>-1</sup> above the ground in the case of CH<sub>2</sub> and CD<sub>2</sub>, respectively. None of these ground-state transitions has yet been measured with microwave accuracy.

It is also worthwhile mentioning that the  $7_{07} \leftarrow 6_{16}$  transition at 0.94 THz lies in the centre of one of the “atmospheric windows” around 1 THz (Matsushita et al. 2000), through which astronomical observations are feasible from ground-based observatories.

## 5. Conclusions

The two strongest field-free pure rotational transitions of the CHD radical in the electronic ground state ( $\bar{X}^3A''$ ) have been successfully observed below 1 THz for the first time. It is necessary to increase the CHD production efficiency and/or the detection sensitivity of the spectrometer for further detection of the unobserved lines below or above 1 THz. We intend in the near future to carry out such measurements using the “conventional” method, that is, in situ flash pyrolysis of partially deuterated diketene (to generate partially deuterated ketene) combined with continuous glow discharge.

*Acknowledgements.* The National French Programme “Physique et Chimie du Milieu Interstellaire” (PCMI) and the French National Research Agency

(ANR-08-BLAN-0225-01-02-03-04 “FORCOMS”) are acknowledged for their support. H.O. gratefully acknowledges Lille 1 University for supporting his stay as an invited professor for two months.

## References

- Amano, T. 2010, A&A, 516, L4  
 Bailleux, S., Bogey, M., Demuynck, C., Liu, Y., & Walters, A. 2002, J. Mol. Spectrosc., 216, 465  
 Brünken, S., Michael, E., Lewen, F., et al. 2004, Can. J. Chem., 82, 676  
 Brünken, S., Müller, H. S. P., Lewen, F., & Giesen, T. F. 2005, J. Chem. Phys., 123, 164315  
 Bunker, P. R. 1985, in Comparison of Ab Initio Quantum Chemistry with Experiment for Small Molecules, ed. R. J. Bartlett (Dordrecht, Holland: D. Reidel Publishing Company), and references therein  
 Bunker, P. R., & Jensen, P. 1983, J. Chem. Phys., 79, 1224  
 Bunker, P. R., & Landsberg, B. M. 1977, J. Mol. Spectrosc., 67, 374  
 Bunker, P. R., Sears, T. J., McKellar, A. R. W., Evenson, K. M., & Lovas, F. J. 1983, J. Chem. Phys., 79, 1211  
 Bunker, P. R., Jensen, P., Kraemer, W. P., & Beardsworth, R. 1986, J. Chem. Phys., 85, 3724  
 Gärtner, S., Krieg, J., Klemann, A., Asvany, O., & Schlemmer, S. 2010, A&A, 516, L3  
 Herbst, E. 2001, Chem. Soc. Rev., 30, 168  
 Herzberg, G., & Johns, J. W. C. 1971, J. Chem. Phys., 54, 2276  
 Herzberg, G., & Shoosmith, J. 1959, Nature, 183, 1801  
 Hollis, J. M., Jewell, P. R., & Lovas, F. J. 1995, ApJ, 438, 259  
 Jensen, P. 1988, J. Mol. Spectrosc., 128, 478  
 Jensen, P., Bunker, P. R., & Hoy, A. R. 1982, J. Chem. Phys., 77, 5370  
 Lis, D. C., Goldsmith, P. F., Bergin, E. A., et al. 2009, in Submillimeter Astrophysics and Technology, ASP Conf. Ser., 417, 23  
 Lovas, F. J., Suenram, R. D., & Evenson, K. M. 1983, ApJ, 267, L131  
 Matsushita, S., Matsuo, H., Sakamoto, A., & Pardo, J. R. 2000, Proc. SPIE, 4015, 378  
 Michael, E. A., Lewen, F., Winnewisser, G., et al. 2003, ApJ, 596, 1356  
 Moss, R. A., & Jones Jr., M. 1975, in Carbenes (New York: Wiley-Interscience), 2  
 Nolte, J., Temps, F., Wagner, H. Gg., Wolf, M., & Sears, T. J. 1994, J. Chem. Phys., 100, 8706  
 Ozeki, H., & Saito, S. 1995, ApJ, 451, L97  
 Ozeki, H., & Saito, S. 1996, J. Chem. Phys., 104, 2167  
 Parise, B., Leurini, S., Schilke, P., et al. 2009, A&A, 508, 737  
 Pickett, H. M. 1991, J. Mol. Spectrosc., 148, 371  
 Polehampton, E. T., Menten, K. M., Brünken, S., Winnewisser, G., & Baluteau, J. P. 2005, A&A, 431, 203  
 Roueff, E., Parise, B., & Herbst, E. 2007, A&A, 464, 245  
 Turner, B. E. 2001, ApJS, 136, 579  
 Vejby-Christensen, L., Andersen, L. H., Heber, O., et al. 1997, ApJ, 1997, 483, 531

### 3.4 Future prospects

With only two pure rotational transitions observed, additional measurements of rotational transitions of the CHD radical are obviously required. However, the next rotational transition is expected to occur near 1.316 THz. Of astrophysical interest are the  $N_{KaKc} = 1_{10} - 1_{01}$  ( $\sim 15$  K) transition and the  $1_{11} - 0_{00}$  ground-state transition that are predicted to fall near 1.480 and 1.773 THz, respectively. This frequency range is difficult to attain and the hyperfine pattern predicted for these low  $N$  rotational quantum numbers will certainly prevent direct radioastronomical detection. Because the methylene radical is an extremely floppy molecule, the centrifugal distortion terms are very large and strongly dependent on the isotopologues. For example the  $\Delta K$  value varies from 87.6 GHz ( $\text{CH}_2$ ), through 42.1 GHz (CHD) to 16.8 GHz ( $\text{CD}_2$ ). This has precluded the detection of transitions in the (sub)millimetre-wave region with  $K_a \geq 2$ . The investigation of  $K_a = 2$  transitions for the three isotopologues of the methylene radical is therefore of special interest. It is also worthwhile noting that, although the matrix infrared spectrum of the silicon analogue of methylene is known for the three isotopologues  $\text{SiH}_2$ ,  $\text{SiD}_2$  and  $\text{SiHD}$ , and the gas-phase infrared diode laser spectroscopy of the  $\nu_1$ ,  $\nu_2$ ,  $2\nu_2$  and  $\nu_3$  bands were reported for  $\text{SiH}_2$ ,<sup>163</sup> the rotational spectrum of silylene has not been reported yet. Since silicon chemistry is extensive, several theoretical studies recently published on this elusive molecule<sup>164</sup> show once more the interest for its investigation by high-resolution spectroscopy. It is interesting to point out that while the ground state of methylene is a

---

<sup>163</sup> C. Yamada, H. Kanomori, E. Hirota, N. Nishiwaki, N. Itabashi, K. Kato and T. Goto, *J. Chem. Phys.* **91**, 4582 (1989); E. Hirota and H. Ishikawa, *J. Chem. Phys.* **110**, 4254 (1999).

<sup>164</sup> A. Kalemos, T. H. Dunning Jr and A. Mavridis, *Mol. Phys.* **102**, 2597 (2004); S. N. Yurchenko, P. R. Bunker, W. P. Kraemer and P. Jensen, *Can. J. Chem.* **82**, 694 (2004).

triplet state lying only slightly below the lowest singlet excited electronic state, this picture is reversed in silylene: the electronic ground state is  $^1A_1$  and strictly speaking  $SiH_2$  is not a radical. However, Hirota determined that with a lifetime of about 10  $\mu s$ , this molecule is extremely reactive. In the case of ionic species, apart the  $H_2O^+$  ion already cited in chap. 1, the investigation of the protonated molecular oxygen,  $O_2H^+$  is also highly desirable in the context of interstellar oxygen-related chemistry. Indeed,  $H_3^+$  is considered as an efficient source of protonation in interstellar clouds, and  $O_2H^+$  is expected to be formed from proton transfer to  $O_2$  according to the reaction:  $H_3^+ + O_2 \rightarrow O_2H^+ + H_2$ . As early as 1977, Herbst *et al.*<sup>165</sup> suggested that this ion could be used as an  $O_2$  tracer which, very surprisingly, has recently been tentatively detected toward only one molecular cloud,  $\rho$  Ophiuchus A (with both the Odin satellite and the Submillimetre Wave Astronomy Satellite, SWAS). What is more, the fractional abundance of  $O_2$  determined from these observations is well below that predicted by astrochemical models. No laboratory rotational spectrum is available for  $O_2H^+$  whose ground electronic state is  $^3A''$  (like CHD), and high level *ab initio* calculations have recently been published.<sup>166</sup> They revealed equilibrium structural parameters along with ground-state rotational constants, centrifugal distortion parameters and spin-rotation coupling constants in addition to the spin-spin interaction terms  $\alpha_0$  and  $\beta_0$  (equation 1.4). Interestingly, the dipole moment possesses two strong *a*- and *b*- components,  $\mu_a$  ( $\sim 1.5$  D) being roughly parallel to the OO bond axis whilst  $\mu_b$  ( $\sim 1.9$  D) is dominated by the OH bond. Therefore if the production in a DC discharge fed by a suitable mixture (using argon

---

<sup>165</sup> E. Herbst, S. Green, P. Thaddeus, W. Klemperer, *Astrophys. J.* **215**, 503 (2007).

<sup>166</sup> S. L. W. Weaver, D. E. Woon, B. Ruscic and B. J. McCall, *Astrophys. J.* **697**, 601 (2009).

or helium as a buffer gas) is not a problem, the detection of the rotational spectrum of  $\text{O}_2\text{H}^+$  below 1 THz would not pose major difficulties.

The characterization of such labile molecules will undoubtedly be facilitated not only by improving the sensibility of the spectrometer, but as well by extending the frequency coverage toward and well above the terahertz region. While the design of the former is planned in the near future and could be achieved for open-shell species by applying the Zeeman modulation, the latter is currently under development and should have significant impact for a number of observational facilities like ALMA and the HIFI (Heterodyne Instrument for the Far- Infrared) spectrometer on board the Herschel spacecraft.

Yet another alternative to assist the identification of short-lived molecules in the PhLAM laboratory may consist in conducting complementing experiments with the high resolution ( $0.0007\text{ cm}^{-1}$  or 20 MHz) Fourier transform infrared spectrometer of the AILES (Advanced Infrared Line Exploited for Spectroscopy) beamline of SOLEIL (the French national synchrotron facility),<sup>167</sup> in collaboration with O. Pirali. Recently, the spectra of the  $^{15}\text{N}$  isotopologues of both amidogen ( $\text{NH}_2$ ,  $X^2\text{B}_1$ ) and imidogen ( $\text{NH}$ ,  $X^3\Sigma^-$ ) radicals in their vibrational ground state were first measured in SOLEIL up to  $200\text{ cm}^{-1}$  (6 THz) and subsequently in Lille between 600 and 950 GHz, involving L. Margulès (PhLAM), O. Pirali (SOLEIL) and M.-A. Martin-Drumel (SOLEIL). It should be pointed out that compared with the  $^{14}\text{N}$  parent species, the absence of the quadrupolar interaction in both open-shells makes the hyperfine-structures simpler,

---

<sup>167</sup> <http://www.synchrotron-soleil.fr/>

and the analysis of the fine- and hyperfine- structures has thus been carried out without difficulty. This research is complementary to that concerning the recent detection in Lille of the spectra of the  $^{15}\text{N}$  isotopologues of the hydrogen isocyanide close-shell ( $\text{H}^{15}\text{N}^{12}\text{C}$ ,  $\text{H}^{15}\text{N}^{13}\text{C}$ ,  $\text{D}^{15}\text{N}^{12}\text{C}$  and  $\text{D}^{15}\text{N}^{13}\text{C}$ ).

The studies of 15-nitrogen containing species should be placed in the following context. All the 14-nitrogen parent species have been detected in interstellar medium (Table 1) and large isotopic enhancements of nitrogen have been observed in the solar system, *second in range after hydrogen*. In interstellar medium, nitrogen-bearing species are important tracers of cold, dense gas but  $^{15}\text{N}/^{14}\text{N}$  ratios have scarcely been measured. Recently  $\text{N}^{15}\text{NH}^+$ ,  $^{168} \text{ }^{15}\text{NH}_2\text{D}$ ,  $^{169}$  and  $^{15}\text{NH}_3$ ,  $^{170}$  have all been easily detected by Herschel, making it very attractive to search for the  $^{15}\text{N}$  species cited above. The search for these  $^{15}\text{N}$  species in interstellar clouds is thus an on-going project in collaboration with E. Roueff (Observatoire de Paris-Meudon), M. Gerin (Laboratoire d'Etude du Rayonnement et de la Matière en Astrophysique /Laboratoire de Radioastronomie ENS) and A. Faure (Laboratoire d'Astrophysique de l'Observatoire de Grenoble). If successful, their observation should provide clues as to why large isotopic variations of nitrogen are observed. The results obtained on  $^{15}\text{NH}$  and  $^{15}\text{NH}_2$  will be discussed at the 66<sup>th</sup> International Symposium on Molecular Spectroscopy (Columbus, U.S.A., 20 -24 June 2011) and at the 31<sup>st</sup> International Symposium on Free Radicals (Port-Douglas, Australia, 24 -29 July 2011). The most important results will also be presented during the defence of this “accreditation to supervise research” as well.

---

<sup>168</sup> L. Bizzocchi, P. Caselli, L. Dore, *Astron. & Astrophys.* **510**, L5 (2010).

<sup>169</sup> M. Gerin, N. Marcellino, N. Biver, *et al.*, *Astron. & Astrophys.* **498**, 9 (2009).

<sup>170</sup> D. C. Lis, A. Wooten, M. Gerin, E. Roueff, *Astrophys. J.* **710**, L49 (2010).





